



| | |
|--------------|--|
| Title | Anharmonic Effects on the Elementary Excitations in the Ordered Solid Hydrogen |
| Author(s) | 五十嵐, 潤一 |
| Citation | 大阪大学, 1979, 博士論文 |
| Version Type | VoR |
| URL | https://hdl.handle.net/11094/79 |
| rights | |
| Note | |

The University of Osaka Institutional Knowledge Archive : OUKA

<https://ir.library.osaka-u.ac.jp/>

The University of Osaka

Anharmonic Effects on the Elementary
Excitations in the Ordered Solid Hydrogen

Jun-ichi Igarashi

Abstract

The elementary excitations in the ordered solid hydrogen are studied. It is shown that there exists a strong cubic anharmonicity for rotons ($J=3$ excitations) and librins ($J=1$ excitations), which makes one excitation split into two excitations. It is also the case for $J=2$ rotons due to a parahydrogen (or a orthodeuterium) as the impurity. The relevant Green's functions are determined self-consistently in good agreement with the experiment by Hardy, Silvera and McTague. Moreover we calculate the polarization effect on the excitation energies with better agreement with experiments.

Acknowledgements

The author would like to express his sincere thanks to Professor T. Nakamura for helpful suggestions and enlightening discussions and for improving the manuscript.

He also wishes to thank Dr. M. Fujio for the cooperation in the early stage of his study. He also wishes to thank Dr. H. Miyagi and Dr. J. Hama for helpful discussions.

Contents

- Abstract
- Acknowledgements
- I Introductory Part
- II Anharmonic Effect on Rotons in the Ordered Solid Hydrogen,
- III Localized Excitations in the Ordered Solid Hydrogen,
- IV Polarization Effect on the Excitations in the Ordered Solid Hydrogen.

Sections, pages, equations, tables and figures are numbered separately for each part. References are given separately also for each part.

Part I

Introductory Part

§1. Basic properties of solid hydrogen

Hydrogen and deuterium molecules are classified by the parity of the nuclear spin states. Molecules with nuclear spin states of even parity are called "ortho-" molecules and those with nuclear spin states of odd parity are called "para-" molecules. In hydrogen, even J (odd J), $I=0$ ($I=1$) states are called parahydrogen (orthohydrogen), where J denotes the rotational quantum number and I the total nuclear spin quantum number. This is based on the fact that total nuclear wave function must be antisymmetric under the interchange of nuclei according to the statistics of protons. Deuterium in even (odd) J and $I=0, 2$ (1) is called orthodeuterium (paradeuterium).

The transition J (odd) \rightarrow J (even) is nearly forbidden because that requires a simultaneous change of nuclear spin states. For instance the spontaneous conversion rate of $J=1 \rightarrow 0$ in solid state is about 1.9% per hour for H_2 and 0.056% per hour for D_2 .¹⁾

Now the rotational kinetic energy is given by

$$E_J = BJ(J+1) , \quad (1.1)$$

where

$$B = \hbar^2/2I \quad (1.2)$$

with I the moment of inertia of molecule. The rotational constant B is equal to 85.4 K for H_2 and to 43.0 K for D_2 .

The most dominant anisotropic intermolecular force is the electric quadrupole-quadrupole (EQQ) interaction.²⁾ This interaction between two molecules with distance R_{12} is written as

$$W(1,2) = \frac{3}{4} \frac{e^2 Q^2}{R_{12}^5} \frac{16\pi}{15} \sqrt{280\pi} \sum_{m_1 m_2} \begin{pmatrix} 2 & 2 & 4 \\ m_1 & m_2 & -M \end{pmatrix} \cdot Y_{4M}(-\theta, -\phi) Y_{2m_1}(\omega_1) Y_{2m_2}(\omega_2) \quad (1.3)$$

with eQ the electric quadrupole moment of the molecule. Here $Y_{\ell m}(\theta, \phi)$ denotes the spherical harmonic function with (θ, ϕ) the polar angles of the direction of line connecting the centers of two molecules. Here ω_1 and ω_2 denote the polar angles of the direction of two molecules 1 and 2 respectively.

And $\begin{pmatrix} j_1 & j_2 & j_3 \\ m_1 & m_2 & m_3 \end{pmatrix}$ is a Wigner's 3-j symbol. The coupling parameter Γ in solid state is defined by

$$\Gamma = 6e^2 Q^2 / 25a^5, \quad (1.4)$$

where a denotes the nearest neighbor distance. The estimate of Γ is of the order of 1K, being much less than B . Thus each molecule may be regarded essentially as free rotor. At low temperatures each molecule occupies exclusively the lowest rotational state consistent with each nuclear spin state.

Since the Debye temperature is about 100K for H_2 and D_2 , phonons are assumed not to have any important role at low

temperatures. However a large zero-point vibration makes Γ renormalize.³⁾ The anisotropic parts of valence and dispersion forces are very small. Therefore we shall leave out these forces in this study.

§2. Ground-state configuration

The melting point for H_2 and D_2 is about 20K. By X-ray diffraction⁴⁾ and neutron-scattering,⁵⁾ it was found that the solid H_2 and D_2 at high concentrations of $J=1$ molecules cause phase change from a hcp lattice to a fcc lattice with lowering temperature.

In the ordered state, fcc lattice consists of four sc sublattices.^{6,7,8)} The ordered state may be characterized by the following: If the quantized axis for each sublattice is chosen to be parallel to one of four body-diagonals, each molecules is frozen in the state with $J_z=0$, as far as the first approximation is concerned.

§3. Elementary excitations

The elementary excitations in the ordered solid hydrogen have two interesting aspects. First the microscopic forces which govern their behavior are fully known. The EQQ interactions can be studied from the first principle, apart from

a small effect on Γ due to rotation-phonon coupling and dielectric shielding.³⁾ Secondly there exists a strong cubic anharmonicity, which makes one excitation splits two excitations. In this sense the excitations in solid hydrogen resemble more closely to phonons than to magnons.

The anharmonic effect on librions ($J=1$ excitations) was manifested in the Raman scattering experiments.⁹⁾ The Raman spectra, which correspond to $k=0$ libron, have four peaks, while the harmonic theory of librions gives only three peaks. Elliott¹⁰⁾ and Nakamura and Miyagi¹¹⁾ suggested that the extra line is due to two-libron excitations. However they were not able to give a reasonable mechanism.

Harris and his collaborators¹²⁾ have proposed a relevant mechanism which contains a strong cubic anharmonic processes in good agreement with experiments.⁹⁾ A strong anharmonic effect also exists in $J=3$ rotons. It is also the case for $J=2$ rotons in the presence of a parahydrogen (or a orthodeuterium) as the impurity.

It is the object to present the systematic study of the anharmonic effects on the elementary excitations in the ordered solid hydrogen. The treatment in this study is more general than the previous theory¹²⁾ even for libron itself.

References

- 1) W.N. Hardy, I.F. Silvera and J.P. McTague, Phys. Rev. B12 (1975), 753. Theoretical: K. Motizuki and T. Nagamiya, J. Phys. Soc. Japan 11 (1956), 93. K. Motizuki, J. Phys. Soc. Japan 17 (1962), 1192.
- 2) T. Nakamura, Prog. Theor. Phys. 14 (1955), 135.
- 3) A.B. Harris, Phys. Rev. B1 (1970), 1881. S. Luryi and J. Van Kranendonk, to be published.
- 4) A.F. Schuch, R.L. Mills, and D.A. Depatie, Phys. Rev. 165 (1968), 1032.
- 5) K.F. Mucker, P.M. Harris, D. White and R.A. Erickson, J. Chem. Phys. 49 (1968), 1922.
- 6) O. Nagai and T. Nakamura, Prog. Theor. Phys. 24 (1960), 432. [Errata: 30 (1963), 412].
- 7) H.M. James and J.C. Raich, Phys. Rev. 162 (1967), 649.
- 8) J. Felsteiner, Phys. Rev. Lett. 15 (1965), 1025.
- 9) W.N. Hardy, I.F. Silvera and J.P. McTague, Phys. Rev. Lett. 22 (1969), 297; 26 (1971), 127; Phys. Rev. B12 (1975), 753.
- 10) R.J. Elliott, Discussions Faraday Soc. 48 (1969), 7.
- 11) T. Nakamura and H. Miyagi, Prog. Theor. Phys. 44 (1970), 833 [Errata: 44 (1970), 1430].
- 12) C.F. Coll, III and A.B. Harris, Phys. Rev. B4 (1971), 2781.

Part II

Anharmonic Effect on Rotons in the Ordered Solid Hydrogen

In the ordered state of solid ortho- H_2 and para- D_2 the rotons ($J=3$ excitations) are studied in full details. It is shown that the rotons are strongly perturbed by the librons ($J=1$ excitations) through the anharmonic term splitting one roton into a pair of roton and libron. The relevant self-energy part is evaluated self-consistently with the results in satisfactory agreement with the Raman scattering data by Hardy, Silvera and McTague. The previous theory of libron by Coll and Harris is also reexamined, according to the present method.

§1. Introduction

A strong anharmonic effect has been recognized to exist on the librational excitation (libron¹⁾) in the ordered solid hydrogen, owing to the Raman experiments by Hardy et al.²⁾ In the long wavelength limit the harmonic approximation gives the libron modes of one E_g and two T_g with E_g as the lowest energy mode. The above result has been confirmed only by utilizing the angular dependence of the Raman scattering intensity on the single crystal,³⁾ which is sensitive to the mode symmetry.⁴⁾ However Harris and his collaborators⁵⁾ have shown that the libron energies are modified considerably by taking account of the anharmonic effect, in agreement with experiments.²⁾ Moreover the two-libron Raman spectrum comes out with due account of the same effect.⁶⁾ It is mentioned here that the earlier prediction of the two-libron spectrum based on the zero-point effect of librations gives a fairly small figure.⁴⁾

The relevant anharmonic term is cubic in boson operators. Thus the libron has a closer resemblance to phonon than to magnon. The cubic anharmonic term would be crucial in figuring the libron spectrum when a two-libron excitation band is in the vicinity of the top of the one-libron band. This is just what happens in the mentioned problem, resulting in a dramatic energy lowering of the upper T_g -mode.

Now the harmonic theory has proved much more miserable for

rotons ($J=3$ excitations) than for librations, comparing its results (7,8) with the Raman scattering measurements.^{2,9)} (J denotes the rotational quantum number). This is shown in Fig.1, where the roton energy is plotted as a function of the crystalline field parameter G . In the figure Γ is the coupling constant of the electric quadrupole-quadrupole (EQQ) interaction given by

$$\Gamma = 6e^2Q^2/25a^5 \quad (1.1)$$

with eQ the electric quadrupole moment and a the distance to nearest neighbors. By any adjustment of G the predicted spectra with sizable intensity, which are indicated by thick lines, cannot agree with the experimental ones. Moreover the observed higher spectrum is considerably broadened in contradistinction with the libration spectra.

The crystalline field effect is thought small in accordance with Kranendonk's roton ($J=2$ excitation in the pure para-hydrogen).¹⁰⁾ With neglect of the crystalline field the theoretical roton energy should be depressed considerably in comparison with the experiments. The depression comes from the anharmonic terms, making one roton split a pair of roton and libration. Thus a roton must drag librations through the crystal. This means that the molecular field subjected to a roton becomes less effective than the harmonic theory predicts. We note here that the energy depression is more considerable for the higher spectrum; a similar nature as seen in librations.

Now, in the ordered crystal (fcc¹¹) we have four sublattices of $J=1$ molecules, directing respectively along one of four body-diagonals; the lowest energy configuration of the EQQ interaction.^{12,13}) Thus 8 libron- and 28 roton-bands come out. These make our anharmonic problem much complicated. Basing our treatment on Dyson's equation we shall take a simplified procedure to get the frequency-dependent average self-energy, where the matrix element for the anharmonic part of the Hamiltonian is replaced by its average. The resulting self-consistent equation can be solved with the help of the density of states in the harmonic approximation. The average self-energy thus obtained is in turn used to get the $\bar{k}=0$ solution. In the scheme described above we shall treat both libron and roton in agreement with experiments.

We note here that a simple perturbational treatment of anharmonic terms using the density of states in the harmonic approximation brings us a poor improvement; an indication of strong anharmonic effect. We also note that the present method is different from the previous one.⁵⁾ The latter method is based on a frequency-dependent second-order effective Hamiltonian due to the anharmonic term, where the libron energy included in the energy denominator is approximated by its average over renormalized $\bar{k}=0$ modes, resulting in a self-consistent equation. It is mentioned here that the above method has no relevance to the roton case because of overlapping between one-roton and

roton-libron combination bands.

The basic Hamiltonian is described in §2 and our formalism in §3. In §4 the average self-energy shift due to anharmonic terms is obtained from a self-consistent equation. The $k=0$ modes are studied for both libron and roton in §5 and the Raman intensity in §6 where comparison of our theoretical results with experimental ones will be given.

§2. Basic Hamiltonian

In the ordered pure $J=1$ hydrogens the four sublattices will be labeled by $\alpha = A, B, C,$ and D as shown in Fig.2. The quantized axis for each sublattice is chosen to be parallel to one of four body-diagonals, along which the classical molecule orients. In the local coordinates system as described above we write down the EQQ interaction as

$$H = \sum_{j>l} \sum_{\mu, \nu} z_{\mu}(j) f_{\mu\nu}(j, l) z_{\nu}(l) , \quad (2.1)$$

following the notation in Ref. 4. In the above expression, $z_{\mu}(j)$ represents the μ -th quadrupole component at site j , corresponding to $\tilde{z}_{\mu}(j)$ in Ref. 4, as defined by

$$\begin{pmatrix} z_1 \\ z_5 \end{pmatrix} = \left(\frac{4\pi}{10}\right)^{1/2} \left[\begin{pmatrix} 1 \\ -1 \end{pmatrix} Y_{22}(\Omega) + \begin{pmatrix} 1 \\ 1 \end{pmatrix} Y_{2-2}(\Omega) \right] , \quad z_2 = \left(\frac{4\pi}{5}\right)^{1/2} Y_{20}(\Omega) ,$$

$$\begin{pmatrix} z_3 \\ z_4 \end{pmatrix} = \left(\frac{4\pi}{10}\right)^{1/2} \left[\begin{pmatrix} 1 \\ -1 \end{pmatrix} Y_{21}(\Omega) + \begin{pmatrix} 1 \\ 1 \end{pmatrix} Y_{2-1}(\Omega) \right] \quad (2.2)$$

in terms of the spherical harmonic function $Y_{\ell m}(\Omega)$ with Ω the orientational angle of the molecule. $f_{\mu\nu}(j, \ell)$ is a function of $R_{j\ell}$ with distance dependence $R_{j\ell}^{-5}$, including a factor $(eQ)^2$ with eQ the electric quadrupole moment of the molecule. The expression for $f_{\mu\nu}(j, \ell)$ has been given in the other place with the different notation $F_{\mu\nu}^*(j, \ell)$.¹⁴⁾

The roton is a collective excitation in the manifold of $|JM\rangle$ with $J=3$, while the libron is in the manifold of $|1M\rangle$. Confining M to be non-negative integer we shall represent the relevant states as follows.

$$\begin{Bmatrix} |JM^+\rangle \\ |JM^-\rangle \end{Bmatrix} = \frac{1}{\sqrt{2}} \left\{ \begin{pmatrix} 1 \\ -1 \end{pmatrix} (-1)^M Y_{JM}(\Omega) + \begin{pmatrix} 1 \\ 1 \end{pmatrix} Y_{J-M}(\Omega) \right\}, \quad M>0$$

$$|J0\rangle = Y_{J0}(\Omega) \quad (2.3)$$

In the approximate ground-state each molecule is in $|10\rangle \equiv |0\rangle$, where the only non-vanishing quadrupole component is z_2 with expectation value $\langle 0|z_2|0\rangle = 2/5$. In order to take account of the excited configurations collectively we shall use the following bosonic representation:¹⁵⁾

$$z_\mu = \sum_{m>n} \{ \langle m|z_\mu|n\rangle [a_m^\dagger (f-a_n) \delta_{n0} + a_m^\dagger a_n] + \text{h.c.} \}$$

$$+ \sum_m \{ \langle m | z_\mu | m \rangle - \langle 0 | z_\mu | 0 \rangle \} a_m^\dagger a_m + \langle 0 | z_\mu | 0 \rangle \quad (2.4)$$

where $|n\rangle$ stands for $|JM\rangle$. (The inclusion of a_0 , which must have no sense, is due to a formal simplicity.) The annihilation operator a_n and its hermitean conjugate a_n^\dagger are assumed to satisfy the bosonic commutation relation

$$[a_n, a_m^\dagger] = \delta_{nm} . \quad (2.5)$$

And $f = (1 - \sum_m a_m^\dagger a_m)^{1/2}$ is a factor which separates our functional space from the unphysical subspace with the number of occupied excited-states more than one.

Substituting Eq.(2.4) into Eq.(2.1), we have

$$H = H_0 + H_2 + H_3 + \dots \quad (2.6)$$

where H_0 is merely the ground-state energy in the approximate ground state as mentioned before, H_2 the quadratic part in bosonic operators and H_3 the cubic one. We introduce the Fourier transforms

$$a_{\alpha m}(\underline{k}) = \left(\frac{4}{N}\right)^{1/2} \sum_{j[\alpha]} \exp(-ik \cdot \underline{R}_{j[\alpha]}) a_{j[\alpha]m} ,$$

$$f_{\mu\nu}^{\alpha\beta}(\underline{k}) = \sum_{\ell[\beta]} f_{\mu\nu}(j[\alpha], \ell[\beta]) \exp\{ik \cdot (\underline{R}_{j[\alpha]} - \underline{R}_{\ell[\beta]})\} \quad (2.7)$$

where $j[\alpha]$ designates a lattice site belonging to the sublattice α and N is the number of molecules.

Using Eq.(2.7) we obtain

$$\begin{aligned}
 H_2 = & \sum_{\underline{k}} \left[\sum_{\alpha\beta} \sum_m \{ \langle m | z_2 | m \rangle - \langle 0 | z_2 | 0 \rangle \} \langle 0 | z_2 | 0 \rangle f_{22}^{\alpha\beta}(0) a_{\alpha m}^\dagger(\underline{k}) a_{\alpha m}(\underline{k}) \right. \\
 & + \frac{1}{2} \sum_{\alpha\beta} \sum_{\mu\nu} \sum_{mn} \langle m | z_\mu | 0 \rangle \langle n | z_\nu | 0 \rangle f_{\mu\nu}^{\alpha\beta}(-\underline{k}) \\
 & \cdot \{ a_{\alpha m}^\dagger(\underline{k}) + a_{\alpha m}(-\underline{k}) \} \{ a_{\beta n}^\dagger(-\underline{k}) + a_{\beta n}(\underline{k}) \} \\
 & \left. + \sum_{\alpha\beta} \sum_{m>n} \langle m | z_2 | n \rangle \langle 0 | z_2 | 0 \rangle f_{22}^{\alpha\beta}(0) \{ a_{\alpha m}^\dagger(\underline{k}) a_{\alpha n}(\underline{k}) + \text{h.c.} \} \right] , \quad (2.8)
 \end{aligned}$$

$$\begin{aligned}
 H_3 = & (4/N)^{1/2} \sum_{\underline{k}\underline{q}} \sum_{\alpha\beta} \sum_m \sum_{\mu\nu} \langle m | z_\mu | 0 \rangle \{ \sum_{m'>n} (\langle m' | z_\nu | n \rangle - \langle 0 | z_\nu | 0 \rangle \delta_{m'n}) \} \\
 & \cdot f_{\mu\nu}^{\alpha\beta}(-\underline{k}) \{ a_{\alpha m}^\dagger(\underline{k}) + a_{\alpha m}(-\underline{k}) \} \{ a_{\beta m'}^\dagger(\underline{q}) a_{\beta n}(\underline{k}+\underline{q}) + \text{h.c.} \} . \quad (2.9)
 \end{aligned}$$

In writing down the above expression we use

$$\sum_{\underline{l}} f_{\mu 2}(j, \underline{l}) = \sum_{\underline{l}} f_{22}(j, \underline{l}) \delta_{\mu, 2} , \quad (2.10)$$

which stands for the extremum condition satisfied by the classical ground-state configuration as noted in Ref. 4.

The relevant matrix components are expressed in terms of the 3j-symbol as follows.

$$\begin{aligned}
 \langle JM^S | \begin{pmatrix} z_1 \\ z_5 \end{pmatrix} | J'M'S' \rangle &= \begin{pmatrix} C_+(2) \\ -iC_-(2) \end{pmatrix} , & \langle JM^S | z_2 | J'M'S' \rangle &= \sqrt{2} C_+(0) , \\
 \langle JM^S | \begin{pmatrix} z_3 \\ z_4 \end{pmatrix} | J'M'S' \rangle &= \begin{pmatrix} iC_+(1) \\ -C_-(1) \end{pmatrix} . & & (2.11)
 \end{aligned}$$

In the above expression $M, M' \geq 0$ and we put

$$\begin{aligned} \begin{pmatrix} c_+(\mu) \\ c_-(\mu) \end{pmatrix} &= \frac{1}{2\sqrt{2}} [(2J+1)(2J'+1)]^{1/2} \begin{pmatrix} J & J' & 2 \\ 0 & 0 & 0 \end{pmatrix} e^{i(\sigma'-\sigma)\pi/4} \\ &\times \{ (-1)^M [i^{\sigma-\sigma'} \begin{pmatrix} + \\ - \end{pmatrix} (-1)^\mu] \begin{pmatrix} J & J' & 2 \\ M & -M' & \mu \end{pmatrix} \begin{pmatrix} + \\ - \end{pmatrix} \begin{pmatrix} J & J' & 2 \\ -M & M' & \mu \end{pmatrix} \} \\ &+ [i^{1-\sigma'} \begin{pmatrix} + \\ - \end{pmatrix} (-1)^\mu i^{\sigma-1}] \begin{pmatrix} J & J' & 2 \\ -M & -M' & \mu \end{pmatrix} \begin{pmatrix} + \\ - \end{pmatrix} \begin{pmatrix} J & J' & 2 \\ M & M' & \mu \end{pmatrix} \} \quad (2.12) \end{aligned}$$

where $\sigma = +1, -1$ for $s = +, -$ respectively. Expression (2.11) with Eq.(2.12) works when $M=0$ and/or $M'=0$ if one puts $\sigma=0$ and/or $\sigma'=0$ for relevant case.

We finally note that in our Hamiltonian (2.6) the terms of order Γ/B are neglected owing to a large rotational constant B . The inclusion of the mentioned terms gives rise to H_1 , standing for the single-molecule transition between $J=1$ and $J=3$.

§3. Formalism

Let us introduce the thermal Green's functions

$$\begin{aligned} G_{mm'}(k, \tau) &= - \langle T_\tau [a_m(k, \tau) a_m^\dagger(k, 0)] \rangle, \\ \hat{G}_{mm'}(k, \tau) &= - \langle T_\tau [a_m^\dagger(-k, \tau) a_m^\dagger(k, 0)] \rangle, \end{aligned} \quad (3.1)$$

following the current convention.¹⁶⁾ Here we designate (m, α) simply by m . And $a_m(k, \tau) = \exp(\tau H) a_m(k) \exp(-\tau H)$ with τ the

imaginary time. The Fourier transform of $G_{\underline{mm}}(k, \tau)$:

$$G_{\underline{mm}}(k, \omega_n) = \int_0^\beta e^{i\omega_n \tau} G_{\underline{mm}}(k, \tau) d\tau \quad (3.2)$$

is denoted simply by $G_{\underline{mm}}(p)$ with p the four dimensional momentum (k, ω) , where $\omega_n = 2\pi n/\beta$ and $\beta^{-1} = k_B T$.

Let us start with the following Dyson's equation¹⁶⁾

$$G(p) = G^0(p) + G^0(p)\Sigma_{11}(p)G(p) + G^0(p)\Sigma_{20}(p)\hat{G}(p), \quad (3.3)$$

$$\hat{G}(p) = G^0(-p)\Sigma_{11}(-p)\hat{G}(p) + G^0(-p)\Sigma_{02}(p)G(p) \quad (3.4)$$

in the matrix form, where the free-propagator matrix $G = (G_{\underline{mm}}^0)$ is chosen appropriately as described later. The self-energy matrices Σ_{11} , ..., Σ_{20} are defined in accord with Ref.16. As a formal solution of Eqs.(3.3) and (3.4) we obtain

$$G(p) =$$

$$[[G^0(p)]^{-1} - \Sigma_{11}(p) - \Sigma_{20}(p)\{[G^0(-p)]^{-1} - \Sigma_{11}(-p)\}^{-1}\Sigma_{02}(p)]^{-1}. \quad (3.5)$$

The excitation energies are given by the root of the equation

$$\text{Re det } |\check{G}^{-1}| = 0, \quad (3.6)$$

where a retarded Green's function $\check{G}(k, \epsilon)$ is obtained from $G(k, \omega)$ by replacing ω by $-i(\epsilon+i\delta)$ with $\delta=0^+$.

(a) Libron. Consider Eq.(2.8) in the $J=1$ manifold. The first term in H_2 is taken to be the unperturbed Hamiltonian

and hence

$$G_L^0(\omega) = (i\omega - \omega_0)^{-1} I, \quad (3.7)$$

with I the unit matrix, where

$$\omega_0 = -(6/25)f_2, \quad f_2 = \sum_{\alpha'} f_{22}^{\alpha\alpha'}(0). \quad (3.8)$$

The second term in H_2 gives us Σ_{11} , Σ_{02} and Σ_{20} in the same 8×8 matrix $\Sigma_L^{(2)}$, whose non-vanishing components are given by

$$(\Sigma_L^{(2)})_{\alpha m, \alpha' m'} = \sum_{\mu \mu'} \langle m | z_\mu | 0 \rangle \langle 0 | z_{\mu'} | m' \rangle f_{\mu \mu'}^{\alpha \alpha'}(\underline{k}). \quad (3.9)$$

Let $S^L(\underline{k})$ be the unitary transformation which diagonalizes $\Sigma_L^{(2)}$:

$$[(S^L)^{-1} \Sigma_L^{(2)} S^L]_{ii'} = \sigma_i(\underline{k}) \delta_{ii'}. \quad (3.10)$$

Here $\sigma_i(\underline{k})$ corresponds to $(3/25)\lambda_i(\underline{k})$ in Ref. 4. Then, in the harmonic approximation we have

$$[G^L(p)]_{ii'} = \frac{1}{i\omega - \omega_0 - \sigma_i(\underline{k}) + \sigma_i^2(\underline{k}) [i\omega + \omega_0 + \sigma_i(\underline{k})]^{-1}} \delta_{ii'} \quad (3.11)$$

whence the excitation energy $\omega_i(\underline{k})$ is obtained as

$$\omega_i(\underline{k}) = [\omega_0^2 + 2\omega_0 \sigma_i(\underline{k})]^{1/2}. \quad (3.12)$$

(b) Roton. Confine ourselves to the $J=3$ manifold. Then the third term in Eq.(3.3) is very small, because the kinetic energy of roton is much greater than the EQQ interaction. Neglecting Σ_{20} , we have simply

$$G^R(p) = [(G_R^0)^{-1} - \Sigma_{11}]^{-1} \quad (3.13)$$

in place of Eq.(3.7), where G_R^0 is taken to be

$$G_R^0(\omega) = (i\omega - \Omega_0)^{-1} I, \quad \Omega_0 = 10B. \quad (3.14)$$

Let $\Sigma_{11}^{(2)}$ be the self-energy part in the harmonic approximation whose $(\alpha M, \alpha' M')$ -component is then written down as

$$\begin{aligned} (\Sigma_{11}^{(2)})_{\alpha M, \alpha' M'} &= \{ \langle 3M | z_2 | 3M \rangle - \langle 10 | z_2 | 10 \rangle \} \langle 10 | z_2 | 10 \rangle f_2 \delta_{\alpha\alpha'} \delta_{MM'} \\ &+ \sum_{\mu\mu'} \langle 3M | z_\mu | 10 \rangle \langle 10 | z_{\mu'} | 3M' \rangle f_{\mu\mu'}^{\alpha\alpha'}(\underline{k}) \end{aligned} \quad (3.15)$$

with the help of Eq.(2.8). Let $S^R(\underline{k})$ be the unitary transformation which diagonalizes $\Sigma_{11}^{(2)}$:

$$[(S^R)^{-1} \Sigma_{11}^{(2)} S^R]_{ii'} = \Omega_i(\underline{k}) \delta_{ii'}. \quad (3.16)$$

Here $\Omega_i(\underline{k})$ stands for the roton energy shift in the harmonic approximation.

(c) Self-energy part due to the cubic terms is denoted by $\Sigma_{11}^{(3)}$. We shall take account of the diagrams illustrated in Fig.3 and hence neglect the interaction between two excitations in the intermediate states. Then the matrix components of $\Sigma_{11}^{(3)}$ for roton are written down as

$$\begin{aligned} [\Sigma_{11}^{(3)}(\underline{k}, \omega)]_{\alpha M, \alpha' M'} &= -\beta^{-1} \sum_{\underline{q}\omega'} \sum_{\alpha'' M''} \sum_{\alpha''' M'''} \sum_{\gamma m \gamma' m'} V_{\alpha M, [\alpha'' M'', \gamma m]}(\underline{k}, \underline{q}) \end{aligned}$$

$$\begin{aligned}
 & \cdot G_{\alpha M''}^R, \alpha M''(k-q, \omega-\omega') G_{\gamma m, \gamma' m'}^L(q, \omega') \\
 & \cdot V_{[\alpha M'', \gamma' m'], \alpha' M'}(-k, -q) \quad (3.17)
 \end{aligned}$$

with the help of Eq.(2.9), where m designates (11^\pm) and the non-vanishing components of V are given by

$$\begin{aligned}
 V_{\alpha M, [\alpha M', \alpha' m]}(k, q) &= \left(\frac{4}{N}\right)^{1/2} \sum_{\mu \mu'} \{ \langle 3M | z_\mu | 3M' \rangle - \langle 10 | z_\mu | 10 \rangle \delta_{MM'} \} \\
 & \cdot \langle 10 | z_{\mu'} | 1m \rangle f_{\mu \mu'}^{\alpha \alpha'}(q) \quad (3.18a)
 \end{aligned}$$

$$V_{\alpha M, [\alpha' M', \alpha m]}(k, q) = \left(\frac{4}{N}\right)^{1/2} \sum_{\mu \mu'} \langle 3M | z_\mu | 1m \rangle \langle 10 | z_{\mu'} | 3M' \rangle f_{\mu \mu'}^{\alpha \alpha'}(k-q) \quad (3.18b)$$

if $\alpha' \neq \alpha$, and

$$\begin{aligned}
 & V_{\alpha M, [\alpha M', \alpha m]}(k, q) \\
 &= \left(\frac{4}{N}\right)^{1/2} \sum_{\mu \mu'} [\{ \langle 3M | z_\mu | 3M' \rangle - \langle 10 | z_\mu | 10 \rangle \delta_{MM'} \} f_{\mu \mu'}^{\alpha \alpha'}(q) \\
 &+ \langle 3M | z_\mu | 1m \rangle \langle 10 | z_{\mu'} | 3M' \rangle f_{\mu \mu'}^{\alpha \alpha'}(k-q)] \quad (3.18c)
 \end{aligned}$$

For libron the matrix components for $\Sigma_{11}^{(3)}$, making one libron split into two librions, are given by Eq.(3.17) with replacement of M, \dots, M'' by n, \dots, n'' and of $G_{\dots}^R(k-q, \omega-\omega')$ by $G_{\dots}^L(k-q, \omega-\omega')$. With the same replacement, Eq.(3.18a) remains unaltered while $\langle 1n | z_\mu | 1m \rangle$ in Eq.(3.18b) is to be replaced by $\langle 1n | z_\mu | 1m \rangle - \langle 10 | z_\mu | 10 \rangle \delta_{nm}$. The same modification occurs for the last term

in Eq.(3.18c). These are also evident in Eq.(2.8).

§4. Self-consistent solution for $\langle \Sigma_{11}^{(3)} \rangle$

Only the diagonal component of $\Sigma_{11}^{(3)}$ will be considered in the representation diagonalizing $\Sigma_{11}^{(2)}$, where by $s_{\alpha M, i}^R(\underline{k})$ we denote a component of the transformation matrix $S^R(\underline{k})$ defined by Eq.(3.16) and by $s_{\alpha m, i}^L$ that for $S^L(\underline{k})$ defined by Eq.(3.10). In rewriting the diagonal component of Eq.(3.17): $[\Sigma_{11}^{(3)}]_{ii} \equiv \Sigma_i^R$ in the considered representation, we confine ourselves to the terms with $[\alpha^{\sim} M^{\sim}, \gamma^{\sim} m^{\sim}] = [\alpha^{\sim} M^{\sim}, \gamma m]$. Then

$$\begin{aligned} \Sigma_i^R(\underline{k}, \omega) = & -\beta^{-1} \sum_{\underline{q}, \omega'} \sum_{\alpha M \alpha' M'} \sum_{\alpha^{\sim} M^{\sim} \gamma m} s_{\alpha M, i}^{R*}(\underline{k}) s_{\alpha' M', i}^R(\underline{k}) \\ & \cdot V_{\alpha M, [\alpha^{\sim} M^{\sim}, \gamma m]}(\underline{k}, \underline{q}) V_{[\alpha^{\sim} M^{\sim}, \gamma m], \alpha' M'}(-\underline{k}, -\underline{q}) \\ & \cdot G_{\alpha^{\sim} M^{\sim}}^R(\underline{k}-\underline{q}, \omega-\omega') G_{\gamma m}^L(\underline{q}, \omega'). \end{aligned} \quad (4.1)$$

Here the diagonal components of G^R and G^L in the (αM) - or (αm) - representation:

$$G_{\alpha M}^R(\underline{k}, \omega) = \sum_i \frac{|s_{\alpha M, i}^R(\underline{k})|^2}{i \omega - \Omega_0 - \Omega_i(\underline{k}) - \Sigma_i^R(\underline{k}, \omega)} \quad (4.2)$$

$$G_{\alpha m}^L(\underline{k}, \omega) =$$

$$= \sum_i \frac{|s_{\alpha m, i}^L(\underline{k})|^2}{i \omega - \omega_0 - \sigma_i(\underline{k}) - \Sigma_i^L(\underline{k}, \omega) + \sigma_i^2(\underline{k}) [i\omega + \omega_0 + \sigma_i(\underline{k}) + \Sigma_i^L(-\underline{k}, -\omega)]^{-1}} \quad (4.3)$$

are evident in Eqs.(3.13) and (3.11) with the help of Eqs.(3.16) and (3.10) respectively. The expression for $\Sigma_i^L(\underline{k}, \omega)$ is written down similarly as

$$\begin{aligned} \Sigma_i^L(\underline{k}, \omega) = & -\beta^{-1} \sum_{\underline{q}, \omega'} \sum_{\alpha m \alpha' m'} \sum_{\alpha'' m'' \gamma n} s_{\alpha m, i}^{L*}(\underline{k}) s_{\alpha' m', i}^L(\underline{k}) \\ & \cdot V_{\alpha m, [\alpha'' m'', \gamma n]}(\underline{k}, \underline{q}) V_{[\alpha'' m'', \gamma n], \alpha' m'}(-\underline{k}, -\underline{q}) \\ & \cdot G_{\alpha'' m''}^L(\underline{k}-\underline{q}, \omega-\omega') G_{\gamma n}^L(\underline{q}, \omega') . \end{aligned} \quad (4.4)$$

(a) Average self-energy for libron. Let us first look into the libron case. In Eq.(4.4) we replace $\Sigma_i^L(\underline{k}, \omega)$ by its average over (\underline{k}, i) , $\Sigma^L(\omega)$. Namely we sum both sides of Eq.(4.4) over (\underline{k}, i) , being divided by $8 \cdot (N/4) = 2N$. With the help of the unitary property of S^L we have

$$\Sigma^L(\omega) = -\beta^{-1} \sum_{\omega'} \sum_{m' n} w_{m, [m' n]} G_{m'}^L(\omega-\omega') G_n^L(\omega') . \quad (4.5)$$

Here we replace $|V_{\alpha m, [\alpha' m', \gamma n]}(\underline{k}, \underline{q})|^2$ by its average over $(\underline{k}, \underline{q})$ and put

$$w_{m, [m' n]} = (N/4) \sum_{\alpha' \gamma} \langle |V_{\alpha m, [\alpha' m', \gamma n]}(\underline{k}, \underline{q})|^2 \rangle . \quad (4.6)$$

In Eq.(4.5) the Green's function averaged over \underline{k} : $G_m^L(\omega) = \langle G_{\alpha m}^L(\underline{k}, \omega) \rangle$ must be independent of $m = 1^\pm$. Hence Eq.(4.5) becomes

$$\Sigma^L(\omega) = -\beta^{-1} w \sum_{\omega'} G^L(\omega-\omega') G^L(\omega') , \quad (4.7)$$

where we drop the suffix in G_m^L and put similarly

$$w = \sum_{m'n} w_{m,[m'n]} . \quad (4.8)$$

Now Eq.(4.7) is combined with the average of Eq.(4.3) with replacement of $\Sigma_i^L(k, \omega)$ by $\Sigma^L(\omega)$. The combined result provides us a self-consistent equation in $\Sigma^L(\omega)$. Let us introduce the density of states $D(\sigma)$ by

$$D(\sigma) = \frac{1}{2N} \sum_{ki} \delta(\sigma - \sigma_i(k)) , \quad (4.9)$$

which is normalized to unity such that $\int D(\sigma) d\sigma = 1$. Then Eq.(4.3) with replacement of $\Sigma_i^L(k, \omega)$ by $\Sigma^L(\omega)$ reduces to

$$G^L(\omega) = \int \frac{D(\sigma) d\sigma}{i\omega - \omega_0 - \sigma - \Sigma^L(\omega) + \sigma^2 [i\omega + \omega_0 + \sigma + \Sigma^L(-\omega)]^{-1}} . \quad (4.10)$$

In Eq.(4.7) the sum over $\omega' = 2\pi n'/\beta$ (n' : integer) is replaced by a contour integral encircling the imaginary axis

$$\Sigma^L(\omega) = \frac{w}{2\pi i} \int \frac{dz}{e^{\beta z} - 1} G^L(\omega + iz) G^L(-iz) \quad (4.11)$$

We evaluate the integral by replacing the above contour by the two closed contours, where the one encircles the real axis and the other the straight line obtained by sifting the real axis by $i\omega$. Thus, noting $\omega = 2\pi n/\beta$, we have

$$\Sigma^L(\omega) = -\frac{w}{\pi} \int_{-\infty}^{\infty} d\varepsilon \coth \frac{\beta\varepsilon}{2} G^L(\omega+i\varepsilon) \text{Im} \tilde{G}^L(\varepsilon). \quad (4.12)$$

The self-consistent equation (4.12) can be solved by an iteration method. For instance, the first approximation to $\Sigma^L(\omega)$ is given by

$$\begin{aligned} \Sigma^L(\omega) = & \frac{w}{(4\omega_0)^2} \int D^L(\omega') \frac{d\omega'}{\omega'} \int D^L(\omega'') \frac{d\omega''}{\omega''} \\ & \times \left[\coth \frac{\beta\omega'}{2} \left\{ \frac{(\omega'+\omega_0)^2(\omega''+\omega_0)^2}{i\omega-\omega'-\omega''} - \frac{(\omega'-\omega_0)^2(\omega''-\omega_0)^2}{i\omega+\omega'+\omega''} \right\} \right. \\ & \left. + \left(\coth \frac{\beta\omega''}{2} - \coth \frac{\beta\omega'}{2} \right) \frac{(\omega'+\omega_0)^2(\omega''-\omega_0)^2}{i\omega-\omega'+\omega''} \right], \quad (4.13) \end{aligned}$$

whence the retarded function $\tilde{\Sigma}^L(\varepsilon) \equiv \Sigma^L(-i\varepsilon+\delta)$ immediately follows. In the above expression $D^L(\omega') = (\omega'/\omega_0)D(\omega')$ denotes the density of states for the free libron, as was given previously.¹⁷⁾ The self-consistent solution for $\tilde{\Sigma}^L(\varepsilon)$ at zero temperature is computed by the use of $w = 84.8\Gamma^2$, an estimate confined to the nearest-neighbor sum, and is shown in Fig.4. In the same figure is shown also $\tilde{\Sigma}^L(\varepsilon)$ in the molecular field approximation, where Eq.(4.10) is replaced by $G^L(\omega) = [i\omega - \omega_0 - \Sigma^L(\omega)]^{-1}$.

(b) Average self-energy for roton can be evaluated similarly as in (a). In the harmonic approximation, $|3M\rangle = |33^\pm\rangle$ is not

propagating through crystal with excitation energy independent of \underline{k} . Accordingly we shall introduce two kinds of average self-energies: Σ_0^R and $\Sigma_{M^*}^R$, where $\Sigma_{M^*}^R$ denotes the self-energy for the isolated band ($M^* = 3^\pm$) and Σ_0^R the average self-energy over the other roton-bands.

In the same approximation as in (a) we obtain

$$\begin{aligned}\Sigma_0^R(\omega) &= -\beta^{-1} \sum_{\omega'} \sum_M w_M G_M^R(\omega-\omega') G^L(\omega'), \\ \Sigma_{M^*}^R(\omega) &= -\beta^{-1} \sum_{\omega'} \sum_M w_{M^*M} G_M^R(\omega-\omega') G^L(\omega')\end{aligned}\quad (4.14)$$

from Eq.(4.1), where $G_M^R(\omega)$ is the average of Eq.(4.2) over \underline{k} : $G_M^R(\omega) = \langle G_{\alpha M}^R(\underline{k}, \omega) \rangle$, being independent of two states belonging to $M \neq 0$. In Eq.(4.14) we put

$$w_{MM'} = \sum_m w_{M, [M'm]}, \quad w_M = \frac{1}{5} \sum_{M' \neq M^*} w_{M'M} \quad (4.15)$$

Estimates of $w_{MM'}$ are given in Table I.

Let us introduce the effective density of states by

$$D_M^R(\Omega) = (4/N) \sum_{\underline{k}i} |s_{\alpha M, i}^R(\underline{k})|^2 \delta(\Omega_i(\underline{k}) - \Omega), \quad (4.16)$$

with the aid of Eq.(3.16). Then $G_M^R(\omega)$ may be given by

$$\begin{aligned}G_M^R(\omega) &= \int \frac{D_M^R(\Omega) d\Omega}{i\omega - \Omega_0 - \Omega - \Sigma_0^R(\omega)}, \quad (M \neq M^*) \\ G_{M^*}^R(\omega) &= [i\omega - \Omega_0 - \Omega_{M^*} - \Sigma_{M^*}^R(\omega)]^{-1},\end{aligned}\quad (4.17)$$

where Ω_{M^*} denotes $(\alpha M^*, \alpha M^*)$ -component of $\Sigma_{11}^{(2)}$ given by Eq. (3.15). The effective density of states $D_M^R(\Omega)$ in the harmonic approximation is computed with the result plotted in Fig.5.

In evaluating $\Sigma_0^R(E) \equiv \Sigma_0^R(-iE+\delta)$ and $\Sigma_{M^*}^R(E)$ at zero temperature we use

$$\Sigma_0^R(E) = -\frac{1}{\pi} \sum_M w_M \int_0^\infty d\varepsilon \Sigma_M^R(E-\varepsilon) \text{Im} \Sigma^L(\varepsilon), \quad (4.18)$$

and a similar expression for $\Sigma_{M^*}^R(E)$, which are derived from Eq.(4.14) with neglect of a very small contribution of $\text{Im} \Sigma^L(\varepsilon)$ in the negative region of ε . We solve numerically a set of equations (4.17) and (4.18), where $\Sigma^L(\varepsilon)$ is obtained from Eq. (4.10) with the help of the computed result for $\Sigma^L(\varepsilon)$. The average self-energies thus obtained are plotted in Fig.6.

§5. Excitation in the $\underline{k}=0$ limit

(a) For roton let us consider $\Sigma(\underline{k}, E)$ in the limit $\underline{k}=0$, which is responsible for the Raman spectrum. We shall first consider the harmonic term in $(G^R)^{-1}$. Following Ref.4 we introduce an orthogonal matrix $O = (o_{\Delta_i \alpha})$ by

$$O = \begin{array}{c|cccc} \Delta_i \alpha & A & B & C & D \\ \hline \Delta_0 & 1/2 & 1/2 & 1/2 & 1/2 \\ \Delta_1 & 1/2 & 1/2 & -1/2 & -1/2 \\ \Delta_2 & 1/2 & -1/2 & 1/2 & -1/2 \\ \Delta_3 & 1/2 & -1/2 & -1/2 & 1/2 \end{array} \quad (5.1)$$

Define also $\underline{0}$ by a direct product $0 \otimes I$ with I the 7×7 unit matrix. Then, with the use of $\Sigma_{11}^{(2)}$ given by Eq.(3.16)

$$\Sigma^{(2)} = \underline{0}^{-1} \Sigma_{11}^{(2)} \underline{0} \quad (5.2)$$

proves to be decomposed into fourteen matrices: nine 1×1 , two 2×2 and three 5×5 matrices. Here eight 1×1 matrices stand merely for the isolated modes with the same energy $\Omega_{M*} = 25.92$. Since the degeneracy is partially accidental, we shall below treat them according to the transformation property.

Of the sub-matrices the inequivalent ones are given numerically in Table II. One equivalent 2×2 matrix proves to be $S_2^{-1} \Sigma_2^{(2)} S_2$ referring to the transformed states $|\Delta_2, 32^-\rangle$ and $|\Delta_2, 31^-\rangle$ in order, where

$$S_2 = \begin{pmatrix} -1 & 0 \\ 0 & 1 \end{pmatrix}. \quad (5.3)$$

Two equivalent 7×7 matrices prove to be $S_3^{-1} \Sigma_3^{(2)} S_3$ and $S_3 \Sigma_3^{(2)} S_3^{-1}$ with S_3 given by

$$S_3 = \begin{pmatrix} X & Y & 0 & 0 & 0 & 0 & 0 \\ -Y & X & 0 & 0 & 0 & 0 & 0 \\ 0 & 0 & X & -Y & 0 & 0 & 0 \\ 0 & 0 & Y & X & 0 & 0 & 0 \\ 0 & 0 & 0 & 0 & X & Y & 0 \\ 0 & 0 & 0 & 0 & -Y & X & 0 \\ 0 & 0 & 0 & 0 & 0 & 0 & 1 \end{pmatrix}, \quad \begin{matrix} X \\ Y \end{matrix} = \begin{matrix} \cos \\ \sin \end{matrix} \left(\frac{2\pi}{3} \right) \quad (5.4)$$

where the transformed matrices refer to the basis $|\Delta_3, 33^+\rangle$, $|\Delta_1, 33^-\rangle$, $|\Delta_3, 32^+\rangle$, $|\Delta_1, 32^-\rangle$, $|\Delta_3, 31^+\rangle$, $|\Delta_1, 31^-\rangle$, $|\Delta_3, 30\rangle$ for the former and $|\Delta_1, 33^+\rangle$, $|\Delta_3, 33^-\rangle$, $|\Delta_1, 32^+\rangle$, $|\Delta_3, 32^-\rangle$, $|\Delta_1, 31^+\rangle$, $|\Delta_3, 31^-\rangle$, $|\Delta_1, 30\rangle$ for the latter, both in order. Since the equivalent matrices bring us the same eigenvalues, we have two doublets and seven triplets with respective symmetries of E_g and T_g . Thus the $\underline{k}=0$ rotons are decomposed as $3A_g + 2E_g + 7T_g$ according to the symmetry.

Let us next consider $\Sigma_{11}^{(3)}(\underline{k}, \omega)$, which is given by Eq.(3.17). Define the Fourier coefficient $w_{\alpha M, \alpha^{-M}}^{M''}(\underline{\rho})$ by

$$\begin{aligned} & (N/4) \sum_{\alpha'' \gamma m} V_{\alpha M, [\alpha'' M'', \gamma m]}^{(0, q)} V_{[\alpha'' M'', \gamma m], \alpha^{-M}}^{(0, -q)} \\ & = \sum_{\underline{\rho}} w_{\alpha M, \alpha^{-M}}^{M''}(\underline{\rho}) e^{-i \underline{q} \cdot \underline{\rho}} \end{aligned} \quad (5.5)$$

with $\underline{\rho}$ a sc lattice vector. Then $\chi_{11}^{(3)}(E) \equiv \Sigma_{11}^{(3)}(0, -iE + \delta)$ may be written down as

$$\begin{aligned} & [\chi_{11}^{(3)}(E)]_{\alpha M, \alpha^{-M}} \\ & = -\frac{1}{\pi} \sum_{M''} \sum_{\underline{\ell} \underline{\ell}'} w_{\alpha M, \alpha^{-M}}^{M''}(\underline{r}_{\underline{\ell}} - \underline{r}_{\underline{\ell}'}) \int_0^{\infty} \chi_{M''}^R(\underline{r}_{\underline{\ell}}, E - \epsilon) \text{Im} \chi_{\underline{\ell}'}^L(\underline{r}_{\underline{\ell}'}, \epsilon) d\epsilon \end{aligned} \quad (5.6)$$

with the help of Eq.(4.18) with modification, where we neglect non-diagonal components of the Green's function. In the above expression, $\chi_M^R(\underline{r}_{\underline{\ell}}, E)$ with sc lattice vector $\underline{r}_{\underline{\ell}}$ is the Fourier transform of $\chi_M^R(\underline{k}, E)$:

$$\tilde{G}_M^R(\underline{r}_\ell, E) = (4/N) \sum_{\underline{k}} \tilde{G}_{\alpha M}^R(K, E) e^{i\underline{k} \cdot \underline{r}_\ell} \quad (5.7)$$

and $\tilde{G}^L(\underline{r}_\ell, \epsilon)$ the similar one. We shall retain only the term with $\underline{r}_\ell = \underline{r}_\ell' = 0$ on the right-hand side of Eq.(5.6). Then the diagonal sum of the resultant equations, excluding $M=M^\#$, leads to Eq.(4.18). Note that $w_{\alpha M, \alpha M}^{M'}(0) = w_{MM}$.

In the $|\Delta_i M\rangle$ -scheme, Eq.(5.6) with $\underline{r}_\ell = \underline{r}_\ell' = 0$ turns out to be

$$\Sigma^{(3)}(E) = \underline{O}^{-1} \Sigma_{11}^{(3)}(E) \underline{O}. \quad (5.8)$$

The expression for $[\Sigma^{(3)}(E)]_{\Delta_i M, \Delta_i M'}$ is given by Eq.(5.6) if one substitutes

$$w_{\Delta_i M, \Delta_i M'}^{M''}(\underline{r}_\ell) = \sum_{\alpha \alpha'} \sigma_{\Delta_i \alpha} \sigma_{\Delta_i \alpha'} w_{\alpha M, \alpha' M'}^{M''}(\underline{r}_\ell), \quad \underline{r}_\ell = 0 \quad (5.9)$$

for $w_{\alpha M, \alpha' M'}^{M''}(0)$. In the decomposed form of a matrix $W(M'') = (w_{\Delta_i M, \Delta_i M'}^{M''}(0))$ we have three inequivalent matrices W_1, W_2 and W_3 . Here W_1 and W_3 prove to have similar forms to $\Sigma_1^{(2)}$ and $\Sigma_3^{(2)}$ respectively, while W_2 is a 4×4 matrix and given in Table III. Two equivalent matrices to W_3 are $S_3 W_3 S_3^{-1}$ and $S_3^{-1} W_3 S_3$.

Thus $[\tilde{G}^R(E)]^{-1}$ proves to be decomposed into

$$\begin{aligned} [\tilde{G}_\lambda^R(E)]^{-1} &= (E - \Omega_0) I_\lambda - \Sigma_\lambda^{(2)} - \Sigma_\lambda^{(3)}(E), \quad \lambda=1,3 \\ &= (E - \Omega_0) I_\lambda - \Sigma_\lambda^{(2)} - \Sigma_\lambda^{(3)}(E), \quad \lambda=2 \end{aligned} \quad (5.10)$$

and the equivalent ones, where I_λ is a unit matrix, $\Sigma_2^{(2)}$ a box-diagonal matrix composed of $\Sigma_2^{(2)}$ and $S_2^{-1} \Sigma_2^{(2)} S_2$, and

$$\Sigma_{\lambda}^{(3)}(E) = -\frac{1}{\pi} \sum_M W_{\lambda}(M) \int_0^{\infty} \tilde{G}_M^R(E-\epsilon) \text{Im} G^L(\epsilon) d\epsilon, \quad \lambda \neq 2 \quad (5.11)$$

and $\Sigma_2^{(3)}(E)$ with the corresponding expression. Here $[\tilde{G}_{\lambda}^R(E)]^{-1}$ for $\lambda=2$ has a similar form to W_2' shown in Table III. A matrix of that form may be brought to a semidiagonal form by applying a unitary transformation of the form

$$S_2' = \begin{pmatrix} \gamma & \delta & 0 & 0 \\ -\delta & \gamma & 0 & 0 \\ 0 & 0 & \gamma & -\delta \\ 0 & 0 & \delta & \gamma \end{pmatrix}, \quad (5.12)$$

whence two doublets of E_g -symmetry prove to be included in $[\tilde{G}_2^R(E)]^{-1}$. (See also Appendix A).

(b) For libron it is also worth while to examine the $k=0$ solutions, because accuracy of our roton solution largely depends upon that of libron one.

In the decomposition of $\Sigma_{11}^{(2)}$, we have two inequivalent matrices $\Sigma_2^{(2)}$ and $\Sigma_3^{(2)}$ in accord with the designations in (a), being given numerically in Table II. Two equivalent matrices to $\Sigma_3^{(2)}$ prove to be $S \Sigma_3^{(2)} S^{-1}$ and $S^{-1} \Sigma_3^{(2)} S$, referring respectively to $|\Delta_{3,11}^+\rangle$, $|\Delta_{1,11}^-\rangle$ and $|\Delta_{1,11}^+\rangle$, $|\Delta_{3,11}^-\rangle$, both in order. Here $S = \begin{pmatrix} X & -Y \\ Y & X \end{pmatrix}$ with X, Y given by Eq.(5.4).

The matrix W includes two inequivalent submatrices W_2 and W_3 whose respective similarities to $\Sigma_2^{(2)}$ and $\Sigma_3^{(2)}$ are complete,

as shown numerically in Table III. Two equivalent matrices to W_3 are SW_3S^{-1} and $S^{-1}W_3S$.

Thus $[\hat{G}^L(\epsilon)]^{-1}$ proves to be decomposed into

$$[\hat{G}_\lambda^L(\epsilon)]^{-1} = (\epsilon - \omega_0)I_\lambda - \Sigma_\lambda^{(2)} - \Sigma_\lambda^{(3)}(\epsilon) + \Sigma_\lambda^{(2)} [(\epsilon + \omega_0)I_\lambda + \Sigma_\lambda^{(2)} + \Sigma_\lambda^{(3)}(-\epsilon)]^{-1} \Sigma_\lambda^{(2)}, \quad \lambda=2,3 \quad (5.13)$$

and the equivalent ones, where

$$\Sigma_\lambda^{(3)}(\epsilon) \approx -\frac{1}{\pi} W_\lambda \int_0^\infty \hat{G}^L(\epsilon - \epsilon') \text{Im} \hat{G}^L(\epsilon') d\epsilon' . \quad (5.14)$$

In writing down Eq.(5.13) we use Eq.(3.5). Our Green's function is different from the previous one⁵⁾ only in the content of $\Sigma_\lambda^{(3)}(\epsilon)$.

§6. Raman intensities and comparison with experiments

By using the expressions given in Ref.4, the differential cross section of Raman scattering may be written as

$$I(\omega, \underline{n}) = \frac{\omega^4}{2\pi c^3} \left(\frac{2}{3}\right)^3 \sum_{\nu\nu'} \{ \underline{n}^{(1)} \times \underline{E} \}_\nu \{ \underline{n}^{(1)} \times \underline{E} \}_{\nu'} \Pi_{\nu\nu'}(\omega - \omega^0), \quad (6.1)$$

where \underline{E} denotes the electric field vector for the incident light with frequency ω^0 , $(\underline{n}^{(1)}, \underline{n}^{(2)})$ the unit polarization vectors for the scattered light with propagation direction $\underline{n} = \underline{n}^{(1)} \times \underline{n}^{(2)}$ and

with frequency ω , and $[\underline{n}^{(1)} \times \underline{E}]_{\nu}$ the ν -th component of the second-rank irreducible tensors constructed by $\underline{n}^{(1)}$ and \underline{E} , being in accord with Eq.(2.2). In the above expression we put

$$\Pi_{\nu\nu}(\omega) = (2\pi)^{-1} \int_{-\infty}^{\infty} \langle P_{\nu}(t) P_{\nu}(0) \rangle e^{-i\omega t} dt . \quad (6.2)$$

Here P_{ν} stands for the ν -th component of the orientation-dependent polarizability tensor of the system and is given by

$$P_{\nu} = \sum_{i,\mu} c_{\nu\mu}(\Delta_i) \chi_{\mu}(\Delta_i) \quad (6.3)$$

$$\chi_{\mu}(\Delta_i) = 2\Delta\chi \sum_{\alpha} o_{\Delta_i\alpha} z_{\mu\alpha} \quad (6.4)$$

with $(o_{\Delta_i\alpha})$ given by Eq.(5.1). In the above expressions, $\Delta\chi$ denotes the difference of parallel and perpendicular polarizabilities of a molecule, referring to the molecular axis, $z_{\mu\alpha}$ the sum of Eq.(2.4) over all sites belonging to a sublattice α , and the coefficients $c_{\nu\mu}(\Delta_i)$ can be obtained from Eq.(5.4) of Ref.4.

By retaining only the terms linear in boson operators, Eq.(6.4) may be written as

$$\chi_{\mu}(\Delta_i) \simeq \sqrt{N} \Delta\chi \sum_{n \neq 0} \langle n | z_{\mu} | 0 \rangle a_{\Delta_i n}^{\dagger} + \text{h.c.} , \quad (6.5)$$

$$a_{\Delta_i n}^{\dagger} = \sum_{\alpha} o_{\Delta_i\alpha} a_{\alpha n}^{\dagger} (k=0) , \quad (6.6)$$

where n designates a (JM^{\pm}) -state. Substituting Eq.(6.5) into Eq.(6.3), we get the relevant expression for P_{ν} to roton excitation as follows:

$$P_{\nu} = (\sqrt{21}/105)\sqrt{N} \Delta\chi(\pi_{\nu} + \pi_{\nu}^{\dagger}) . \quad (6.7)$$

Here we note only the following ones

$$\begin{aligned} \pi_2 &= \sqrt{15} a_{\Delta_0,32^+} - 4\sqrt{3} a_{\Delta_0,31^+} , \\ \pi_5 &= 2\sqrt{5} a_{\Delta_2,32^+} + 4a_{\Delta_2,31^+} + 3\sqrt{3} a_{\Delta_2,30} , \end{aligned} \quad (6.8)$$

being in accord with Table II. Of the omitted components, π_1 is obtained from a column vector made of the coefficients in π_2 , $(\sqrt{15}, -4\sqrt{3})$, by the transformation (5.3) and (π_3, π_4) similarly from that in π_5 by the transformation (5.4), where the transformed vectors stand respectively for the coefficients of the annihilation operators in accord with the new basic states described before (§5).

Owing to the symmetry mentioned above, one has

$$\Pi_{\nu\nu'}(\omega) = \Pi_{tg}(\omega)\delta_{\nu\nu'} , \quad \nu \text{ and/or } \nu' = 3, 4, 5 . \quad (6.9)$$

In the same approximation as Σ_{20} was neglected (§3 (b)), $\Pi_{tg}(\omega)$ is written as

$$\Pi_{tg}(\omega) \simeq -\frac{1}{525} N(\Delta\chi)^2 (e^{\beta\omega} - 1)^{-1} \frac{1}{\pi} \text{Im} [G_{tg}(\omega) - G_{tg}(-\omega)] , \quad (6.10)$$

where $G_{tg}(\omega)$ is the Fourier transform of a retarded Green's function

$$G_{tg}(t) = -i\theta(t) \langle [\pi_5(t), \pi_5^{\dagger}(0)] \rangle \quad (6.11)$$

with $\theta(t)$ the step function. Thus the right-hand side of Eq. (6.10) is evaluated by utilizing $\tilde{G}_3^R(E)$ given in Eq.(5.10):

$$G_{tg}(\omega) = 20[\tilde{G}_3^R(\omega)]_{\Delta_2^{2+}, \Delta_2^{2+}} + 8\sqrt{5}[\tilde{G}_3^R(\omega)]_{\Delta_2^{2+}, \Delta_2^{1+}} \dots$$

With $\Pi_{tg}(\omega)$ thus evaluated the T_g -part of $I(\omega, \underline{n})$ is given by

$$I_{tg}(\omega, \underline{n}) = \frac{2\omega^4}{3\pi c^3} F_{tg}(\underline{n}) \Pi_{tg}(\omega - \omega^0), \quad (6.12)$$

$$F_{tg}(\underline{n}) = 1/3 \cdot \sum_{i=1}^2 \sum_{v=3}^5 [\{ \underline{n}^{(i)} \times \underline{E} \}_v]^2. \quad (6.13)$$

For the E_g -part of $I(\omega, \underline{n})$ we have some complication due to the transformation (5.12) which is necessary for decomposing the Greenian matrix $\tilde{G}_2^R(E)$ given in Eq.(5.10). However it will be shown in Appendix A that in the considered part there should exist a similar factor to Eq.(6.13). Therefore one must have

$$I_{eg}(\omega, \underline{n}) = \frac{4\omega^4}{9\pi c^3} F_{eg}(\underline{n}) \Pi_{eg}(\omega - \omega^0), \quad (6.14)$$

$$F_{eg}(\underline{n}) = 1/2 \cdot \sum_{i=1}^2 \sum_{v=1}^2 [\{ \underline{n}^{(i)} \times \underline{E} \}_v]^2. \quad (6.15)$$

Here $\Pi_{eg}(\omega)$ is given by Eq.(6.10) with replacement of $G_{tg}(\omega)$ by $G_{eg}(\omega)$, which is the Fourier transform of

$$G_{eg}(t) = -i\theta(t) \langle [\pi_{eg}(t), \pi_{eg}^\dagger(0)] \rangle, \quad \pi_{eg} = \frac{\pi_1 + \pi_2}{\sqrt{2}}. \quad (6.16)$$

It is needless to say that $G_{eg}(\omega)$ is obtained from Eq.(5.10):

In Fig.7 we plot the differential cross sections computed separately for E_g and T_g , which is the average over two sets of pure E_g - and pure T_g - modes of the theoretical suppression formulas (Appendix B). Our result seems to be in satisfactory agreement with the experimental ones,⁹⁾ which are also shown in Fig.7.

As can be seen in the same figure we have considerable overlapping between E_g - and T_g - spectra. Hardy et al (HSM)⁹⁾ resolved the above two components of spectra by the following way. They set the incident light to be parallel to the [111]-axis of the crystal, which is chosen to be Z-axis, and observe the intensity of scattered light along X-axis. In the above arrangement they get four kinds of scattering data: [XY], [YY], [XZ] and [YZ], in which, for instance, [XY] stands for the intensity of scattered light with polarization parallel to the Y-axis in the case when the polarization of incident light is parallel to the X-axis. Thus HSM have observed for libron that either E_g or T_g is suppressed in certain linear combinations of [XY], [YY], ..., being applied to resolution of the roton spectra. The suppression formulas will be discussed in Appendix B.

In Table IV we recapitulate our theoretical results, including the Raman inactive modes. The omitted $\underline{k}=0$ modes with higher energy are so much broadened due to considerable increase of $\text{Im } \Sigma^R(E)$ in the relevant region (See Fig.6).

Let us finally look into the libron excitation. For this case

$$P_{\nu} = (\sqrt{6}/15)\sqrt{N}\Delta\chi(\pi_{\nu} + \pi_{\nu}^{\dagger}) \quad (6.17)$$

in place of Eq.(6.7), where one has

$$\pi_2 = -\sqrt{3} a_{\Delta_0, 11^+}, \quad \pi_5 = a_{\Delta_2, 11^+} \quad (6.18)$$

in place of Eq.(6.8). Thus $\Pi_{tg}(\omega)$ is written similarly as Eq. (6.10), in which $[G_{tg}(\omega) - G_{tg}(-\omega)]$ should be replaced by

$$[G_{tg}(\omega) + \hat{G}_{tg}(\omega) - G_{tg}(-\omega) - \hat{G}_{tg}(-\omega)] . \quad (6.19)$$

Here $\hat{G}_{tg}(\omega)$ is the Fourier transform of the retarded Green's function

$$\hat{G}_{tg}(t) = -i\theta(t)\langle[\pi_5^{\dagger}(t), \pi_5^{\dagger}(0)]\rangle . \quad (6.20)$$

With the help of Eq.(3.4) in the retarded form, we get

$$G_{tg}(\omega) + \hat{G}_{tg}(\omega) = \left\{ [1 - [(\omega + \omega_0)I_3 + \Sigma_3^{(2)} + \Sigma_3^{(3)}(-\omega)]^{-1} \Sigma_3^{(2)}] \cdot G_3^L(\omega) \right\}_{\Delta_2 1^+, \Delta_2 1^+} \quad (6.21)$$

in accord with Eq.(5.13). The corresponding expression for E_g may be omitted.

The computed results are shown in Table V. For the excitation energies the results by Coll and Harris (CH)⁵⁾ is somewhat closer to the experiments than ours, while for the Raman intensities the situations are reversed. CH obtained a larger

energy depression of $T_g^{(2)}$ where their self-consistent equation is confined to the $k=0$ manifold, resulting from a simple pole approximation to the self-energy part.

Throughout the present part we have neglected contributions of the order Γ/B . They are not negligibly small for each contribution and hence have been somewhat controversial.^{8,9,18)} However the net effect is shown to be small as a result of cancellation. The result is given in part IV.

Appendix A

In the transformation S_2' given by Eq.(5.12), γ and δ are chosen so that the matrix $[\tilde{G}_2^R(E)]^{-1}$ may be transformed as

$$\begin{bmatrix} a & -c & 0 & d \\ -c & b & d & 0 \\ 0 & d & a & c \\ d & 0 & c & b \end{bmatrix} \longrightarrow \begin{bmatrix} \epsilon & 0 & b & d \\ 0 & \epsilon' & d & 0 \\ 0 & d & \epsilon & 0 \\ d & 0 & 0 & \epsilon' \end{bmatrix}. \quad (\text{A.1})$$

Accordingly, we shall introduce the following operators

$$\begin{aligned} a_{1+} &= \gamma a_{\Delta_0, 32+} + \delta a_{\Delta_0, 31+}, & a_{2+} &= \delta a_{\Delta_2, 32-} + \delta a_{\Delta_2, 31-}, \\ a_{1-} &= \gamma a_{\Delta_2, 32-} - \delta a_{\Delta_2, 31-}, & a_{2-} &= -\delta a_{\Delta_0, 32+} + \gamma a_{\Delta_0, 31+}. \end{aligned} \quad (\text{A.2})$$

Note that the sub-matrix of \tilde{G}_2^R referring to $\{|1-\rangle, |2-\rangle\}$ must be equivalent to that referring to $\{|1+\rangle, |2+\rangle\}$.

Consider an operator $Q = \pi_1 u_1 + \pi_2 u_2$ with π_ν defined by Eq.(6.8) and with $u_\nu = \{n^{(1)} \times E\}_\nu$. Then we have

$$\begin{aligned} Q &= (\sqrt{15}\gamma - 4\sqrt{3}\delta)u_2 a_{1+} - (\sqrt{15}\delta + 4\sqrt{3}\gamma)u_1 a_{2+} \\ &\quad - (\sqrt{15}\gamma - 4\sqrt{3}\delta)u_1 a_{1-} - (\sqrt{15}\delta + 4\sqrt{3}\gamma)u_2 a_{2-} \end{aligned} \quad (\text{A.3})$$

with the help of Eq.(A.2). We shall now introduce $G(A,B)$ by $G(A,B) = -i\theta(t)\langle[A(t), B(0)]\rangle$. Then

$$\begin{aligned}
& G(Q, Q^\dagger) \\
&= (\sqrt{15}\gamma - 4\sqrt{3}\delta)^2 u_2^2 G(a_{1+}, a_{1+}^\dagger) + (\sqrt{15}\delta + 4\sqrt{3}\gamma)^2 u_1^2 G(a_{2+}, a_{2+}^\dagger) \\
&- (\sqrt{15}\gamma - 4\sqrt{3}\delta)(\sqrt{15}\delta + 4\sqrt{3}\gamma) u_1 u_2 \cdot \{G(a_{1+}, a_{2+}^\dagger) + G(a_{2+}, a_{1+}^\dagger)\} \\
&+ \dots, \tag{A.4}
\end{aligned}$$

where the omitted terms belonging to the subspace $\{|1-\rangle, |2-\rangle\}$ can easily be seen from Eq.(A.3).

Owing to the equivalent form of sub-matrices we may put

$$G(a_{n+}, a_{n+}^\dagger) = G(a_{n-}, a_{n-}^\dagger), \quad n, n = 1, 2, \tag{A.5}$$

which tells us the third term in Eq.(A.4) to be cancelled by the corresponding term in the other subspace. In this way $G(Q, Q^\dagger)$ proves to include $u_1^2 + u_2^2$ as a factor.

Appendix B

According to the frame of HSM's scattering experiment described in §6, we may put $\theta = \arccos(1/\sqrt{3})$, $\psi = 3\pi/4$ in the expressions for $\{n^{(1)} \times E\}_v \equiv u_v^{(1)}$, which were given in §6 of Ref. 4.^{†)} Here (ϕ, θ, ψ) denote the Euler angles, by which the crystal fixed frame referred to the cubic axes is specified in the laboratory-fixed frame. Thus we get

$$\begin{bmatrix} u_1^{(1)} \\ u_2^{(1)} \end{bmatrix} = -\frac{1}{\sqrt{2}} \begin{bmatrix} -\sin \phi & \cos \phi \\ \cos \phi & \sin \phi \end{bmatrix} \begin{bmatrix} E_1 \\ E_2 \end{bmatrix}, \quad (\text{B.1})$$

$$\begin{bmatrix} u_1^{(2)} \\ u_2^{(2)} \end{bmatrix} = -\frac{1}{2} \begin{bmatrix} \cos 2\phi & \sin 2\phi \\ -\sin 2\phi & \cos 2\phi \end{bmatrix} \begin{bmatrix} E_1 \\ E_2 \end{bmatrix} \quad (\text{B.2})$$

for the E_g -components and

$$\begin{bmatrix} u_3^{(1)} \\ u_4^{(1)} \\ u_5^{(1)} \end{bmatrix} = \frac{1}{\sqrt{6}} \begin{bmatrix} \cos(\phi+\alpha) & \sin(\phi+\alpha) \\ \cos(\phi+2\alpha) & \sin(\phi+2\alpha) \\ \cos \phi & \sin \phi \end{bmatrix} \begin{bmatrix} E_1 \\ E_2 \end{bmatrix}, \quad (\text{B.3})$$

$$\begin{bmatrix} u_3^{(2)} \\ u_4^{(2)} \\ u_5^{(2)} \end{bmatrix} = -\frac{1}{2\sqrt{3}} \begin{bmatrix} -2 \sin 2(\phi+\alpha) & 1+2 \cos 2(\phi+\alpha) \\ -2 \sin (2\phi+\alpha) & 1+2 \cos (2\phi+\alpha) \\ -2 \sin 2\phi & 1+2 \cos 2\phi \end{bmatrix} \begin{bmatrix} E_1 \\ E_2 \end{bmatrix} \quad (\text{B.4})$$

for the T_g -components, where $\alpha = 2\pi/3$.

In the above expressions, the electric field vector associated with the incident light is defined by $(E_1, E_2, 0)$ and the polarization vectors associated with the scattered light respectively by $n^{(1)} = (0, 0, -1)$ and $n^{(2)} = (0, 1, 0)$, all referring to the laboratory frame (XYZ). Keeping these in mind, one easily evaluates $F_{eg}(n)$ defined by Eq.(6.15) to be $1/8, 1/8, 1/4, 1/4$ respectively for [XY], [YY], [XZ], [YZ],

assuming $E = (1,0,0)$ or $= (0,-1,0)$. In evaluating $F_{tg}(n)$ defined by Eq.(6.12) we notice $\sum_{m=0}^2 \exp(im\alpha) = 0$; $F_{tg}(n) = 1/6, 1/4, 1/12, 1/12$ respectively for $[XY], [YY], [XZ], [YZ]$.

Therefore $[XY] - \frac{1}{2}[XZ], [YY] - \frac{1}{2}[YZ]$ suppress E_g while $[XZ] - \frac{1}{2}[XY], [YZ] - \frac{1}{3}[YY]$ suppress T_g . The corresponding experimental results are $[XY] - 0.53[XZ], [YY] - 0.57[YZ]$ for the suppression of E_g and $[XZ] - 0.60[XY], [YZ] - 0.45[YY]$ for that of T_g .⁹⁾

References

- 1) S. Homma, K. Okada and H. Matsuda, Prog. Theor. Phys. 38 (1967), 767 [Errata: 45 (1971), 330].
F.G. Mertens, W. Biem and H. Hahn, Z. Phys. 213 (1968), 33.
H. Ueyama and T. Matsubara, Prog. Theor. Phys. 38 (1967), 784.
J.C. Raich and R.D. Ethers, Phys. Rev. 168 (1968), 425.
- 2) W.N. Hardy, I.F. Silvera and J.P. McTague, Phys. Rev. Letters 22 (1969), 297.
- 3) W.N. Hardy, I.F. Silvera and J.P. McTague, Phys. Rev. Letters 26 (1971), 127.
- 4) T. Nakamura and H. Miyagi, Prog. Theor. Phys. 44 (1970), 833. [Errata: 44 (1970), 1430].
- 5) C.F. Coll, III, A.B. Harris and A.J. Berlinsky, Phys. Rev. Letters 25 (1970), 858.
C.F. Coll, III and A.B. Harris, Phys. Rev. B4 (1971), 2781.
- 6) A.J. Berlinsky and A.B. Harris, Phys. Rev. B4 (1971), 2808.
A.J. Berlinsky, Ph. D. thesis (University of Pennsylvania, 1972).
- 7) R.J. Lee, J.C. Raich and R.D. Ethers, J. Low Temp. Phys. 2 (1970), 255.
- 8) T. Nakamura, H. Miyagi and M. Fujio, in Proceedings of the Twelfth International Conference of Low Temperature Physics, edited by Eizo Kanda (Academic of Japan, Kyoto, 1970).
- 9) W.N. Hardy, I.F. Silvera and J.P. McTague, Phys. Rev. B12

- (1975), 753.
- 10) J. Van Kranendonk and G. Karl, Rev. Mod. Phys. 40 (1968), 531.
 - 11) A.F. Schuch, R.L. Mills and D.A. Depatie, Phys. Rev. 165 (1968), 1032.
 - 12) O. Nagai and T. Nakamura, Prog. Theor. Phys. 24 (1960), 432.
[Errata: 30 (1963), 412].
 - 13) J. Felsteiner, Phys. Rev. Letters 15 (1965), 1025.
 - 14) H. Miyagi and T. Nakamura, Prog. Theor. Phys. 37 (1967), 641.
 - 15) L. Biegala, Phys. Letters 56A (1976), 125.
 - 16) A.A. Abrikosov, L.P. Gorkov and I.E. Dzyaloshinski,
Methods of Quantum Field Theory in Statistical Physics,
(Dover, New York 1969).
 - 17) A.J. Berlinsky and C.F. Coll, III, Phys. Rev. B5 (1972), 1587.
 - 18) A.B. Harris, A.J. Berlinsky and H. Meyer, Phys. Rev. B7 (1973), 4720.

Table I Numerical values of $w_{MM'}$ a)

| M \ M' | 0 | 1 ⁺ | 1 ⁻ | 2 ⁺ | 2 ⁻ | 3 ⁺ | 3 ⁻ |
|----------------|------|----------------|----------------|----------------|----------------|----------------|----------------|
| 0 | 9.7 | 6.7 | 6.7 | 22.7 | 22.7 | 0 | 0 |
| 1 ⁺ | 11.3 | 19.3 | 21.6 | 10.5 | 11.1 | 4.0 | 4.0 |
| 1 ⁻ | 11.3 | 21.6 | 19.3 | 11.1 | 10.5 | 4.0 | 4.0 |
| 2 ⁺ | 28.7 | 13.0 | 13.0 | 29.5 | 11.1 | 5.5 | 5.5 |
| 2 ⁻ | 28.7 | 13.0 | 13.0 | 11.1 | 29.5 | 5.5 | 5.5 |
| 3 ⁺ | 31.6 | 30.6 | 30.6 | 12.6 | 12.6 | 61.9 | 0 |
| 3 ⁻ | 31.6 | 30.6 | 30.6 | 12.6 | 12.6 | 0 | 61.9 |

a) Estimates up to the nearest neighbors are given in units of Γ^2 .

Table II Inequivalent matrices for $\Sigma_{11}^{(2)}$ in the $|\Delta_i, M\rangle$ scheme and in the $\underline{k}=0$ limit. a)

A) Roton^{b)}

$$\Sigma_1^{(2)}: \begin{matrix} |\Delta_0, 33^+\rangle & |\Delta_2, 33^-\rangle & |\Delta_0, 30\rangle \\ \left[\begin{array}{ccc} 25.92 & 0 & 0 \\ 0 & 25.92 & 0 \\ 0 & 0 & -8.92 \end{array} \right] \end{matrix}, \quad \Sigma_2^{(2)}: \begin{matrix} |\Delta_0, 32^+\rangle & |\Delta_0, 31^+\rangle \\ \left[\begin{array}{cc} 8.14 & -2.82 \\ -2.82 & -0.01 \end{array} \right] \end{matrix},$$

$\Sigma_3^{(2)}$:

$$\begin{matrix} |\Delta_2, 33^+\rangle & |\Delta_0, 33^-\rangle & |\Delta_2, 32^+\rangle & |\Delta_0, 32^-\rangle & |\Delta_2, 31^+\rangle & |\Delta_0, 31^-\rangle & |\Delta_2, 30\rangle \\ \left[\begin{array}{ccccccc} 25.92 & 0 & 0 & 0 & 0 & 0 & 0 \\ 0 & 25.92 & 0 & 0 & 0 & 0 & 0 \\ 0 & 0 & 14.63 & 0.85 & 2.14 & -7.61 & 0.33 \\ 0 & 0 & 0.85 & 17.30 & 7.61 & 3.38 & -7.91 \\ 0 & 0 & 2.14 & 7.61 & 5.94 & 5.44 & 0.29 \\ 0 & 0 & -7.61 & 3.38 & 5.44 & 15.15 & 7.07 \\ 0 & 0 & 0.33 & -7.91 & 0.29 & 7.07 & 7.37 \end{array} \right] \end{matrix}$$

B) Libron^{b)}

$$\Sigma_2^{(2)}: \begin{matrix} |\Delta_0, 11^+\rangle \\ (-6.20) \end{matrix}, \quad \Sigma_3^{(2)}: \begin{matrix} |\Delta_2, 11^+\rangle & |\Delta_0, 11^-\rangle \\ \left[\begin{array}{cc} -0.99 & 4.76 \\ 4.76 & 7.07 \end{array} \right] \end{matrix},$$

a) Estimates with lattice summation over all neighbors are given in units of Γ .

b) $\Sigma_1^{(2)}$, $\Sigma_2^{(2)}$, $\Sigma_3^{(2)}$ refer to the A_g , E_g and T_g -manifolds respectively.

Table III Inequivalent sub-matrices of $W(M)$ ^{a)}

(A) Roton^{b),c)}

$$W_2'(M) = \begin{matrix} & |\Delta_0, 32^+\rangle & |\Delta_0, 31^+\rangle & |\Delta_2, 32^-\rangle & |\Delta_2, 31^-\rangle \\ \left[\begin{array}{cccc} a(M) & -c(M) & 0 & d(M) \\ -c(M) & b(M) & d(M) & 0 \\ 0 & d(M) & a(M) & c(M) \\ d(M) & 0 & c(M) & b(M) \end{array} \right] \end{matrix}$$

with

| M | a(M) | b(M) | c(M) | d(M) |
|---|-------|-------|------|-------|
| 0 | 8.65 | 15.56 | 1.74 | -2.18 |
| 1 | 31.79 | 55.14 | 1.36 | 0.20 |
| 2 | 20.45 | 13.79 | 3.39 | 4.58 |
| 3 | 11.03 | 8.03 | 0 | 0 |

(B) Libron^{c)}

$$W_2 = (5.47) \quad \begin{matrix} |\Delta_0, 11^+\rangle & & |\Delta_2, 11^+\rangle & |\Delta_0, 11^-\rangle \\ & & \left[\begin{array}{cc} 5.84 & -0.11 \\ -0.11 & 13.67 \end{array} \right] \end{matrix}$$

a) $W(M)$ is defined by $W(M) = \sum_{s=\pm} W(M^s)$.

b) $W_1(M)$ and $W_3(M)$ are omitted.

c) Estimates based on the nearest neighbor approximation (unit: Γ^2).

Table IV The $k=0$ roton spectrum and Raman intensity.

| Mode | Energy shift ^{a)} (unit: Γ) | | | Raman intensity ^{b)} | | |
|-------------|--|---------|----------------------|-------------------------------|---------|----------------------|
| | H.A. ^{c)} | Present | Exp. ^{d,e)} | H.A. ^{c)} | Present | Exp. ^{d)} |
| $A_g^{(1)}$ | -8.92 | -11.7 | | 0 | 0 | 0 |
| $E_g^{(1)}$ | -0.89 | -4.1 | -4.74 | 1.00 | 1.00 | 1.00 |
| $T_g^{(1)}$ | -1.92 | -3.8 | (-4.09) | 0.35 | 0.28 | (0.74) ^{f)} |
| $T_g^{(2)}$ | 0.10 | -3.0 | (-4.09) | 0.14 | 0.16 | (0.74) ^{f)} |
| $E_g^{(2)}$ | 9.02 | 4.4 | 3.12 | 1.12 | 1.15 | 0.92 |
| $T_g^{(3)}$ | 13.12 | 5.8 | 4.45 | 2.70 | 2.74 | 3.70 |

- a) The energy shift relatively to the free roton value $\Omega_0=10B$.
- b) The intensities for a powder sample are normalized to that of $E_g^{(1)}$.
- c) Ref.8 based on the harmonic approximation.
- d) HSM's data for p-D₂ with 98% J=1 molecules (Ref.9). The values in parenthesis are not resolved.
- e) The energy shifts relatively to the disordered state are scaled by $\Gamma=0.802 \text{ cm}^{-1}$ after Ref.9.
- f) The resultant value of $T_g^{(1)}$ and $T_g^{(2)}$ based on a numerical interaction of HSM's experimental curve is converted into the powder value.

Table V The $k=0$ libron spectrum and Raman intensity.

| Mode | Energy ^{a)} (unit: Γ) | | | Raman intensity ^{b)} | | |
|-------------|--|--------------------|--------------------|-------------------------------|---------|--------------------|
| | CH ^{c)} | Present | Exp. ^{d)} | CH ^{c)} | Present | Exp. ^{d)} |
| E_g | 11.29 | 11.4 | 11.3 | 1.000 | 1.00 | 1.00 |
| $T_g^{(1)}$ | 14.07 | 14.2 | 14.0 | 0.211 | 0.25 | 0.26 |
| $T_g^{(2)}$ | 19.55 | 20.8 | 19.1 | 0.080 | 0.07 | 0.06 |
| two-libron | 28.2 ^{e),f)} | 35.5 ^{f)} | 31.1 ^{f)} | 0.25 | 0.21 | 0.18 |

a) The energy values in the harmonic approximation are 13.68, 17.73, 29.04 (Ref.4).

b) The intensities are normalized to that of E_g .

c) Coll and Harris (Ref.5).

d) HSM's data for p-D₂ (Ref.9), where the energies extrapolated to 100% p-D₂ are scaled by $\Gamma=0.81 \text{ cm}^{-1}$.

e) The value evaluated from Berlinsky's result (Ref.6).

f) The mean positions of the energy spectra are given. The peak positions are 25.8 Γ and 26.8 Γ respectively for Berlinsky and HSM while our peak is located at 35 Γ with broader width.

Figure Captions

Fig.1. Energy diagram of the $k=0$ rotors as a function of G/Γ . The roton energies in the harmonic approximation (Ref.8) are compared with the Raman feature of $p\text{-D}_2$ observed by HSM (Ref.9). The crystalline field energy V_c is defined by $V_c = -(2/9)(4\pi)^{1/2}G[Y_{40}(\Omega) + (10/7)^{1/2}\{-Y_{43}(\Omega) + Y_{4-3}(\Omega)\}]$. Only the modes shown by thick lines have sizable Raman intensity.

Fig.2. Designation of the sublattices.

Fig.3. Diagrammatic representation of $\Sigma_{11}^{(3)}$. The wavy lines represent the EQQ interaction.

Fig.4. Curves for $\tilde{\Sigma}^L(\epsilon)$ vs. ϵ/Γ . Here $\tilde{\Sigma}^L(\epsilon)$ is plotted in units of Γ and the broken line shows $\text{Re } \tilde{\Sigma}^L(\epsilon)$ in the molecular field approximation. The density of states $D^L(\epsilon)$ in the harmonic approximation are also shown in the same energy scale, whereas the corresponding ordinate is taken arbitrarily.

Fig.5. Effective density of states $D_M^R(\Omega)$ in the harmonic approximation. Here $D_M^R(\Omega) \equiv D_{Ms}^R(\Omega)$ with $s=\pm$.

Fig.6. Curves for $\tilde{\Sigma}_0^R(E)$ vs. $(E-\Omega_0)/\Gamma$ and for $\tilde{\Sigma}_{M^*}^R(E)$ vs. $(E-\Omega_0)/\Gamma$. The both self-energies are in units of Γ .

Fig.7. Raman features for E_g - and T_g - modes. The intensities are in arbitrarily units. The theoretical curves are obtained with account of the experimental resolution width 1.25 cm^{-1} , where $\Gamma = 0.802 \text{ cm}^{-1}$ and $\Omega_0 = 298.75 \text{ cm}^{-1}$ are assumed in accord with the experiments on $p\text{-D}_2$ by HSM (Ref.9).

FIG.1

Exp.

Theor.

P-D₂ (98.8%)

T=1.16K

POLARIZATION:

XY+ XZ

$\Gamma=0.80\text{ CM}^{-1}$

$\Omega_0=298.75\text{ CM}^{-1}$

a: T_g⁽⁷⁾

b: A_g⁽³⁾

c: A_g⁽²⁾+T_g⁽⁶⁾

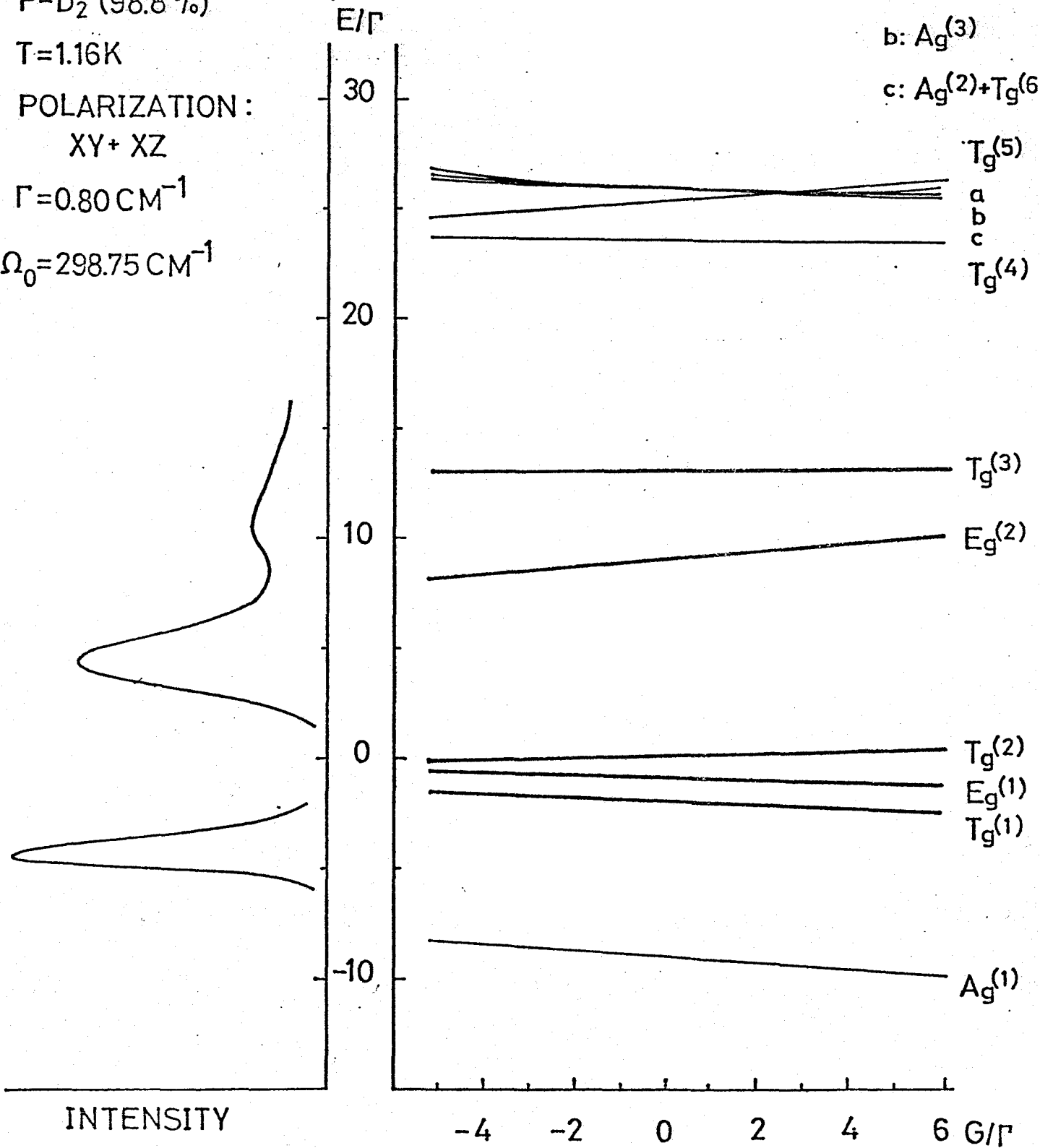


FIG.2

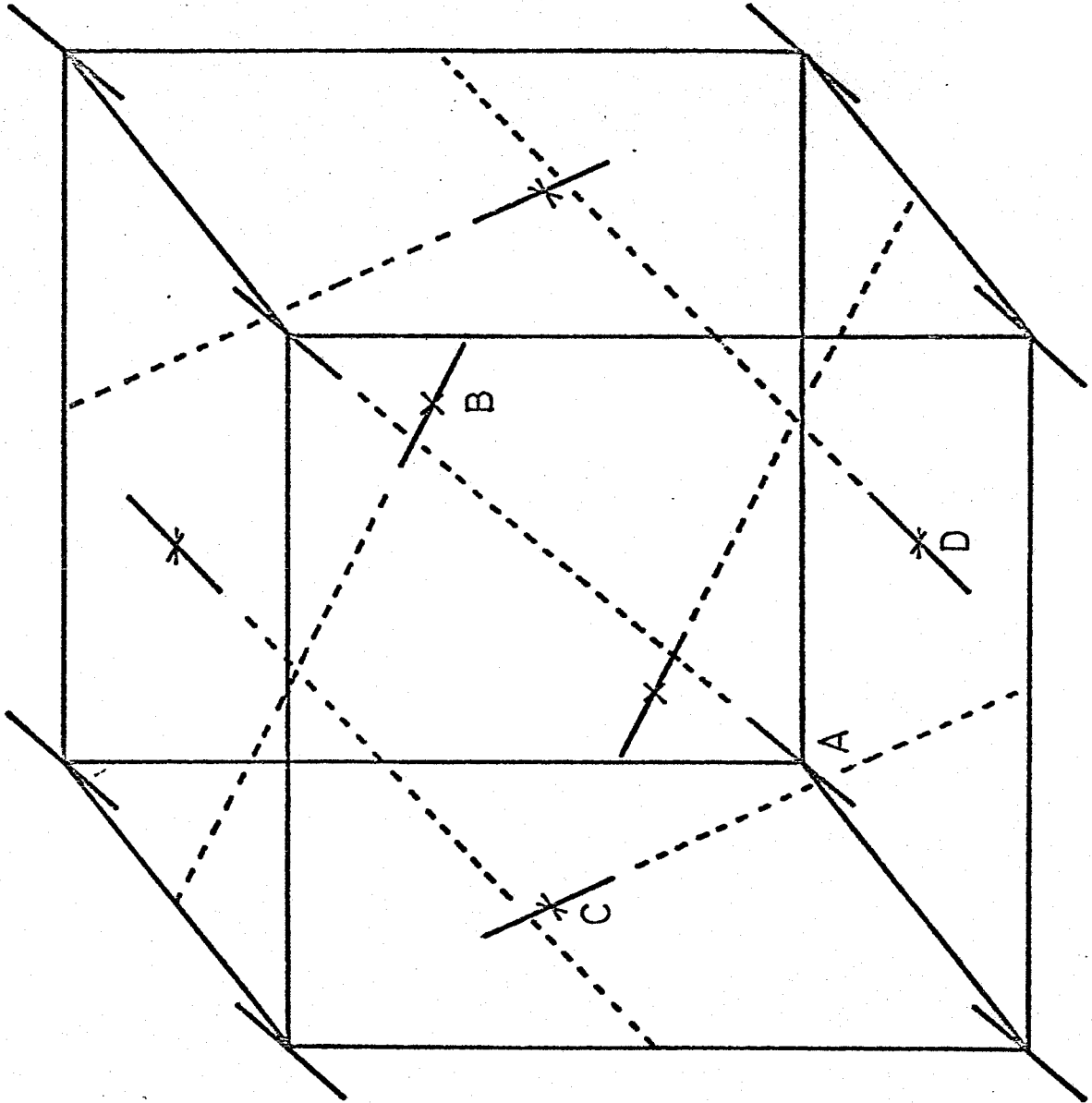
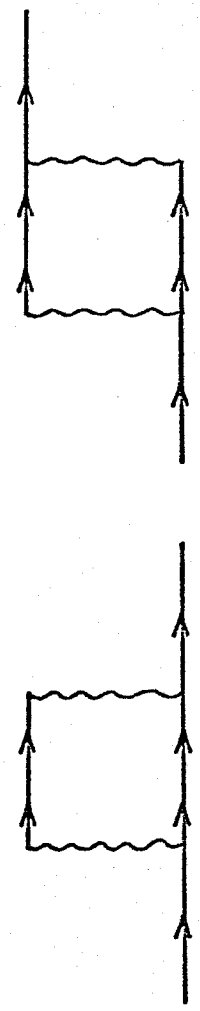
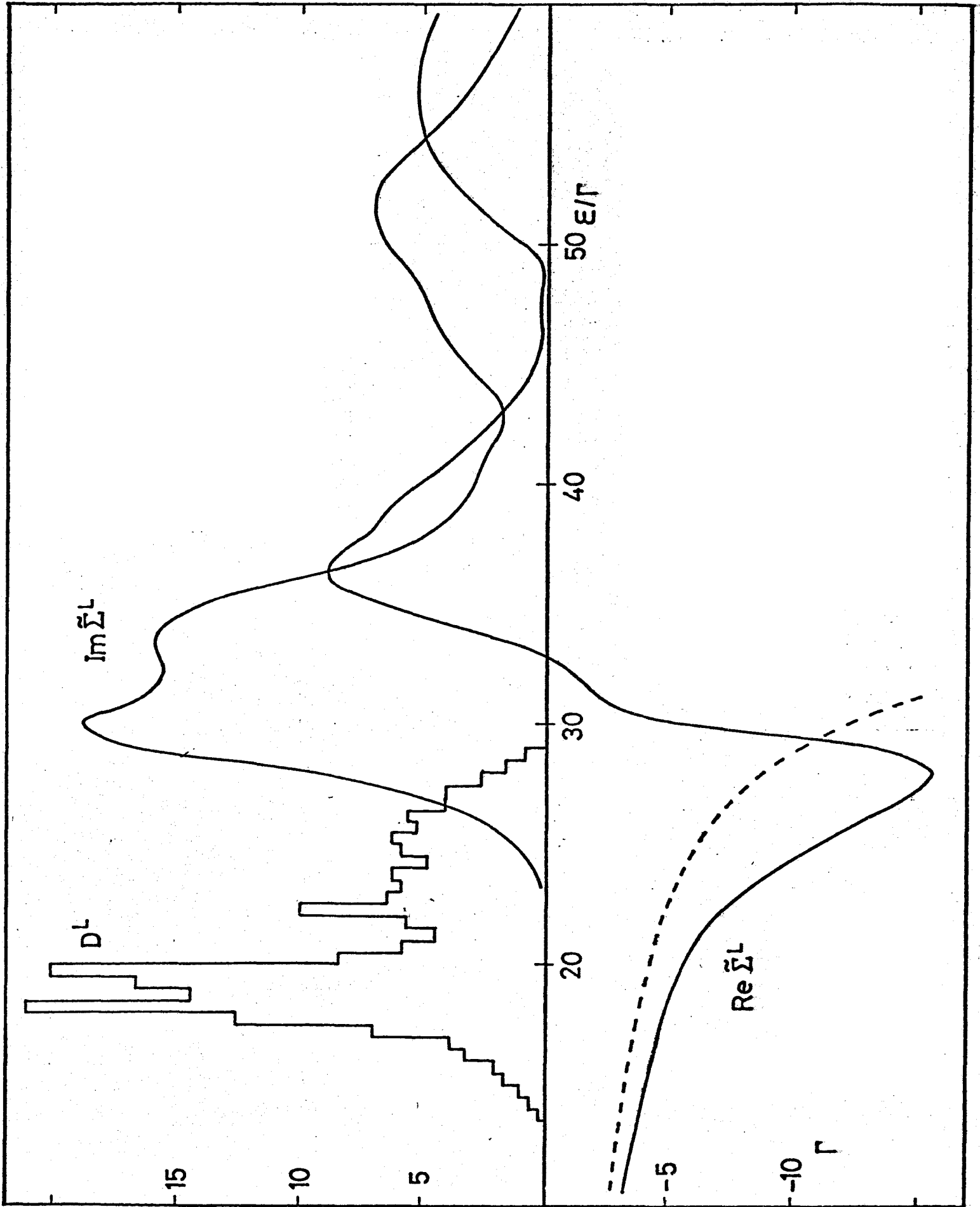
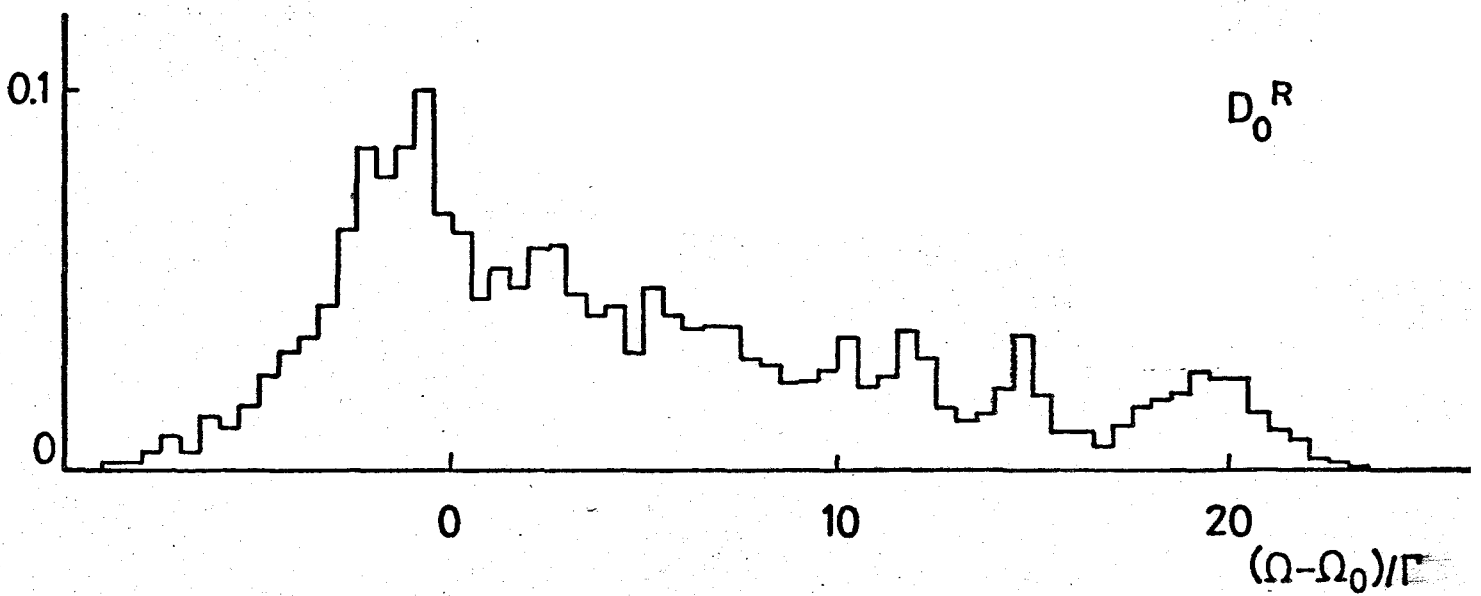
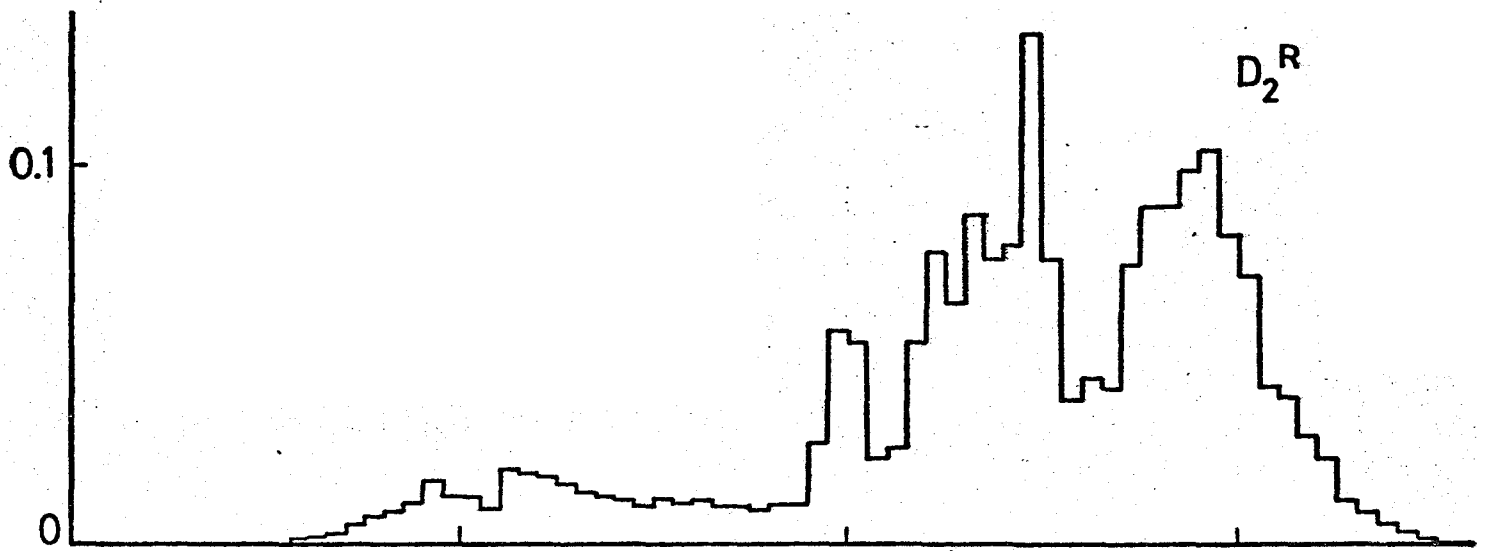


FIG. 3







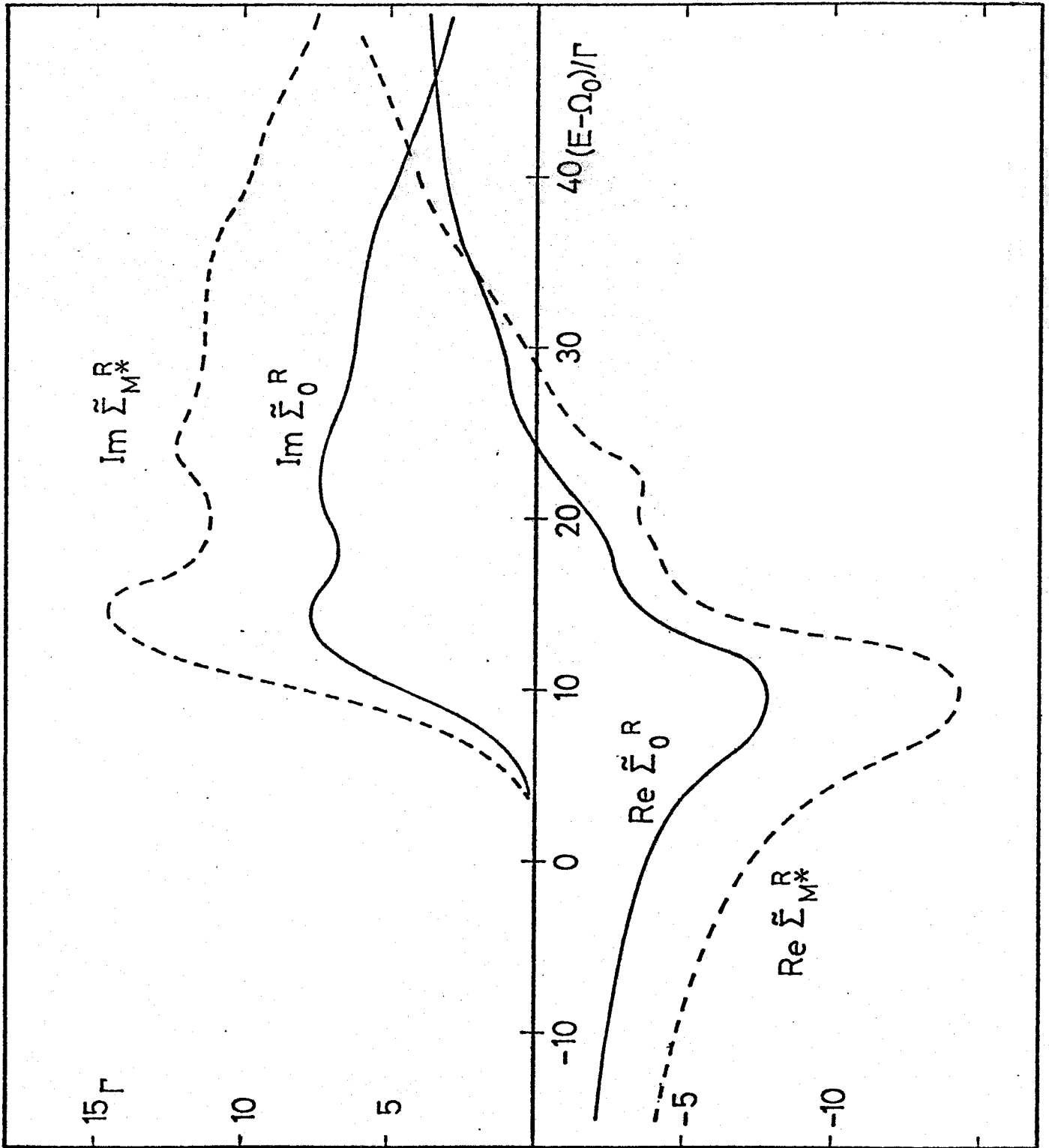
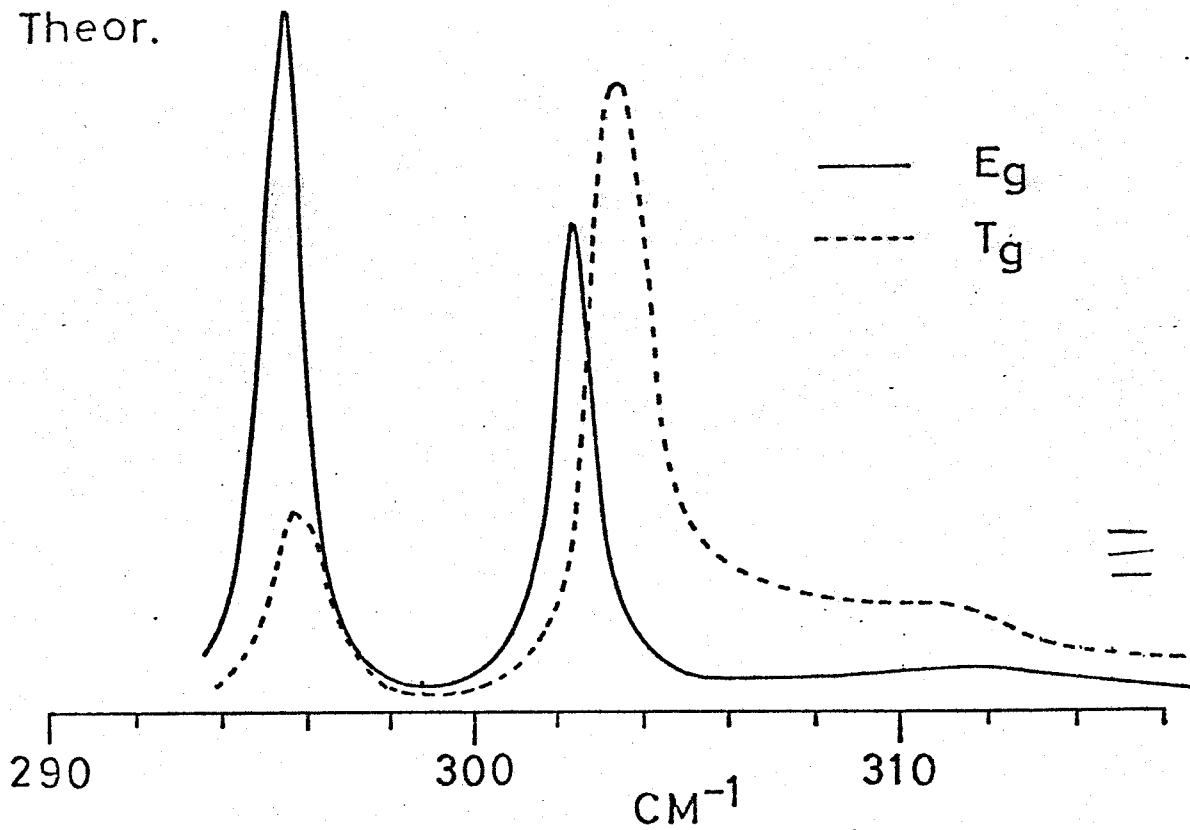


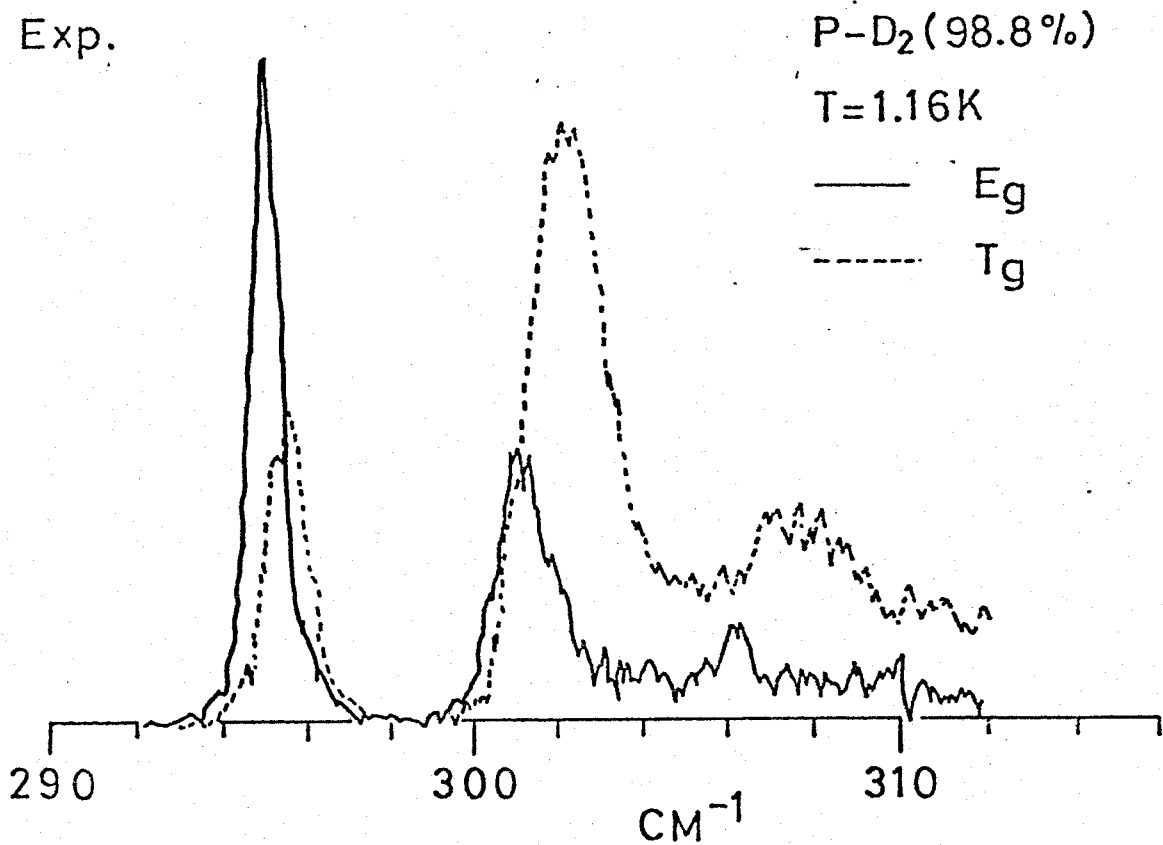
FIG.7

INTENSITY

Theor.



Exp.



Part III

Localized Excitations in the Ordered Solid Hydrogen

The excitations due to a parahydrogen in the ordered state of solid orthohydrogens are studied. The anharmonic processes prove to give significant effects on $J=2$ rotons. The virtual creation of libron ($J=1$ excitation) in the vicinity of roton is taken into account with the interactions between roton and libron, where the relevant Green's function is determined self-consistently. The results for Raman intensities are in good agreement with the experiment by Hardy, Silvera and McTague. It is shown that the local perturbation in the presence of a parahydrogen gives large effects on libron. The concentration dependences of the $k=0$ libron energy at very low concentrations of parahydrogens are also studied in a fair agreement with the Raman experiment by Hardy et al.

§1 Introduction

In Part II¹⁾ referred to as II, a study has been presented for the rotational excitation in the ordered solid hydrogen, particularly for J=3 excitation. The ground state of pure J=1 hydrogen system is of the Pa3 structure.^{2,3)} The dominant interactions between molecules are EQQ interactions.^{3,4)} The rotation-phonon interaction does not alter the angular dependence of EQQ interactions.⁵⁾ This effect is taken into account as a renormalization of the EQQ coupling parameter Γ , $\Gamma = 6e^2Q^2/25a^5$ with eQ the electric quadrupole moment and a the distance to nearest neighbors.

It was first shown by Harris et al.⁶⁾ that librations (J=1 excitations) are strongly perturbed by the anharmonic processes. With due account of the mentioned processes, they got a good agreement with experiments.⁷⁾ It is also the case for rotors (J=3 excitations),¹⁾ where the anharmonic processes are considerably effective in achieving the agreement of theory with experiment.⁷⁾

In the present paper, we study J=2 rotors localized at the parahydrogen site in J=1 hydrogens on the same footing. The Raman scattering experiment⁷⁾ shows four lines with the higher two lines broadend considerably, compared with the molecular field theory giving only three lines. Hardy et al. pointed out⁷⁾ the second highest line to be mainly $|2\ 2^\pm\rangle$

with a large frequency shift due to the anharmonic effect. (See Eq.(2.3) for our state as designated by $|JM^\pm\rangle$.) They also pointed out the highest broad line to be $|21^\pm\rangle$ combined with a libron, i.e. $\{|21^\pm\rangle + \text{libron}\}$.

In contradistinction with Hardy's interpretation, it appears that the highest broad line is mainly $|22^\pm\rangle$. The broad width of it comes from the virtual processes of libron creation. However there is no large frequency shift for the considered line. This follows simply from a second order perturbation; the energy of $|22^\pm\rangle$ is larger than that of $\{|20\rangle + \text{libron}\}$, while it is smaller than that of $\{|22^\pm\rangle + \text{libron}\}$. The energy shifts due to these energy levels cancel each other. It should be noted that $|22^\pm\rangle$ combines strongly with $\{|21^\pm\rangle + \text{libron}\}$ through the anharmonic term, because they are nearly degenerate. While this gives the highest line, the second highest line also comes from $|22^\pm\rangle$ strongly combined with $\{|20\rangle + \text{libron}\}$ again through the anharmonic term with considerable lowering of the energy. The situations are shown in Fig. 1 schematically.

The local perturbation in the presence of impurity gives large effects on libron, though no local mode comes out. This change of libron state in turn affects roton. This effect is also taken into account in our study.

The above effect gives rise to change of $k=0$ libron if the concentration of parahydrogens is finite. The

concentration dependence of the libron energy thus produced is studied in good agreement with the Raman experiment.⁷⁾ The treatment has been confined to the system at very low concentration of impurities.

Our Hamiltonian is described in §2. In §3, we discuss the local character of libron in the presence of a J=0 molecule. §4 is devoted to the study of J=2 excitation. In §5, the Raman intensity is evaluated in agreement with experiments. The concentration dependence of the energy of $k=0$ libron is studied in §6.

§2. Hamiltonian

The molecular configuration in the ordered pure J=1 hydrogens is a fcc lattice consisting of four sc sublattices. We choose new coordinate systems with z-axis parallel to the molecular direction, which is directed along one of four body-diagonals as is shown in Table I.

In the local frame, EQQ interactions are written as

$$H = \sum_{j>\ell} \sum_{\mu, \nu} z_{\mu}(j) f_{\mu\nu}(j, \ell) z_{\nu}(\ell), \quad (2.1)$$

$$\begin{pmatrix} z_1 \\ z_5 \end{pmatrix} = \left(\frac{4\pi}{10}\right)^{1/2} \left[\begin{pmatrix} 1 \\ -1 \end{pmatrix} Y_{22}(\Omega_j) + \begin{pmatrix} 1 \\ 1 \end{pmatrix} Y_{2-2}(\Omega_j) \right],$$

$$\begin{pmatrix} z_3 \\ z_4 \end{pmatrix} = \left(\frac{4\pi}{10}\right)^{1/2} \left[\begin{pmatrix} 1 \\ -1 \end{pmatrix} Y_{21}(\Omega_j) + \begin{pmatrix} 1 \\ 1 \end{pmatrix} Y_{2-1}(\Omega_j) \right],$$

$$z_5 = \left(\frac{4\pi}{5}\right)^{1/2} Y_{20}(\Omega_j), \quad (2.2)$$

where $Y_{\ell m}(\Omega_j)$ denotes the spherical harmonic function with Ω_j the orientational angle of the molecule at site j . The coupling parameter Γ is included in $f_{\mu\nu}(j, \ell)$, a function of $R_{j\ell}$ with the distance dependence $R_{j\ell}^{-5}$.

Let us introduce the real basic states by

$$\begin{cases} \langle \Omega | JM^+ \rangle \\ \langle \Omega | JM^- \rangle \end{cases} = \frac{1}{\sqrt{2}} \left\{ \begin{pmatrix} 1 \\ -1 \end{pmatrix} (-1)^M Y_{JM}(\Omega) + \begin{pmatrix} 1 \\ 1 \end{pmatrix} Y_{J-M}(\Omega) \right\}, \quad M > 0$$

$$\langle \Omega | J0 \rangle = Y_{J0}(\Omega). \quad (2.3)$$

Let us then consider the system with a parahydrogen substituted into the matrix of $J=1$ system. In the approximate ground state, all molecules are in $|10\rangle$, except the origin with state $|00\rangle$. In order to get the elementary excitation, we adopt the bosonic representation:

$$\begin{aligned} z_\mu(j) = \sum_{m>n} \{ \langle m | z_\mu | n \rangle [a_m^\dagger(j) (f - a_n(j) \delta_{n0} + a_m^\dagger(j) a_n(j)) + \text{h.c.}] \\ + \sum_m \{ \langle m | z_\mu | m \rangle - \langle 0 | z_\mu | 0 \rangle \} a_m^\dagger(j) a_m(j) + \langle 0 | z_\mu | 0 \rangle \}, \quad (2.4) \end{aligned}$$

where $f = (1 - \sum_m a_m^\dagger(j) a_m(j))^{1/2}$. Here in the case of $j \neq 0$, $|n\rangle$ stands for $|JM\rangle$ with odd J -number and $|0\rangle$ for $|10\rangle$.

At the origin, $|n\rangle$ stands for $|JM\rangle$ with even J -number and $|0\rangle$ for $|00\rangle$. (The inclusion of a_0 which must have no sense is due to a formal simplicity.) We assume that $a_n(j)$ and

$a_n^\dagger(j)$ satisfy the boson commutation relations.

(a) The case when the parahydrogen is in J=0 state.

In this case, one has $z_\mu(j) = 0$ for $j=0$. It is here noted that in Eq.(2.4) for $j \neq 0$ $|n\rangle$ is restricted to J=1 manifold, because the energies of J=3 states are higher than those of J=1 by $10B$ with B the rotational constant. From Eq.(2.4), we obtain

$$H^L = E_0 + H_{\text{pure}}^L + V_1 + V_2 + V_3 + \dots \quad (2.5)$$

Here E_0 denotes the energy of the approximate ground state, and H_{pure}^L the Hamiltonian of pure J=1 hydrogen system as classified into the quadratic, cubic and quartic terms in boson operators:

$$H_{\text{pure}}^L = H_2^L + H_3^L + \dots ,$$

$$H_2^L = \frac{1}{2} \sum_{ij} \sum_{mm'} \sum_{\mu} \{ \langle m | z_{\mu} | m' \rangle - \langle 10 | z_{\mu} | 10 \rangle \delta_{mm'} \} f_{\mu 2}(i, j) \\ \cdot \langle 10 | z_2 | 10 \rangle \{ a_m^\dagger(i) a_{m'}(i) + \text{h.c.} \} ,$$

$$+ \frac{1}{2} \sum_{ij} \sum_{mn} \sum_{\mu\nu} \langle m | z_{\mu} | 10 \rangle f_{\mu\nu}(i, j) \langle n | z_{\nu} | 10 \rangle \\ \{ a_m^\dagger(i) + a_m(i) \} \{ a_n^\dagger(j) + a_n(j) \} , \quad (2.6)$$

$$H_3^L = \frac{1}{2} \sum_{ij} \sum_{\mu\nu} \sum_{mm'n} \langle m | z_{\mu} | 10 \rangle f_{\mu\nu}(i, j) \{ \langle m' | z_{\nu} | n \rangle - \langle 10 | z_{\nu} | 10 \rangle \delta_{m'n} \}$$

$$\{a_m^\dagger(i) + a_m(i)\} \{a_m^\dagger(j) a_n(j) + \text{h.c.}\} . \quad (2.7)$$

The terms of V_1, V_2, V_3, \dots stand for the local perturbations in the presence of a $J=0$ molecule. Here V_1 is written as

$$V_1 = - \sum_j \sum_m \sum_\mu \langle m | z_\mu | 10 \rangle f_{\mu 2}(j, 0) \langle 10 | z_2 | 10 \rangle \{a_m^\dagger(j) + a_m(j)\} , \quad (2.8)$$

and we similarly have V_2 and V_3 which in reversed sign are merely a sum of the two terms obtained respectively from Eqs.

(2.6) and (2.7) if we put $i=0$ or $j=0$. Here we use

$\sum_j f_{\mu 2}(ij) = 0$ for $\mu \neq 2$.³⁾ Note that the creation and annihilation operators associated with $|11^\pm\rangle$ can also be effective for the parahydrogen site due to our division of the Hamiltonian.

(b) The case when the parahydrogen is in $J=2$ state.

In this case, from Eq.(2.4) we obtain

$$z_\mu(j=0) = \frac{1}{2} \sum_{mm'} \langle 2m | z_\mu | 2m' \rangle \{b_m^\dagger(0) b_{m'}(0) + \text{h.c.}\} . \quad (2.9)$$

If one substitutes Eq.(2.9) into Eq.(2.1), the correction terms to Eq.(2.5) come out as follows:

$$H^R = 6B \sum_m b_m^\dagger(0) b_m(0) + H_2^R + H_3^R + H_4^R + \dots , \quad (2.10)$$

$$H_2^R = \sum_m \sum_j \langle 2m | z_2 | 2m \rangle f_{22}(0, j) \langle 10 | z_2 | 10 \rangle b_m^\dagger(0) b_m(0) , \quad (2.11)$$

$$H_3^R = \frac{1}{2} \sum_{mm'} \sum_j \sum_{\mu\nu} \langle 2m | z_\mu | 2m' \rangle f_{\mu\nu}(0, j)$$

$$\cdot \langle 1n | z_\nu | 10 \rangle \{b_m^\dagger(0) b_{m'}(0) + \text{h.c.}\} \{a_n^\dagger(j) + a_n(j)\} \quad (2.12)$$

$$\begin{aligned}
H_4^R = & \frac{1}{4} \sum_{mm'} \sum_j \sum_{nn'} \langle 2m | z_\mu | 2m' \rangle f_{\mu\nu}(0, j) \\
& \cdot \{ \langle 1n | z_\nu | 1n' \rangle - \langle 10 | z_\nu | 10 \rangle \delta_{nn'} \} \\
& \cdot \{ b_m^\dagger(0) b_{m'}(0) + \text{h.c.} \} \{ a_n^\dagger(j) a_{n'}(j) + \text{h.c.} \} . \quad (2.13)
\end{aligned}$$

In the above expression b_m^\dagger denotes the creation operator as defined by $b_m^\dagger |00\rangle = |2m\rangle$. We note that Eq.(2.11) corresponds to the molecular field energy.

§3. Libron

We shall for a moment ignore the linear term V_1 , which comes out due to presence of impurities. The effect of it has proved very small, ⁸⁾ as will be discussed in Appendix A.

In the presence of an impurity, let us introduce the temperature Green's function

$$\begin{aligned}
G_{m,m'}(j, j'; \tau) &= - \langle T_\tau (a_m(j, \tau) a_{m'}^\dagger(j', 0)) \rangle , \\
\hat{G}_{mm'}(j, j'; \tau) &= - \langle T_\tau (a_m^\dagger(j, \tau) a_{m'}^\dagger(j', 0)) \rangle , \quad (3.1)
\end{aligned}$$

where j and j' denote the molecular site. Here $a_m(j, \tau) = \exp(\tau H) a_m(j) \exp(-\tau H)$ with τ the imaginary time. We also introduce the Fourier transform of $G_{mm'}(j, j'; \tau)$ by

$$G_{mm'}(j, j'; \omega_n) = \int_0^\beta e^{i\omega_n \tau} G_{mm'}(j, j'; \tau) , \quad (3.2)$$

where $\omega_n = 2\pi n/\beta$ and $\beta^{-1} = k_B T$.

For a pure $J=1$ system described by the Hamiltonian H_{pure}^L , we introduce the Green's functions, $P_{mm'}(j, j'; \omega_n)$ and $\hat{P}_{mm'}(j, j'; \omega_n)$, corresponding respectively to $G_{mm'}(j, j'; \omega_n)$ and $\hat{G}_{mm'}(j, j'; \omega_n)$. Referring to Fig. 2, we write down Dyson's equations

$$P(\omega) = P^0(\omega) + P^0(\omega)\Sigma_{11}(\omega)P(\omega) + P^0(\omega)\Sigma_{20}\hat{P}(\omega), \quad (3.3)$$

$$\hat{P}(\omega) = P^0(-\omega)\Sigma_{11}(-\omega)\hat{P}(\omega) + P^0(-\omega)\Sigma_{02}P(\omega). \quad (3.4)$$

Here j and m are absorbed into the formal matrix notation. In II, we have taken the diagonal term of Eq.(2.6) to be the unperturbed Hamiltonian. In the present paper, however, we introduce the free propagator matrix by

$$[P^0(\omega)]_{jm, j'm'} = (i\omega)^{-1} \delta_{mm'} \delta_{jj'}. \quad (3.5)$$

We note here

$$\Sigma_{11}(\omega) = \Sigma_{11}^{(2)} + \Sigma_{11}^{(3)}(\omega) \quad (3.6)$$

with $\Sigma_{11}^{(2)}$ and $\Sigma_{11}^{(3)}$ as defined in Fig. 2. The effect of the cubic anharmonicity is included in the site-diagonal part $[\Sigma_{11}^{(3)}(\omega)]_{jm, jm'}$, whose expression may be given by

$$\begin{aligned} & [\Sigma_{11}^{(3)}(\omega)]_{jm, jm'} \\ &= -\beta^{-1} \sum_{\ell} \sum_{nn'} \sum_{\mu\nu\nu'} \sum_{\omega'} \langle n | z_{\mu} | 10 \rangle f_{\mu\nu}(\ell, j) \{ \langle m | z_{\nu} | n' \rangle - \langle 10 | z_{\nu} | 10 \rangle \delta_{mn'} \} \end{aligned}$$

$$\begin{aligned}
& \cdot \langle n | z_{\mu} | 10 \rangle f_{\mu\nu}(\ell, j) \{ \langle m' | z_{\nu} | n' \rangle - \langle 10 | z_{\nu} | 10 \rangle \delta_{m'n'} \} \\
& \cdot [P(\omega - \omega')]_{\ell n, \ell n} [P(\omega')]_{jn', jn'} . \quad (3.7)
\end{aligned}$$

We note $[\Sigma_{11}^{(3)}(\omega)]_{jm, jm'} = 0$ if $m \neq m'$.

We can formally solve Eqs.(3.3) and (3.4) as

$$P(\omega)^{-1} = P^0(\omega)^{-1} - \Sigma_{11}(\omega) - \Sigma_{20} \{ P^0(-\omega) - \Sigma_{11}(-\omega) \}^{-1} \Sigma_{02} . \quad (3.8)$$

In the right side of Eq.(3.8), $\Sigma_{11}(\omega)$ includes $P(\omega)$, and hence the self-consistent solution of Eq.(3.8) must be solved. The solution is obtained by a transformation of Eq.(3.8) from the coordinate space to the momentum one.¹⁾ (See Appendix B.)

By the same consideration as above, we get the formal equation of $G(\omega)$ as

$$G^{-1}(\omega) = P^0(\omega)^{-1} - \Sigma_{11}'(\omega) - \Sigma_{20}' \{ P^0(-\omega)^{-1} - \Sigma_{11}'(-\omega) \} \Sigma_{02}' . \quad (3.9)$$

Here $\Sigma_{11}'(\omega)$, Σ_{20}' and Σ_{02}' are the self-energy parts in the presence of the impurity, where the notation follows Fig. 2. Needless to say, the $(jm, j'm')$ components of the above self-energy parts should be zero if either of j and j' is at the impurity site 0. Similarly $\Sigma_{11}^{(3) \prime}$ corresponds to $\Sigma_{11}^{(3)}$ in the perfect lattice as given by Eq.(3.7) and vanishes if one of j and ℓ is at the origin. The expression for $\Sigma_{11}^{(3) \prime}$ includes $G(\omega)$ in place of $P(\omega)$.

It should be noted that $[G^{-1}(\omega)]_{0m, 0m} = i\omega$. This is

the Green's function at the impurity site. Here a spurious resonance comes in at zero frequency because excess degrees of freedom are brought into the impurity site. However, the mentioned singular term can be isolated from our libron solution.

Let us now subtract Eq.(3.9) from Eq.(3.8). We obtain

$$P^{-1}(\omega) - G^{-1}(\omega) = C(\omega) , \quad (3.10)$$

where

$$\begin{aligned} [C(\omega)]_{jm, j'm'} = & -\{ \langle m | z_2 | m' \rangle - \langle 10 | z_2 | 10 \rangle \} \{ \sum_i f_{22}(0, i) \} \\ & \cdot \langle 10 | z_2 | 10 \rangle \delta_{jj'} \delta_{j0} \delta_{mm'} \\ & - \sum_{\mu} \{ \langle m | z_{\mu} | m' \rangle - \langle 10 | z_{\mu} | 10 \rangle \delta_{mm'} \} f_{\mu 2}(j, 0) \langle 10 | z_2 | 10 \rangle \delta_{jj'} \\ & - \sum_{\mu\nu} \langle m | z_{\mu} | 10 \rangle f_{\mu\nu}(j, j') \langle m' | z_{\nu} | 10 \rangle (\delta_{j0} + \delta_{j'-0}) \\ & + \beta^{-1} \sum_{\omega'} \sum_{nn'} \sum_{\mu\nu\nu'} \sum_{\ell} [\langle n | z_{\mu} | 10 \rangle f_{\mu\nu}(\ell, j) \{ \langle m | z_{\nu} | n' \rangle - \langle 10 | z_{\nu} | 10 \rangle \delta_{mn'} \}] \\ & \cdot [\langle n | z_{\mu} | 10 \rangle f_{\mu\nu'}(\ell, j) \{ \langle m' | z_{\nu'} | n' \rangle - \langle 10 | z_{\nu'} | 10 \rangle \delta_{m'n'} \}] \\ & \cdot P_{\ell n, \ell n}(\omega') P_{j n', j n'}(\omega - \omega') \delta_{jj'} \cdot (\delta_{j0} + \delta_{\ell 0}) . \quad (3.11) \end{aligned}$$

In the right-hand side of Eq.(3.11), the first three terms come from V_2 , and the others from V_3 . The frequency sum in $C(\omega)$ is performed by the same procedure as was done in Eq.(4.12) of II.

In deriving Eq.(3.11), we neglect the difference between

$\Sigma_{20}\{P^0(-\omega)^{-1} - \Sigma_{11}(-\omega)\}^{-1}\Sigma_{02}$ and $\Sigma_{20}\{P^0(-\omega)^{-1} - \Sigma_{11}(-\omega)\}^{-1}\Sigma_{02}$, because it has proved very small. In $\Sigma_{11}^{(3)}(\omega)$, we may also replace G by P by the same reason.

In Eq.(3.10) with replacement of ω by $-i\omega+0^+$, we write the Dyson equation for the retarded functions as

$$\tilde{G}(\omega) = \tilde{P}(\omega) + \tilde{P}(\omega)\tilde{C}(\omega)\tilde{G}(\omega) . \quad (3.12)$$

Here the retarded functions are defined, for instance, by $\tilde{G}(\omega) = G(-i\omega+0^+)$. (The temperature is assumed zero throughout the present paper.)

Solving Eq.(3.12), we have

$$\tilde{G}(\omega) = \tilde{P}(\omega) + \tilde{P}(\omega)\tilde{T}(\omega)\tilde{P}(\omega) , \quad (3.13)$$

where

$$\tilde{T}(\omega) = \tilde{C}(\omega)[I - \tilde{P}(\omega)\tilde{C}(\omega)]^{-1} \quad (3.14)$$

with I the unite matrix.

In our site representation, the defect matrix $\tilde{C}(\omega)$ is the most effective for the diagonal term with respect to the impurity site, decreasing rapidly with increasing distance from it. Thus the effective sites of $\tilde{C}(\omega)$ can be confined to the nearest neighbors to the origin. Then $\tilde{C}(\omega)$ is a 26×26 matrix. Accordingly, $\tilde{P}(\omega)$ and $\tilde{G}(\omega)$ can also be assumed to have the same dimensionality.

Let ω_0 be the bottom of the libron band. For $\omega < \omega_0$, both $\tilde{P}(\omega)$ and the diagonal part of $\tilde{C}(\omega)$ are negative, and hence

some local modes may appear at the frequency satisfying $\det [I - \hat{P}(\omega)\hat{C}(\omega)] = 0$. However no local mode appears according to the numerical inspection.

For $\omega > \omega_0$, we look into $-(1/24\pi) \sum_{j \neq 0} \sum_m \text{Im}[\hat{G}(\omega)]_{jm, jm}$. This spectral density for libron at the neighboring site is different from that in the perfect lattice. The result is shown in Fig. 3. The computations of $\hat{P}(\omega)$ were performed for 1,000 points in the $1/8$ part of k -space.

§4. Localized roton at parahydrogen

Let us consider the roton associated with a parahydrogen. Consider the Green's function of roton

$$D_{m m'}(\tau) = - \langle T_{\tau} (b_m(0, \tau) b_{m'}^{\dagger}(0, 0)) \rangle . \quad (4.1)$$

whose Fourier transform is denoted by $D_{m m'}(\omega)$. The total Hamiltonian is given by

$$H = H_2^R + H_3^R + H_4^R + H^L , \quad (4.2)$$

according to §2. As mentioned before, V_1 in H^L may be eliminated by a canonical transformation. In Appendix A, the effect of the elimination on the Hamiltonian for roton will be given. Using that result we obtain

$$H' = H_2^R + H_3^R + H_4^R + H^{L'} , \quad (4.3)$$

where

$$H_2^{R'} = \sum_m \{ 6B + \langle 2m | z_2 | 2m \rangle \{ \sum_j f_{22}(0, j) \} \langle 10 | z_2 | 10 \rangle + \Delta \epsilon_m \} \cdot b_m^\dagger(0) b_m(0) . \quad (4.4)$$

Here $\Delta \epsilon_m$ is the term coming from the elimination as given by Eq.(A.4) and hence $H^{L'} = H_{\text{pure}}^L + V_2 + V_3 + \dots$. Let $H_2^{R'}$ be the unperturbed Hamiltonian. Thus the free propagator matrix becomes

$$D_{mm'}^{(0)}(\omega) = (i\omega - 6B - \epsilon_m)^{-1} \delta_{mm'} , \quad (4.5)$$

$$\epsilon_m = \langle 2m | z_2 | 2m \rangle \{ \sum_j f_{22}(0, j) \} \langle 10 | z_2 | 10 \rangle + \Delta \epsilon_m . \quad (4.6)$$

Let us now consider the Dyson equation as shown in Fig. 4:

$$[D^{-1}(\omega)]_{mm'} = (i\omega - 6B - \epsilon_m) \delta_{mm'} - \Sigma_{mm'}(\omega) , \quad (4.7)$$

$$\Sigma_{mm'}(\omega) = -\beta^{-1} \sum_j \sum_{m_1 m_2} \sum_{n_1 n_2} \sum_{\omega'} \Gamma_{m_1 n_1, m}^{(0)}(j) G_{n_1 n_2}(j, j; \omega') \cdot D_{m_1 m_2}(\omega - \omega') \Gamma_{m_2 n_2, m'}(j; \omega - \omega', \omega'; \omega) . \quad (4.8)$$

In the above, $G_{n_1 n_2}(j, j; \omega')$ is the libron Green's function as derived from $H^{L'}$. In Eq.(4.8), $\Gamma^{(0)}(j)$ is defined by

$$\Gamma_{m_1 n_1, m}^{(0)}(j) = \sum_{\mu\nu} \langle 2m | z_\mu | 2m_1 \rangle f_{\mu\nu}(0, j) \langle n_1 | z_\nu | 10 \rangle . \quad (4.9)$$

We shall below use Eq.(3.2) for $G_{n_1 n_2}(j, j'; \omega')$. Only the site-diagonal part of G will be taken into account.

For the vertex part, we might have

$$\begin{aligned} \Gamma_{mn,m'}(j; \omega - \omega', \omega'; \omega) &= \Gamma_{mn,m'}^{(0)}(j) \\ &- \beta^{-1} \sum_{\omega''} \sum_{m_1 m_2} \sum_{n_1 n_2} U_{mn, m_1 n_1}(j) G_{n_1 n_2}(j, j; \omega'') D_{m_1 m_2}(\omega - \omega'') \\ &\cdot \Gamma_{m_2 n_2, m'}(j; \omega - \omega'', \omega''; \omega) \end{aligned} \quad (4.10)$$

in a ladder approximation (Fig. 4), where U is defined by

$$\begin{aligned} U_{mn, m' n'}(j) \\ = \sum_{\mu\nu} \langle 2m | z_\mu | 2m' \rangle f_{\mu\nu}(0, j) \{ \langle n | z_\nu | n' \rangle - \langle 10 | z_\nu | 10 \rangle \delta_{nn'} \} . \end{aligned} \quad (4.11)$$

In order to solve Eq.(4.10), we introduce

$$\begin{aligned} F_{mn, m'}(j; \omega) &= -\beta^{-1} \sum_{\omega'} \sum_{m_1 n_1} G_{nn_1}(j, j; \omega') \\ &\cdot D_{mm_1}(\omega - \omega') \Gamma_{m_1 n_1, m'}(j; \omega - \omega', \omega'; \omega) . \end{aligned} \quad (4.12)$$

And $F^{(0)}(j; \omega)$ is defined by Eq.(4.12) with replacement of Γ by $\Gamma^{(0)}$. From Eq.(4.10) we have

$$F(j; \omega) = F^{(0)}(j; \omega) + K(j; \omega) U(j) F(j; \omega) \quad (4.13)$$

in the matrix form, where $K(j; \omega)$ is defined by

$$[K(j; \omega)]_{mn, m' n'} = -\beta^{-1} \sum_{\omega'} G_{mm'}(\omega') D_{nn'}(\omega - \omega') . \quad (4.14)$$

Then $F^{(0)}(j; \omega) = K(j; \omega) \Gamma^{(0)}(j)$. Thus Eq.(4.13) is solved to be

$$F(j; \omega) = [I - K(j; \omega)U(j)]^{-1}K(j; \omega)\Gamma^{(0)}(j) . \quad (4.15)$$

By the use of Eq.(4.15), Eq.(4.8) is rewritten as

$$\Sigma_{mm'}(\omega) = \sum_j \sum_{m_1 n_1} \Gamma_{m_1 n_1, m}^{(0)}(j) F_{m_1 n_1, m'}(j; \omega) . \quad (4.16)$$

Equations (4.7), (4.14), (4.15) and (4.16) are a set of equations, which will below be solved self-consistently.

By the same procedure as we obtained Eq.(4.18) of II

$$[\tilde{K}(j; \omega)]_{mn, m' n'} = -\frac{1}{\pi} \int_0^{\infty} \tilde{D}_{mm'}(\omega - \varepsilon) \text{Im} \tilde{G}_{nn'}(j, j; \varepsilon) d\varepsilon , \quad (4.17)$$

where $\tilde{K}(j; \omega)$ and $\tilde{D}(\omega)$ are the corresponding retarded functions.

Using Eq.(4.17), we evaluate $\tilde{\Sigma}(\omega) \equiv \Sigma(-i\omega + 0^+)$ by an iterative method, where the summation over j in Eq.(4.16) is taken up to the nearest neighbors of the parahydrogen.

The self-consistent solution for $\tilde{\Sigma}(\omega)$ has a simple form as shown in Table II. This form brings us two two-fold degenerate levels, as required from a symmetry reason. In Table II, d should be reversed in sign if the parahydrogen site belongs to B- and D-sublattices.

The computed results for $\tilde{\Sigma}(\omega)$ are given in Fig. 5, where only the diagonal parts of $\tilde{\Sigma}(\omega)$ are shown. The off-diagonal parts of $\tilde{\Sigma}(\omega)$ are fairly small. In Fig. 6 is shown the density of states as given by $-(1/\pi)\text{Im}[\tilde{D}_{mm}(\omega)]$. The line $|2 \ 2^\pm\rangle$ is now splitted into two parts, where each part appears with considerably broad width.

§5. Raman intensities for $J = 0 \rightarrow 2$ transition

According to II, the differential cross section of light scattered by the system is given by

$$I(\omega, \underline{n}) = \frac{\omega^4}{2\pi c^3} \left(\frac{2}{3}\right)^2 \sum_{\nu\nu'} \{ \underline{n}^{(\ell)} \times \underline{E} \}_{\nu} \{ \underline{n}^{(\ell)} \times \underline{E} \}_{\nu'} \Pi_{\nu\nu'}(\omega - \omega^0) . \quad (5.1)$$

Here $\underline{n}^{(1)}$ and $\underline{n}^{(2)}$ denote the unit polarization vectors of the scattered light with propagation direction $\underline{n} = \underline{n}^{(1)} \times \underline{n}^{(2)}$ and with frequency ω , \underline{E} the electric field vector for the incident light with frequency ω^0 , and $\{ \underline{n}^{(\ell)} \times \underline{E} \}_{\nu}$ the ν -th component of the second-rank irreducible tensors constructed by $\underline{n}^{(\ell)}$ and \underline{E} in accordance with Eq.(2.2). And $\Pi_{\nu\nu'}(\omega)$ is defined by

$$\Pi_{\nu\nu'}(\omega) = (2\pi)^{-1} \int_{-\infty}^{\infty} \langle P_{\nu}(t) P_{\nu'}(0) \rangle e^{-i\omega t} dt , \quad (5.2)$$

with P_{ν} the polarizability tensor of the system.

Let us consider the system at very low concentrations. Now P_{ν} for roton may be given by the orientation-dependent polarizability tensors of parahydrogens. Hence we have

$$P_{\nu} = \Delta\chi \sum_i z'_{\nu}(i) , \quad (5.3)$$

where $\Delta\chi = \chi_{\parallel} - \chi_{\perp}$ with χ_{\parallel} and χ_{\perp} the polarizabilities of molecule parallel and perpendicular to the molecular axis respectively. The summation is taken over parahydrogen sites. And $z'_{\nu}(i)$ defined in the crystal-fixed frame is transformed into

our $z_{\mu}(i)$ in the local coordinate frame by

$$z'_{\nu}(i) = \sum_{\mu} T_{\nu\mu}(\theta_i, \phi_i) z_{\mu}(i), \quad (5.4)$$

where $T_{\nu\mu}(i)$ is given in Table VII of Ref. 9. Here $\theta_i = \arccos(1/\sqrt{3})$, and $\phi_i = \pi/4, -\pi/4, -3\pi/4, 3\pi/4$, corresponding to A, B, C, D sublattices, respectively.

The primary terms of Eq.(5.4) prove to be

$$z'_{\nu}(i) = \sum_{\mu m} T_{\nu\mu}(\theta_i, \phi_i) \langle 2m | z_{\mu} | 00 \rangle \{ b_m^{\dagger}(i) + b_m(i) \}. \quad (5.5)$$

We introduce the following function:

$$R_{\nu\nu'}(\omega) = 1/4 \cdot \sum_{\alpha} \sum_{\mu\mu'} \sum_{mm'} T_{\nu\mu}^{\alpha} \langle 2m | z_{\mu} | 00 \rangle \cdot T_{\nu'\mu'}^{\alpha} \langle 2m' | z_{\mu'} | 00 \rangle D_{mm'}^{\alpha}(\omega) \quad (5.6)$$

after averaging over sublattice α . Then $R_{\nu\nu'}(\omega) = R_1(\omega)\delta_{\nu\nu'}$ for $\nu = 1, 2$ and $R_2(\omega)\delta_{\nu\nu'}$ for $\nu = 3, 4, 5$, where

$$R_1(\omega) = 1/5 \cdot \{ 1/3 \cdot \tilde{D}_{2\pm 2}^{\pm}(\omega) + 2/3 \cdot \tilde{D}_{1\pm 1}^{\pm}(\omega) \} \quad (5.7)$$

$$R_2(\omega) = 1/5 \cdot \{ 4/9 \cdot \tilde{D}_{2\pm 2}^{\pm}(\omega) + 2/9 \cdot \tilde{D}_{1\pm 1}^{\pm}(\omega) + 1/3 \cdot \tilde{D}_{00}(\omega) \}. \quad (5.8)$$

Thus we obtain $\Pi_{\nu\nu'}(\omega) = \Pi_1(\omega)\delta_{\nu\nu'}$ for $\nu = 1, 2$ and $\Pi_2(\omega)\delta_{\nu\nu'}$ for $\nu = 3, 4, 5$, where

$$\Pi_1(\omega) = -N_1(\Delta\chi)^2 (e^{\beta\omega} - 1)^{-1} (1/\pi) \text{Im} [R_1(\omega) - R_1(-\omega)] \quad (5.9)$$

and $\Pi_2(\omega)$ given by Eq.(5.9) with replacement of R_1 by R_2 .

Here N_i is the number of parahydrogens.

Then we have

$$I(\omega, \underline{n}) = \frac{\omega^4}{2\pi c^3} \left(\frac{2}{3}\right)^2 [2F_1(\underline{n})\Pi_1(\omega) + 3F_2(\underline{n})\Pi_2(\omega)] \quad (5.10)$$

$$F_1(\underline{n}) = 1/2 \cdot \sum_{\ell=1}^2 \sum_{\nu=1}^2 [\{\underline{n}^{(\ell)} \times \underline{E}\}_{\nu}]^2 \quad (5.11)$$

$$F_2(\underline{n}) = 1/3 \cdot \sum_{\ell=1}^2 \sum_{\nu=3}^5 [\{\underline{n}^{(\ell)} \times \underline{E}\}_{\nu}]^2 . \quad (5.12)$$

According to the experiment,⁷⁾ we assume the incident light to be parallel to [111]-axis of the crystal, being parallel to Z-axis, and the scattered light to be observed along X-axis. Using the formula of Appendix B in II, we can evaluate Eq.(5.10) for arbitrary polarization.

In Fig. 7, we show the calculated differential cross section for the polarization XY + XZ, in agreement with the experiment.⁷⁾ Here XY stands for the polarization of the scattered light along Y-axis for the incident light polarization parallel to X-axis.

Table III shows the peak positions and the Raman intensities. The theoretical peak positions deviate slightly from the experiment.⁷⁾ However we can get the further improvement by taking account of the neglected effects of the order Γ/B . These contributions are estimated to be about 1.5 Γ for D_2 , as are shown in Part IV.

§6. Energy shift of $k=0$ libron at very low concentration

For the system of impurity concentration x , we must take the configurational average of the Green's function, $\tilde{Q}(\omega)$. In the low concentration limit, by the well-known procedure¹⁰⁾ we obtain

$$\tilde{Q}(\omega) = \tilde{P}(\omega) + \tilde{P}(\omega)\tilde{\Sigma}(\omega)\tilde{Q}(\omega), \quad \tilde{\Sigma}(\omega) = x \sum_{\ell} \tilde{T}^{\ell}(\omega), \quad (6.1)$$

where $\tilde{T}^{\ell}(\omega) = \tilde{C}^{\ell}(\omega) [I - \tilde{P}(\omega)\tilde{C}^{\ell}(\omega)]^{-1}$. Here $\tilde{C}^{\ell}(\omega)$ is the defect matrix due to the impurity at ℓ -site.

By the Fourier transformation of $\tilde{Q}(\omega)$ we obtain

$$[\tilde{Q}^{-1}(\underline{k}, \omega)]_{\alpha m, \alpha' m'} = [\tilde{P}^{-1}(\underline{k}, \omega)]_{\alpha m, \alpha' m'} - \tilde{\Sigma}_{\alpha m, \alpha' m'}(\underline{k}, \omega), \quad (6.2)$$

where

$$\begin{aligned} \tilde{\Sigma}_{\alpha m, \alpha' m'}(\underline{k}, \omega) = x(4/N) \sum_{\ell} \sum_{j[\alpha]} \sum_{j'[\alpha']} \tilde{T}_{jm, j'm'}^{\ell}(\omega) \\ \cdot \exp\{i\underline{k}(\underline{r}_{j[\alpha]} - \underline{r}_{j'[\alpha']})\}. \end{aligned} \quad (6.3)$$

Here N denotes the number of lattice sites, and $j[\alpha]$ stands for a lattice site belonging to the sublattice α .

Remember that we have brought degrees of freedom into the impurity site for our impurity problem. The spurious resonance associated with these degrees of freedom are completely decoupled from libron in $\tilde{G}(\omega)$.

At finite concentrations, however, this spurious resonance couples to libron through $\tilde{T}^{\ell}(\omega)$ of Eq.(6.3).

In order to remove it, we must impose $[\hat{G}(\omega)]_{0m,0m} = 0$ for the single impurity case, because the impurity site should not involve the excitation. This is satisfied by adding a hard core potential at the impurity site of the form¹¹⁾

$$\Delta V(0) = \Delta_0 \sum_m a_m^\dagger(0) a_m(0) \quad (6.4)$$

with a very large Δ_0 . Thus we obtain $\hat{T}^k(\omega)$ in the low concentration limit.

We note here that the symmetry of $\hat{\Sigma}(\underline{k}=0, \omega)$ is the same as that of $\hat{P}^{-1}(\underline{k}=0, \omega)$. We evaluate the libron energy

$$\epsilon = \epsilon_0(1 - Kx) \quad (6.5)$$

with estimates $K=1.69$ for E_g , 0.12 for $T_g^{(1)}$ and 0.38 for $T_g^{(2)}$. It is noted that $\text{Re } \hat{\Sigma}(\underline{k}=0, \epsilon_0)$ depends sensitively on ϵ_0 's, the libron energies in the pure system: $\epsilon_0 = 10.5\Gamma$ for E_g , 14.0Γ for $T_g^{(1)}$ and 22.0Γ for $T_g^{(2)}$ in accordance with §3. Our calculation is based on the neglect of the site-nondiagonal components of \hat{P} in \hat{T}^k farther than the second neighbors. This treatment does not make any serious error for the results given up to §5, because the over-all nature of libron is relevant there. In the present problem, it is not the case. However the error is believed to be not so large. In view of the experimental errors, our results seem consistent with the experimental ones for D_2 :⁷⁾ $K=1.42$ for E_g and 0.57 for $T_g^{(2)}$.

Appendix A: Elimination of V_1

The linear term V_1 may be eliminated by a well known transformation. The transformed Hamiltonian is assumed to be $H' = e^{-S} H e^S$ with

$$S = \sum_j \sum_m t_m(j) \{a_m^\dagger(j) - a_m(j)\}, \quad (\text{A.1})$$

where j runs over nearest neighbors to a impurity.

We replace H in $[H, S]$ by the sum of the diagonal parts of Eq.(2.6) and V_2 in the site representation, since they are most dominant in the quadratic terms. The above terms cancels V_1 , if $t_m(j)$ is determined by

$$\begin{aligned} & \left[\sum_{i \neq 0} \{ \langle m | z_2 | m \rangle - \langle 10 | z_2 | 10 \rangle \} f_{22}(j, i) \langle 10 | z_2 | 10 \rangle \right] t_m(j) \\ & = \langle m | z_\mu | 10 \rangle f_{\mu 2}(j, 0) \langle 10 | z_2 | 10 \rangle, \quad \mu = 3, 4 \end{aligned} \quad (\text{A.2})$$

Equation (A.2) gives $|t_m(j)| \lesssim 0.052$. Since $|t_m(j)|$ is small, the other terms from $[H^L, S]$ prove small and hence ignorable.

If the parahydrogen is in $J=2$, we obtain

$$\begin{aligned} [H_3^R, S] &= \sum_j \sum_{mm'n} \sum_{\mu\nu} \langle 2m | z_\mu | 2m' \rangle f_{\mu\nu}(0, j) \langle n | z_\nu | 10 \rangle \\ &\quad \cdot \{ b_m^\dagger(0) b_{m'}(0) + \text{h.c.} \} t_n(j) \end{aligned} \quad (\text{A.3})$$

from Eqs.(2.16) and (A.2). Thus we get

$$[H_3^R, S] = \sum_m \Delta \epsilon_m b_m^\dagger(0) b_m(0), \quad (\text{A.4})$$

with the estimates $\Delta\varepsilon_{2\pm} = -1.34\Gamma$, $\Delta\varepsilon_{1\pm} = 0.67\Gamma$ and $\Delta\varepsilon_0 = 1.34\Gamma$.

Appendix B: Derivation of $P_{jm, j'm'}(\omega)$

The Fourier transform of $P_{jm, j'm'}(\omega)$ is denoted by $P_{\alpha m, \alpha' m'}(k, \omega)$, which is identical with $G_{\alpha m, \alpha' m'}(k, \omega)$ in II. We also define $[\Sigma(k, \omega)]_{\alpha m, \alpha' m'}$ similarly.

By the same procedure as I, the self-consistent solution for $\Sigma_{11}^{(3)}$ may be written as

$$[\Sigma_{11}^{(3)}(k, \omega)]_{\alpha m, \alpha' m'} = \Sigma^L(\omega) \delta_{\alpha\alpha'} \delta_{mm'} , \quad (\text{B.1})$$

where $\Sigma^L(\omega)$ is given by Eq.(4.11) in I. Moreover we have

$$[\Sigma_{11}^{(2)}(k, \omega)]_{\alpha m, \alpha' m'} = \omega_0 \delta_{\alpha\alpha'} \delta_{mm'} + [\Sigma_L^{(2)}(k)]_{\alpha m, \alpha' m'} , \quad (\text{B.2})$$

where ω_0 is given by Eq.(3.8) and $\Sigma_L^{(2)}(k)$ by Eq.(2.9) in II.

The matrices $\Sigma_{02}(k)$ and $\Sigma_{20}(k)$ are identified with $\Sigma_L^{(2)}(k)$.

Let us introduce $S^L(k)$ such that

$$[S^L(k)^{-1} \Sigma_L^{(2)}(k) S^L(k)]_{ii'} = \sigma_i(k) \delta_{ii'} . \quad (\text{B.3})$$

Then Eq.(3.8) gives

$$P_{\alpha m, \alpha' m'}(k, \omega) = [S^L(k)]_{\alpha m, i} \cdot [S^L(k)]_{\alpha' m', i} \cdot \{i\omega - \omega_0 - \sigma_i(k) - \Sigma^L(\omega) + \sigma_i^2(k) / (i\omega + \omega_0 + \sigma_i(k) + \Sigma^L(-\omega))\} , \quad (\text{B.4})$$

whence one gets $P_{jm, j'm'}(\omega)$.

References

- 1) The part II is based on M. Fujio, J. Igarashi and T. Nakamura, Prog. Theor. Phys. 50 (1978), 329.
- 2) A.F. Schuch, R.L. Mills and D.A. Depaite, Phys. Rev. 165 (1968), 1032.
- 3) O. Nagai and T. Nakamura, Prog. Theor. Phys. 24 (1960), 432 [Errata: 30 (1963), 412].
- 4) T. Nakamura, Prog. Theor. Phys. 14 (1955), 135.
- 5) S. Luryi and J. Van Kranendonk, to be published.
Earlier references there in.
- 6) C.F. Coll, III and A.B. Harris, Phys. Rev. B4 (1971), 2781.
- 7) W.N. Hardy, I.F. Silvera and J.P. McTague, Phys. Rev. B12 (1975), 753.
- 8) H. Miyagi, Thesis (Osaka University, 1970).
- 9) H. Miyagi and T. Nakamura, Prog. Theor. Phys. 37 (1967), 641.
- 10) R.J. Elliott, J.A. Krumhansl and P.L. Leath, Rev. Mod. Phys. 46 (1974), 465.
- 11) A.B. Harris, P.L. Leath, B.G. Nickel and R.J. Elliott, J. Phys. C7 (1974), 1693.

Table I Designation of the local coordinate system

| Sublattice | Position ^{*)} | Direction of z-axis | Direction of x-axis |
|------------|--------------------------------------|---------------------|---------------------|
| A | (0, 0, 0) | (1, 1, 1) | (1, 1, -2) |
| B | (0, $\frac{1}{2}$, $\frac{1}{2}$) | (1, -1, 1) | (1, -1, -2) |
| C | ($\frac{1}{2}$, 0, $\frac{1}{2}$) | (-1, -1, 1) | (-1, -1, -2) |
| D | ($\frac{1}{2}$, $\frac{1}{2}$, 0) | (-1, 1, 1) | (-1, 1, -2) |

*) unit: the lattice constant of s.c. sublattice.

Table II Symmetry of the matrix $\sum_{mm'}^{\nu}(\omega)$

$$\begin{array}{ccccc}
 |2^+\rangle & |2^-\rangle & |1^+\rangle & |1^-\rangle & |0\rangle \\
 \left(\begin{array}{ccccc}
 a & 0 & e & d & 0 \\
 0 & a & d & -e & 0 \\
 e & d & b & 0 & 0 \\
 d & -e & 0 & b & 0 \\
 0 & 0 & 0 & 0 & c
 \end{array} \right)
 \end{array}$$

Table III Theoretical Raman results in comparison
with experiments

| Energy shift ^{a)} (unit: Γ) | | | Raman intensity ^{b)} | | |
|--|---------|-----------------------|-------------------------------|---------|--------------------|
| M.F.A. ^{c)} | Present | Exp. ^{d),e)} | M.F.A. ^{c)} | Present | Exp. ^{d)} |
| -10.1 | -10.2 | -8.09 | 1.00 | 1.00 | 1.00 |
| -5.05 | -6.1 | -4.86 | 2.67 | 2.53 | 2.33 |
| 10.1 | 2.8 | 3.32 | 2.33 | 0.72 | 0.83 |
| | 11.0 | 10.09 | | 1.60 | 1.17 |

- a) The energy shift is measured from the free molecule value.
- b) The intensities for the polarization XY + XZ are normalized to that for the lowest spectrum.
- c) The molecular field approximation.
- d) Data for D_2 based on Ref.7). The origin of the energy is taken as $\bar{\nu}_0 = 178.66\text{cm}^{-1}$.
- e) The energy is scaled by $\Gamma = 0.805\text{cm}^{-1}$ after II.

Figure Captions

- Fig. 1. Schema for energy levels. (a): the energy levels without anharmonic process. (b): the density of states with anharmonic processes.
- Fig. 2. Diagrams for $\Sigma_{11}^{(2)}$, Σ_{02} , Σ_{20} and $\Sigma_{11}^{(3)}$.
- Fig. 3. Curves for $-(1/24\pi) \sum_{j \neq 0} \sum_m \text{Im}[\hat{G}(E)]_{jm,jm}$ vs. E/Γ . The solid line shows the density of states in the presence of a impurity and the broken one that for the perfect $J=1$ system.
- Fig. 4. Diagrammatic representation for the Dyson equation.
- Fig. 5. Curves for $\sum_{nn}^v(E)$ vs. $(E - 6B)/\Gamma$. The solid lines stand for $n=2^\pm$, the broken ones for $n=1^\pm$ and the dotted broken ones for $n=0$.
- Fig. 6. Density of states $-(1/\pi) \text{Im}[\hat{D}_{mm}^v(E)]$ as a function of $(E - 6B)/\Gamma$. The area under the curve with each value of m is normalized to unity. The sharp spectra for $m=0$ and $m=\pm 1$, which are located at -10.2Γ and -6.1Γ , have the area of 0.96 and 0.91, respectively.
- Fig. 7. Raman intensities for the polarization $XY + XZ$ as a function of $(E - 6B)/\Gamma$. The theoretical curve represented by a broken line is obtained by the convolution with a Lorentzian instrumental line-shape function of width 1.25cm^{-1} . Here Γ is taken to be 0.805cm^{-1} , and $6B = 178.66\text{cm}^{-1}$ for $p\text{-D}_2$ in accord with the experiment.⁷⁾

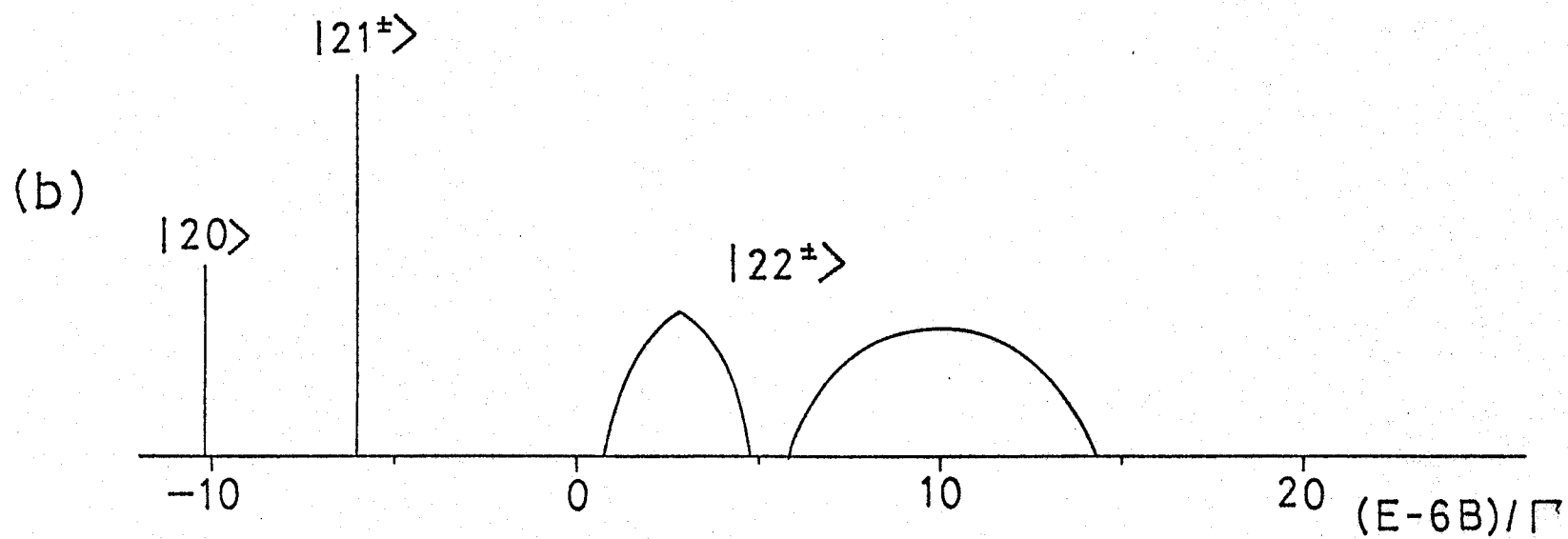
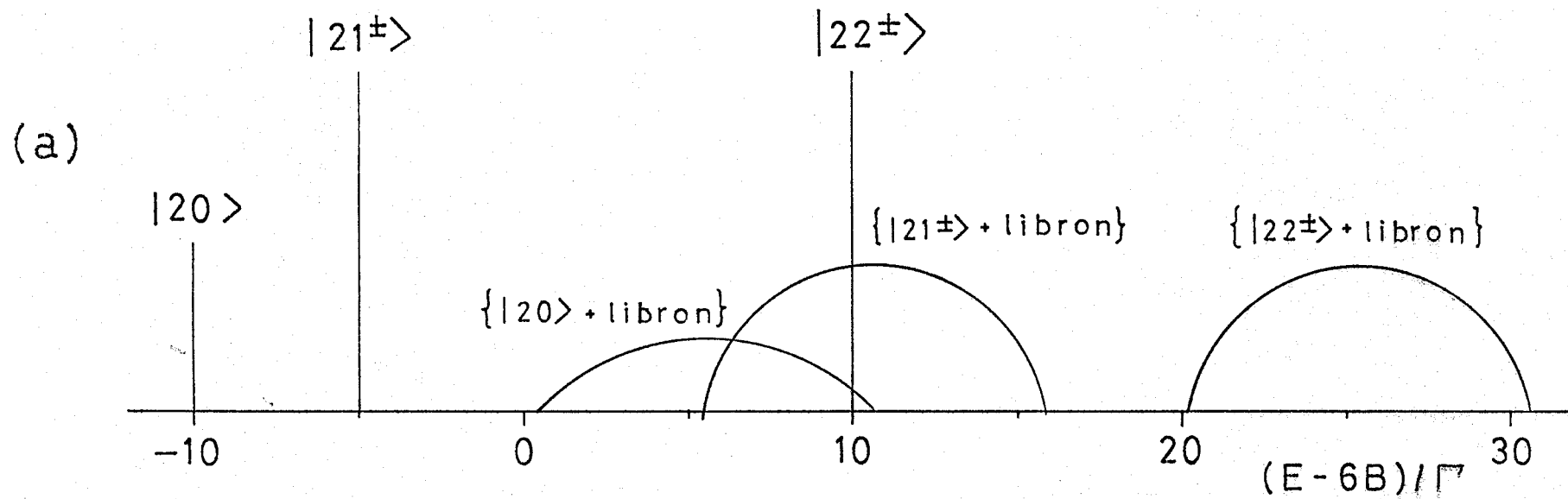


Fig.1

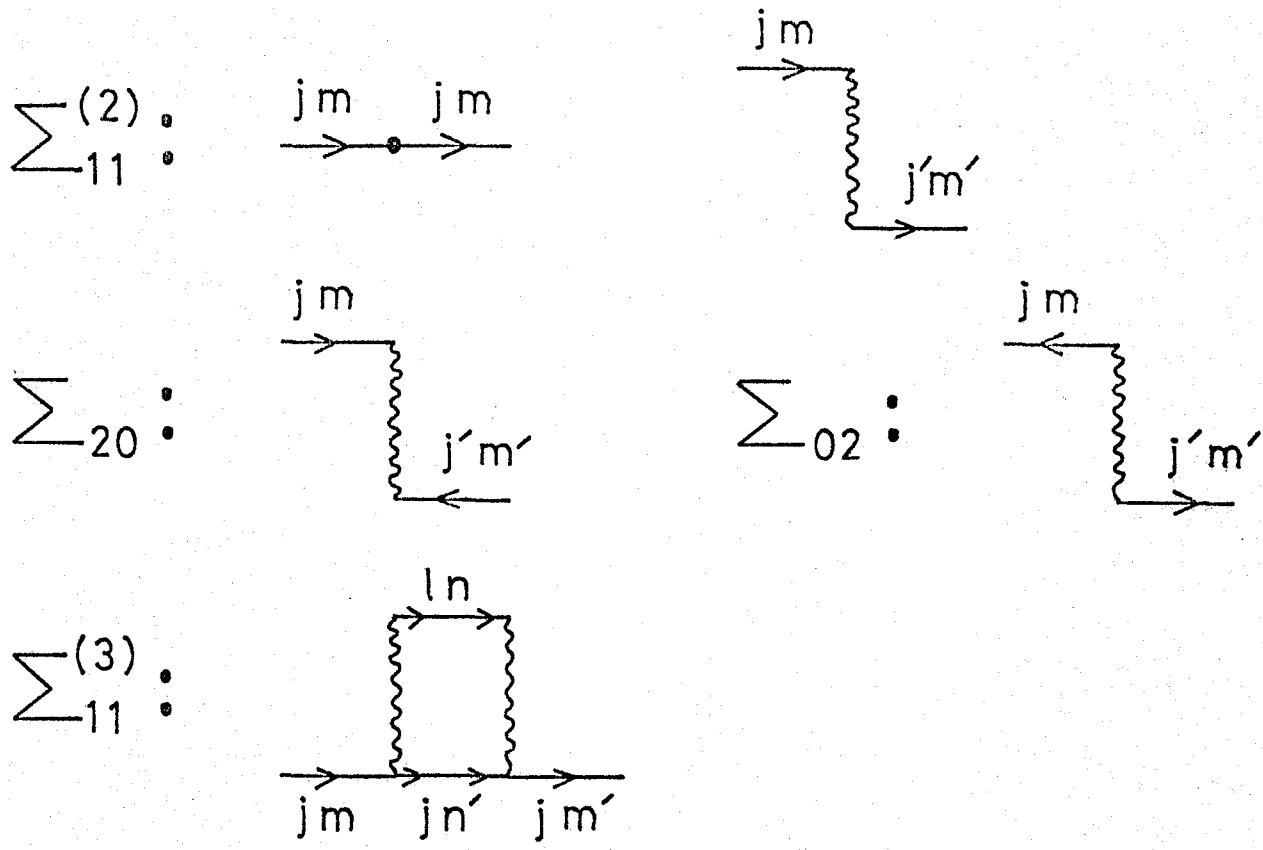
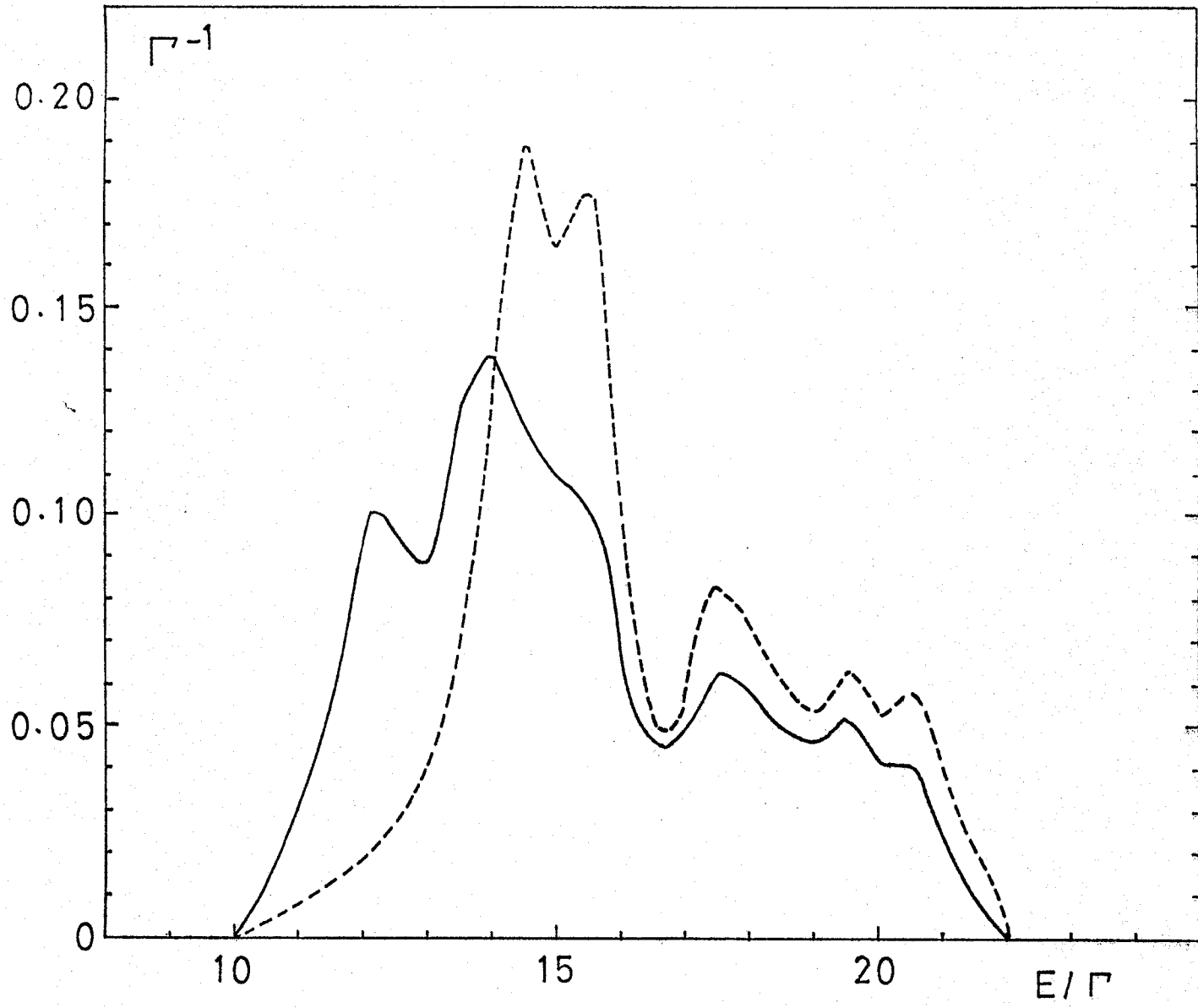


Fig. 2



III-30
Fig. 3

Dyson's equation

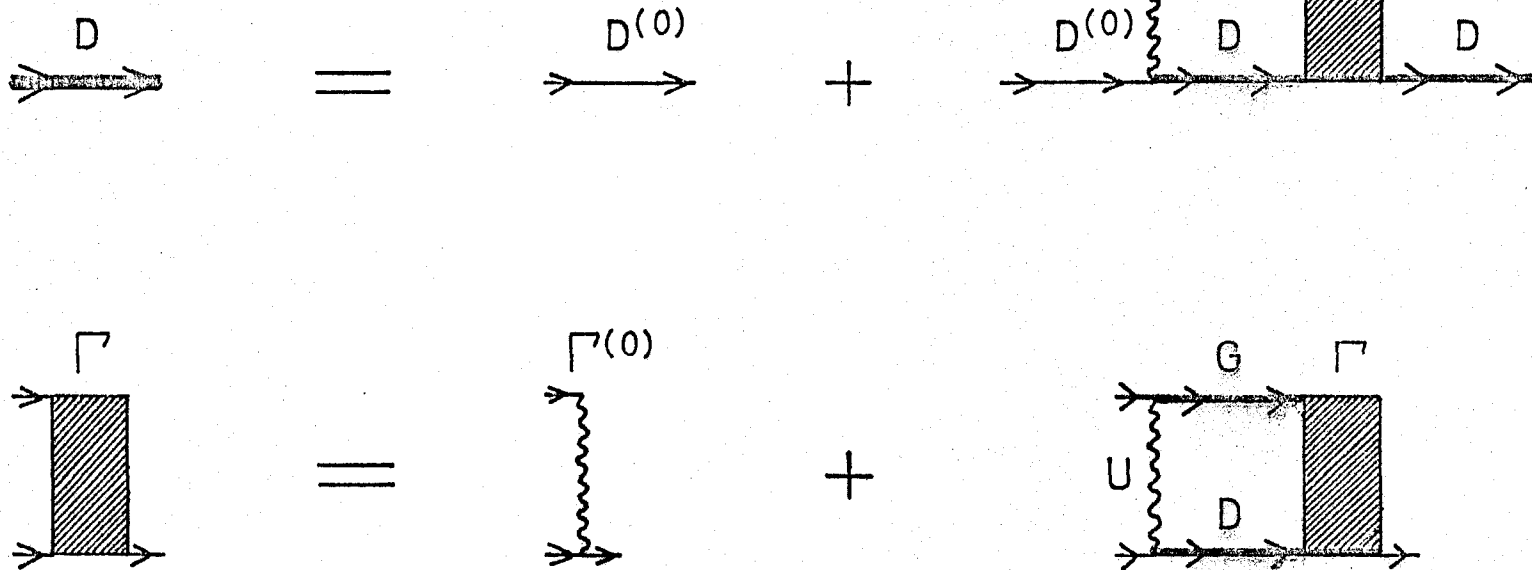
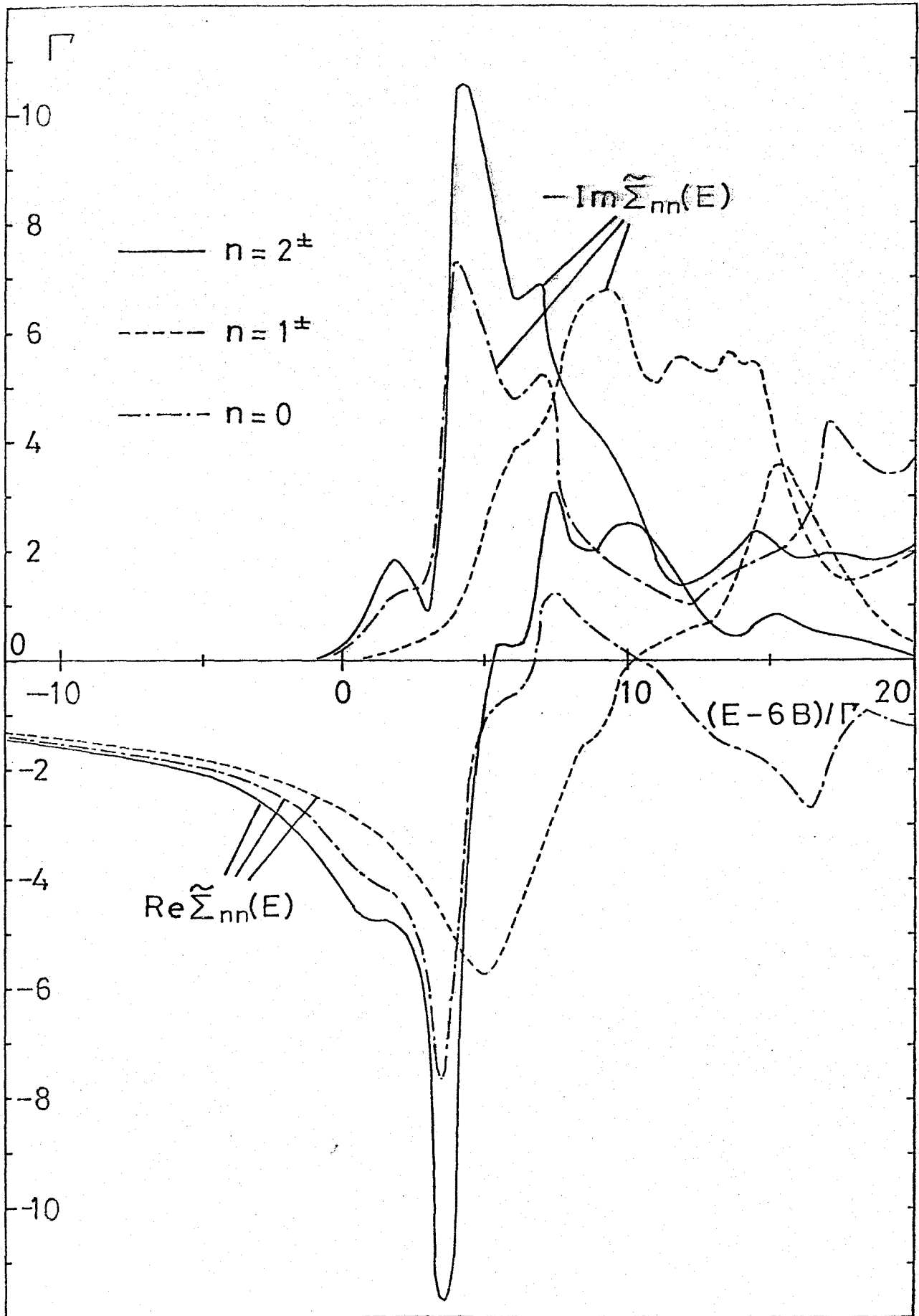


Fig. 4

Fig. 5



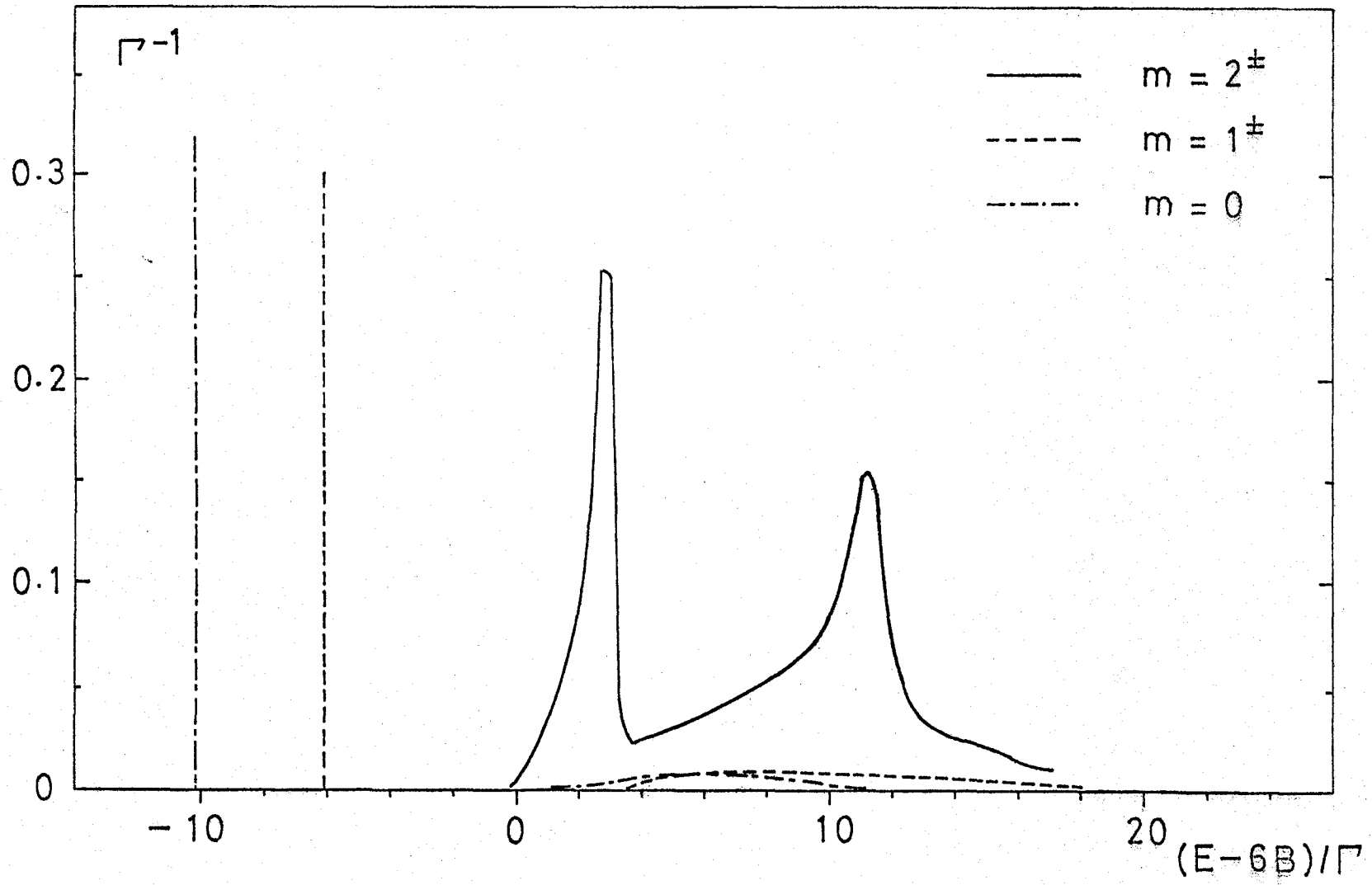


Fig. 6

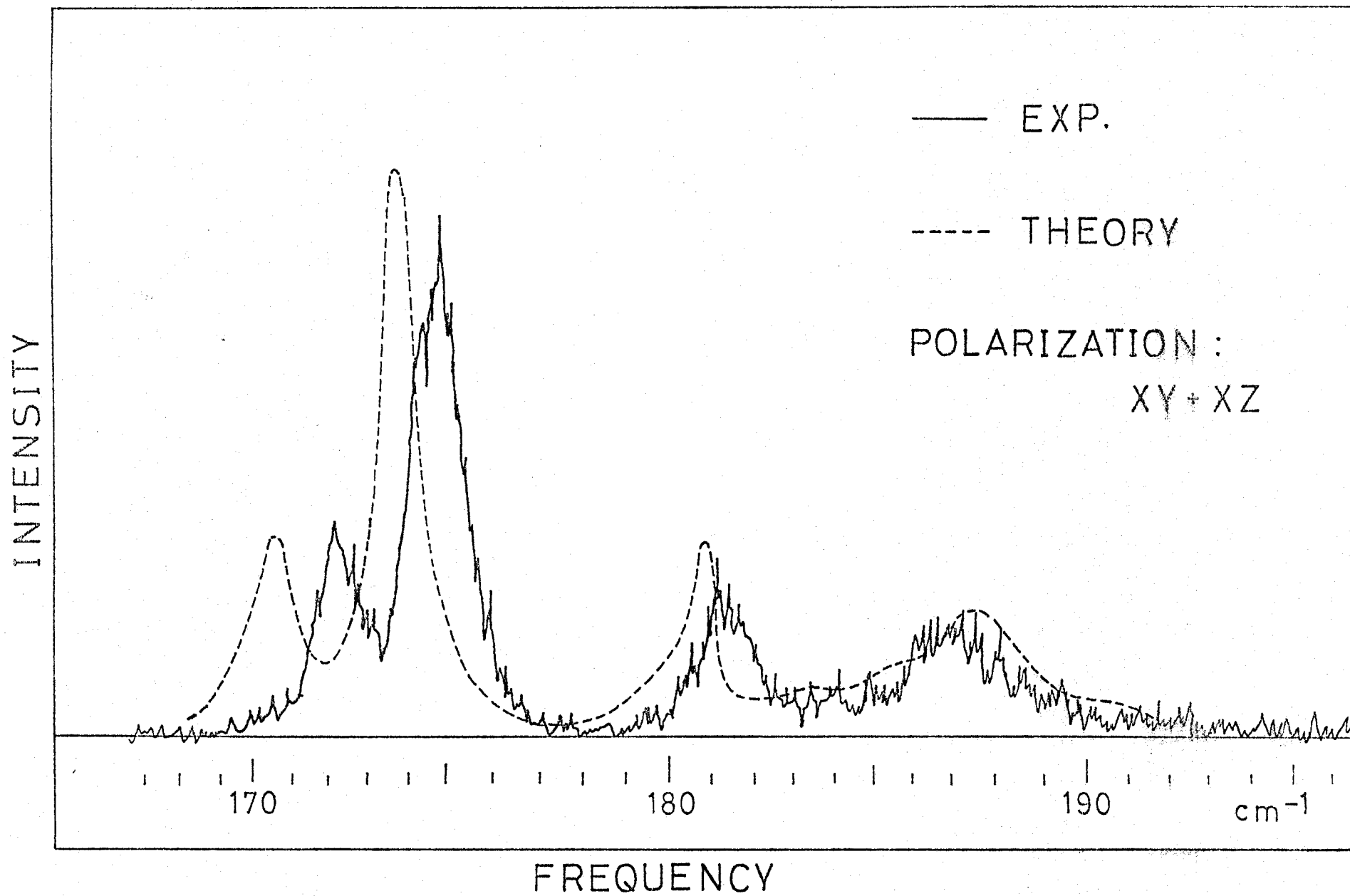


Fig. 7

Part IV

Polarization Effect on the Excitations
in the Ordered Solid Hydrogen

In the ordered solid hydrogen, the polarization effect on the excitation energies of $k=0$ librions ($J=1$ excitations) is studied in the first order of Γ/B , where B is the rotational constant and Γ the electric quadrupole-quadrupole coupling parameter. The similar effect on $J=2$ rotons in the presence of a parahydrogen is also studied. The inclusion of the polarization effect has improved the results without it.

§1. Introduction

In the previous parts referred to as II and III, we have studied the rotational excitations in the ordered solid hydrogen. In II, we have studied the anharmonic effect on both roton ($J=3$ excitations) and libron systematically for pure ortho-hydrogen system in good agreement with the Raman scattering experiment.¹⁾ In III, we have also studied the localized excitations ($J=2$ roton) due to parahydrogen. We have shown a strong anharmonic effect to exist for $J=2$ rotons in good agreement with the experiment.¹⁾ However the theoretical peak positions have slightly shifted from the experimental ones.

In this part, we study the neglected effect of the first order in Γ/B , where B is the rotational constant and Γ the EQQ coupling parameter with the similar notations to II and III. The mentioned effect is important at high pressures, because Γ/B increases there.

First Fujio and Nakamura²⁾ have calculated the energy shift for the $k=0$ libron by taking into account the effect of the virtual excitation to $J=3$ states. However their calculation is based on the harmonic theory. Then Harris et al.³⁾ evaluated the average energy shift for libron by constructing the effective Hamiltonian based on the second order perturbation. The renormalized value of Γ , deduced from the $k=0$ spectrum, seems more consistent with the other experiments.³⁾

First, we evaluate the polarization correction to the $k=0$ libron modes. The average energy shift obtained from the present treatment is smaller than the previous ones by Harris et al. It is noted here that the mode-dependence of the energy shifts is rather small. Secondly we evaluate the similar correction to the energy of $J=2$ rotons in good agreement with experiments.¹⁾ In §2 the correction to the energy of the $k=0$ libron is evaluated. The roton for $J=2$ is treated in §3.

§2. Correction to the $k=0$ libron energy

Let us first consider the pure orthohydrogen ($J=\text{odd}$) system. In §2 of II, we have given the representation for the EQQ interactions in terms of boson operators, where the terms responsible for the non-conserving processes in the number of rotons are neglected. Note that B is considerably large compared with the EQQ coupling constant. Taking account of the neglected terms, we shall now write down the total Hamiltonian as

$$H = H_0 + H^L + H_1^R + H_{\text{kin}}^R + H_2^{RL} + H_3^{RL} + H_4^{RL} + \dots \quad (2.1)$$

Here H_0 denotes the energy of the classical ground state, and H^L the Hamiltonian for librions. Their expressions have been given already. The notations follow the previous parts.

The other terms are new and may be given by the followings:

$$H_1^R = \langle 30 | z_2 | 10 \rangle \langle 10 | z_2 | 10 \rangle \sum_{\alpha \beta} (\sum f_{22}^{\alpha\beta}(0)) (N/4)^{1/2} \{c_{\alpha 0}^\dagger(0) + c_{\alpha 0}(0)\} \quad (2.2)$$

$$H_{kin}^R = 10B \sum_k \sum_{\alpha m} c_{\alpha m}^\dagger(k) c_{\alpha m}(k) \quad (2.3)$$

$$H_2^{RL} = \sum_k [\sum_{\alpha \beta} \sum_{mn} \langle 3m | z_2 | 1n \rangle \langle 10 | z_2 | 10 \rangle f_{22}^{\alpha\beta}(0) \{c_{\alpha m}^\dagger(k) a_{\alpha n}(k) + h.c.\} \\ + \sum_{\alpha \beta} \sum_{\mu\nu} \sum_{mn} \langle 3m | z_\mu | 10 \rangle \langle 1n | z_\nu | 10 \rangle f_{\mu\nu}^{\alpha\beta}(-k) \\ \cdot \{c_{\alpha m}^\dagger(k) + c_{\alpha m}(-k)\} \{a_{\beta n}^\dagger(-k) + a_{\beta n}(k)\}] \quad (2.4)$$

$$H_3^{RL} = (4/N)^{1/2} \sum_k \sum_{q\alpha\beta} [\sum_m (-1/2) \langle 30 | z_2 | 10 \rangle \langle 10 | z_2 | 10 \rangle f_{22}^{\alpha\beta}(0) \\ \cdot \{c_{\alpha 0}^\dagger(k-q) a_{\alpha m}^\dagger(q) a_{\alpha m}(k) + h.c.\} \\ + (1/2) \sum_{mm'n} \sum_{\mu\nu} \langle 3m | z_\mu | 10 \rangle \{ \langle 1m' | z_\nu | 1n \rangle - \langle 10 | z_\nu | 10 \rangle \delta_{m'n} \} \\ \cdot f_{\mu\nu}^{\alpha\beta}(-k) \{c_{\alpha m}^\dagger(k) + c_{\alpha m}(-k)\} \{a_{\beta m'}^\dagger(q) a_{\beta n}(k+q) + h.c.\} \\ + \sum_{\mu\nu} \sum_{mnn'} \langle 1n | z_\mu | 10 \rangle \langle 3m | z_\nu | 1n' \rangle f_{\mu\nu}^{\alpha\beta}(-k) \\ \cdot \{a_{\alpha n}^\dagger(k) + a_{\alpha n}(-k)\} \{c_{\beta m}^\dagger(q) a_{\beta n'}(k+q) + h.c.\} \\ + \sum_{\mu\nu} \sum_{mm'n} \langle 3m | z_\mu | 10 \rangle \langle 3m' | z_\nu | 1n \rangle f_{\mu\nu}^{\alpha\beta}(-k) \\ \cdot \{c_{\alpha m}^\dagger(k) + c_{\alpha m}(-k)\} \{c_{\beta m'}^\dagger(q) a_{\beta n}(k+q) + h.c.\}] , \quad (2.5)$$

$$\begin{aligned}
H_4^{RL} = & (4/N) \sum_k \sum_{k'} \sum_q \sum_{\alpha\beta} \sum_{\mu\nu} \left[\sum_{mnn'} (-1/2) \langle 1n' | z_\mu | 10 \rangle \langle 3m | z_\nu | 10 \rangle f_{\mu\nu}^{\alpha\beta}(-k') \right. \\
& \cdot \{ a_{\alpha n'}^\dagger(k+k'-q) a_{\alpha n}^\dagger(q) a_{\alpha n}(k) + \text{h.c.} \} \{ c_{\beta m}(k') + c_{\beta m}^\dagger(-k') \} \\
& + \sum_{mnn'} (-1/2) \langle 3m | z_\mu | 10 \rangle \langle 1n' | z_\nu | 10 \rangle f_{\mu\nu}^{\alpha\beta}(-k') \\
& \cdot \{ c_{\alpha m}^\dagger(k+k'-q) a_{\alpha n}^\dagger(q) a_{\alpha n}(k) + \text{h.c.} \} \{ a_{\beta n'}(k') + a_{\beta n'}^\dagger(-k') \} \\
& + \sum_{mm'n} (-1/2) \langle 3m | z_\mu | 10 \rangle \langle 3m' | z_\nu | 10 \rangle f_{\mu\nu}^{\alpha\beta}(-k') \\
& \cdot \{ c_{\alpha m}^\dagger(k+k'-q) a_{\alpha n}^\dagger(q) a_{\alpha n}(k) + \text{h.c.} \} \{ c_{\beta m'}(k') + c_{\beta m'}^\dagger(-k') \} \left. \right] .
\end{aligned} \tag{2.6}$$

In the above expressions, H_1^R is the primary term for the polarization, H_{kin}^R the rotational kinetic energy and H_2^{RL} , H_3^{RL} and H_4^{RL} the libron-roton interactions without conserving the number of rotons as classified by the number of operators. The notation follows II, where the previous annihilation operator $a_{\alpha m}(k)$ associated with roton is now replaced by $c_{\alpha m}(k)$. In deriving Eqs.(2.5) and (2.6), we expand $f \equiv (1 - \sum_m a_m^\dagger a_m)^{1/2}$ as $1 - (1/2) \sum_m a_m^\dagger a_m + \dots$. And we utilize

$$\sum_j f_{\mu 2}(i,j) = 0 \quad \text{for } \mu \neq 2. \tag{2.7}$$

In order to eliminate H_1^R we use the following unitary transform:

$$U = \exp \left[(N/4)^{1/2} \sum_{\alpha} g_{\alpha} \{c_{\alpha 0}^{\dagger}(0) - c_{\alpha 0}(0)\} \right] . \quad (2.8)$$

The transformed Hamiltonian is given by

$$H' = U^{-1} H U , \quad (2.9)$$

where

$$\begin{aligned} H_{\text{kin}}^{R'} &= U^{-1} H_{\text{kin}}^R U \\ &= H_{\text{kin}}^R + 10B(N/4) \sum_{\alpha} g_{\alpha}^2 \\ &\quad + 10B(N/4)^{1/2} \sum_{\alpha} g_{\alpha} \{c_{\alpha 0}^{\dagger}(0) + c_{\alpha 0}(0)\} . \end{aligned} \quad (2.10)$$

If we choose g_{α} to be

$$\begin{aligned} g \equiv g_{\alpha} &= \frac{-1}{10B} \langle 30 | z_2 | 10 \rangle \langle 10 | z_2 | 10 \rangle \sum_{\beta} f_{22}^{\alpha\beta}(0) \\ &= 1.388 \Gamma/B , \end{aligned} \quad (2.11)$$

then H_1^R cancels the third terms in the right-hand side of Eq.(2.10). Thus g_{α} proves to be very small, since Γ/B is very small. The other parts of the transformed Hamiltonian are given by

$$H_2^{RL'} = U^{-1} H_2^{RL} U = H_2^{RL} \quad (2.12)$$

$$H_3^{RL'} = U^{-1} H_3^{RL} U$$

$$\begin{aligned}
&= H_3^{RL} + g \sum_k \sum_{\alpha\beta} [\sum_n \langle 30|z_2|10\rangle \{2\langle 1n|z_2|1n\rangle - 3\langle 10|z_2|10\rangle\} \\
&\quad \cdot f_{22}^{\alpha\beta}(0) a_{\alpha n}^\dagger(k) a_{\alpha n}(k) \\
&+ \sum_{\mu\nu} \sum_{mn} \langle 1n|z_\mu|10\rangle \langle 30|z_\nu|1n\rangle f_{\mu\nu}^{\alpha\beta}(-k) \\
&\quad \cdot \{a_{\alpha n}^\dagger(k) + a_{\alpha n}(-k)\} \{a_{\beta n}(k) + a_{\beta n}^\dagger(-k)\} \\
&+ \sum_{\mu\nu} \sum_{mn} \langle 3m|z_\mu|10\rangle \langle 30|z_\nu|1n\rangle f_{\mu\nu}^{\alpha\beta}(-k) \\
&\quad \cdot \{c_{\alpha m}^\dagger(k) + c_{\alpha m}(-k)\} \{a_{\beta n}(k) + a_{\beta n}^\dagger(-k)\} \\
&+ 2 \sum_{mn} \langle 30|z_2|10\rangle \langle 3m|z_2|1n\rangle f_{22}^{\alpha\beta}(0) \{c_{\beta m}^\dagger(k) a_{\beta n}(k) + \text{h.c.}\} \\
&+ \sum_{\mu\nu} \sum_{mn} \langle 3m|z_\mu|10\rangle \langle 30|z_\nu|1n\rangle f_{\mu\nu}^{\alpha\beta}(-k) \\
&\quad \cdot \{c_{\alpha m}^\dagger(k) + c_{\alpha m}(-k)\} \{a_{\beta n}(k) + a_{\beta n}^\dagger(-k)\} + (\text{constant term}).
\end{aligned} \tag{2.13}$$

We neglect the effect of the transformation on H_4^{RL} .

Let us consider the $k=0$ libron Green's function on the same footing as in II with correction terms of the order Γ/B to the self-energy parts.

From the second and third terms in Eq.(2.13) we have the correction to $\tilde{\Sigma}_{11}$, $\tilde{\Sigma}_{20}$ in the unit of Γ^2/B as follows.

$$\tilde{\Delta\Sigma}_{11} : \quad E_g \quad (88.4) \quad T_g \quad \begin{pmatrix} 78.9 & -8.7 \\ -8.7 & 64.3 \end{pmatrix} \begin{matrix} |\Delta_0, 11^+\rangle \\ |\Delta_2, 11^+\rangle \\ |\Delta_0, 11^-\rangle \end{matrix}, \quad (2.14)$$

$$\tilde{\Delta\Sigma}_{20} : \quad E_g \quad (11.3) \quad T_g \quad \begin{pmatrix} 1.8 & -8.7 \\ -8.7 & -12.9 \end{pmatrix} \begin{matrix} |\Delta_0, 11^+\rangle \\ |\Delta_2, 11^+\rangle \\ |\Delta_0, 11^-\rangle \end{matrix}. \quad (2.15)$$

In the above expression the designation of the $k=0$ libron states refers to II. By using Eq.(2.4) and taking account of the processes shown in Fig. 1, we also have

$$\tilde{\Delta\Sigma}_{11} : \quad E_g \quad (-38.0) \quad T_g \quad \begin{pmatrix} -31.6 & 2.9 \\ 2.9 & -33.2 \end{pmatrix} \begin{matrix} |\Delta_0, 11^+\rangle \\ |\Delta_2, 11^+\rangle \\ |\Delta_0, 11^-\rangle \end{matrix}, \quad (2.16)$$

$$\tilde{\Delta\Sigma}_{20} : \quad E_g \quad (-25.2) \quad T_g \quad \begin{pmatrix} -18.8 & 2.9 \\ 2.9 & -20.4 \end{pmatrix} \begin{matrix} |\Delta_0, 11^+\rangle \\ |\Delta_2, 11^+\rangle \\ |\Delta_0, 11^-\rangle \end{matrix}. \quad (2.17)$$

By combining the second, third and fourth terms in Eq.(2.5), we have the following results (See Fig. 2):

$$\tilde{\Delta\Sigma}_{11} : \quad E_g \quad (-46.5) \quad T_g \quad \begin{pmatrix} -42.5 & 1.8 \\ 1.8 & -35.1 \end{pmatrix} \begin{matrix} |\Delta_0, 11^+\rangle \\ |\Delta_2, 11^+\rangle \\ |\Delta_0, 11^-\rangle \end{matrix}. \quad (2.18)$$

In the above expression we neglect the contribution from the repeated processes due to the first term of Eq.(2.5), since these processes may be of the higher order. (The inclusion of this term does not alter the result significantly.)

Let us further take account of the combined actions of H_2^{RL} and H_4^{RL} , which are shown diagrammatically in Fig. 3. The result becomes

$$\tilde{\Delta\Sigma}_{11} : \quad E_g \quad (29.3) \quad T_g \quad \begin{pmatrix} 29.3 & 0 \\ 0 & 29.3 \end{pmatrix} \begin{matrix} |\Delta_0, 11^+\rangle \\ |\Delta_2, 11^+\rangle \\ |\Delta_0, 11^-\rangle \end{matrix}. \quad (2.19)$$

In the calculation of Eqs.(2.18) and (2.19), the interactions are confined to the nearest neighbors. Note that $\Delta\Sigma_{20}^{\lambda} = \Delta\Sigma_{02}^{\lambda}$.

Let us consider the energy shift for each mode. Expanding Eq.(5.13) of II in a small parameter Γ/B , we have

$$\begin{aligned}
[G_{\lambda}^L(\epsilon)]^{-1} &= (\epsilon - \omega_0)I_{\lambda} - \Sigma_{\lambda}^{(2)} - \Sigma_{\lambda}^{(3)}(\epsilon) \\
&+ \Sigma_{\lambda}^{(2)} [(\epsilon + \omega_0)I_{\lambda} + \Sigma_{\lambda}^{(2)} + \Sigma_{\lambda}^{(3)}(-\epsilon)]^{-1} \Sigma_{\lambda}^{(2)} \\
&- \Delta\tilde{\Sigma}_{11}^{\lambda} + \Delta\tilde{\Sigma}_{20}^{\lambda} [(\epsilon + \omega_0)I_{\lambda} + \Sigma_{\lambda}^{(2)} + \Sigma_{\lambda}^{(3)}(-\epsilon)]^{-1} \Sigma_{\lambda}^{(2)} \\
&+ \Sigma_{\lambda}^{(2)} [(\epsilon + \omega_0)I_{\lambda} + \Sigma_{\lambda}^{(2)} + \Sigma_{\lambda}^{(3)}(-\epsilon)]^{-1} \Delta\tilde{\Sigma}_{02}^{\lambda} \\
&- \Sigma_{\lambda}^{(2)} [(\epsilon + \omega_0)I_{\lambda} + \Sigma_{\lambda}^{(2)} + \Sigma_{\lambda}^{(3)}(-\epsilon)]^{-1} \\
&\quad \cdot \Delta\tilde{\Sigma}_{11}^{\lambda} [(\epsilon + \omega_0)I_{\lambda} + \Sigma_{\lambda}^{(2)} + \Sigma_{\lambda}^{(3)}(-\epsilon)]^{-1} \Sigma_{\lambda}^{(2)}, \quad \lambda = 2, 3.
\end{aligned} \tag{2.20}$$

Here the corrections to the self-energy parts are taken to be the E_g -part for $\lambda=2$ and the T_g -part for $\lambda=3$, respectively. We note that E_g part is 1×1 and T_g part is 2×2 matrix. The terms in the first two lines of Eq.(2.20) stand for the zero-th order terms as given in II. Let these be the unperturbed part and the remainders be the perturbed one. By this way we shall perform a perturbation calculation. Thus we expand the unperturbed matrices in $\epsilon - \epsilon_0$, where ϵ_0 denotes the excitation energy in the zero-th order, while ϵ_0 is substituted into ϵ

for the perturbed matrices. The matrices coming from the unperturbed one, being linear in $\epsilon - \epsilon_0$, must cancel the remainders from the perturbed one in the sense of the average, where the average is taken over the relevant eigenvector of the unperturbed matrix.

The resultant energy shifts are given by

$$\Delta\epsilon(E_g) = 30.0 ,$$

$$\Delta\epsilon(T_g^{(1)}) = 32.4 , \quad \Delta\epsilon(T_g^{(2)}) = 35.8 \quad (2.21)$$

in units of Γ^2/B .

The average energy shift proves to be 33.1 which is compared with 45.2 obtained by Harris et al. The difference comes from the neglect of the site nondiagonal correction to $\tilde{\Sigma}_{11}$ and the neglect of $\tilde{\Sigma}_{20}$ and $\tilde{\Sigma}_{02}$ by the mentioned authors, as will be discussed in Appendix. The effective value of Γ is determined by the comparison of our theoretical energies with the Raman experiment.¹⁾ The values are shown in Table I in good agreement with other experiments.

§3. Correction to the J=2 localized rotors

Let us consider the orthohydrogen system containing a parahydrogen as a impurity at the origin. By the similar procedure as in §2, we write down the total Hamiltonian as

$$H = H^L + H^R + h_1 + H_1^R + H_{kin}^R + h_{kin} + h_2 + h_3 + h_4 + \dots \quad (3.1)$$

Here H^L and H^R are the Hamiltonian of librions and $J=2$ rotors, which are given by Eqs.(2.5) and (2.10) of III, respectively.

The kinetic energy term of $J=2$ rotors is given by the first term of Eq.(2.10) in III. The kinetic energy of $J=4$ rotors and of $J=3$ rotors are given by

$$h_{kin} = 20B \sum_m d_m^\dagger(0) d_m(0) , \quad (3.2)$$

$$H_{kin}^R = 10B \sum_m \sum_{j \neq 0} c_m^\dagger(j) c_m(j) , \quad (3.3)$$

respectively. Here we introduce the creation operator $d_m^\dagger(0)$, such that $d_m^\dagger(0)|00\rangle \equiv |4m\rangle$.

The terms of H_1^R , h_1 , h_2 , h_3 and h_4 are responsible for the non-conserving processes of the roton number and given by

$$h_1 = \langle 20 | z_2 | 10 \rangle \langle 10 | z_2 | 10 \rangle \sum_j f_{22}(0,j) \{ b_0^\dagger(0) + b_0(0) \} , \quad (3.4)$$

$$H_1^R = \langle 30 | z_2 | 10 \rangle \langle 10 | z_2 | 10 \rangle \sum_{i,j \neq 0} f_{22}(i,j) \{ c_0^\dagger(i) + c_0(i) \} , \quad (3.5)$$

$$h_2 = \sum_j \sum_{\mu\nu} \sum_m \langle 2m | z_\mu | 00 \rangle \{ b_m^\dagger(0) + b_m(0) \} f_{\mu\nu}(0,j)$$

$$\cdot \left[\sum_n \langle 1n | z_\nu | 10 \rangle \{ a_n^\dagger(j) + a_n(j) \} \right]$$

$$\begin{aligned}
& + \sum_{m'} \langle 3m' | z_\nu | 10 \rangle \{ c_{m'}^\dagger(j) + c_{m'}(j) \} \\
& + \langle 20 | z_2 | 40 \rangle \langle 10 | z_2 | 10 \rangle \sum_j f_{22}(0, j) \{ d_0^\dagger(0) b_0(0) + \text{h.c.} \}, \quad (3.6)
\end{aligned}$$

$$\begin{aligned}
h_3 &= \sum_j \sum_m (-1/2) \langle 20 | z_2 | 00 \rangle \langle 10 | z_2 | 10 \rangle f_{22}(0, j) \\
& \quad \cdot \{ b_0^\dagger(0) b_m^\dagger(0) b_m(0) + \text{h.c.} \} \\
& + \sum_j \sum_{\mu\nu} \sum_{mm'n} \langle 2m | z_\mu | 2m' \rangle \langle 3n | z_\nu | 10 \rangle f_{\mu\nu}(0, j) \\
& \quad \cdot b_m^\dagger(0) b_{m'}(0) \{ c_n^\dagger(j) + c_n(j) \} \\
& + \sum_j \sum_{\mu\nu} \sum_{m'm} \langle 4m | z_\mu | 2m' \rangle \{ d_m^\dagger(0) b_{m'}(0) + \text{h.c.} \} f_{\mu\nu}(0, j) \\
& \quad \cdot [\sum_n \langle 1n | z_\nu | 10 \rangle \{ a_n^\dagger(j) + a_n(j) \} \\
& \quad + \sum_{n'} \langle 3n' | z_\nu | 10 \rangle \{ c_{n'}^\dagger(j) + c_{n'}(j) \}] \quad (3.7)
\end{aligned}$$

$$\begin{aligned}
h_4 &= \sum_j \sum_{\mu\nu} \sum_{mm'} (-1/2) \langle 2m | z_\mu | 00 \rangle f_{\mu\nu}(0, j) \\
& \quad \cdot \{ b_m^\dagger(0) b_{m'}^\dagger(0) b_{m'}(0) + \text{h.c.} \} \\
& \quad \cdot [\sum_n \langle 1n | z_\nu | 10 \rangle \{ a_n^\dagger(j) + a_n(j) \} \\
& \quad + \sum_{n'} \langle 3n' | z_\nu | 10 \rangle \{ c_{n'}^\dagger(j) + c_{n'}(j) \}] \quad (3.8)
\end{aligned}$$

Now we introduce the following canonical transformation:

$$S = \exp\left[\sum_{j \neq 0} g(j)\{c_0^\dagger(j) - c_0(j)\} + g(0)\{b_0^\dagger(0) - b_0(0)\}\right]. \quad (3.9)$$

Then we have the transformed Hamiltonian

$$H' = S^{-1} H S. \quad (3.10)$$

The kinetic energy terms are transformed as

$$\begin{aligned} S^{-1} (6B \sum_m b_m^\dagger(0) b_m(0)) S \\ = 6B \sum_m b_m^\dagger(0) b_m(0) + 6Bg(0)\{b_0^\dagger(0) + b_0(0)\} + 6Bg(0)^2, \end{aligned} \quad (3.11)$$

$$S^{-1} H_{\text{kin}}^R S = H_{\text{kin}}^R + 10B \sum_{j \neq 0} g(j)\{c_0^\dagger(j) + c_0(j)\} + 10B \sum_{j \neq 0} g(j)^2. \quad (3.12)$$

The terms of h_1 and H_1^R cancel with the second terms of Eqs.(3.11) and (3.12) respectively, provided that

$$g(0) = (-1/6B) \langle 20 | z_2 | 00 \rangle \langle 10 | z_2 | 10 \rangle \sum_{\ell} f_{22}(0, \ell), \quad (3.13)$$

$$g(j) = (-1/10B) \langle 30 | z_2 | 10 \rangle \langle 10 | z_2 | 10 \rangle \sum_{i \neq 0} f_{22}(j, i), \quad \text{for } j \neq 0. \quad (3.14)$$

In the transformed Hamiltonian, the corrections coming from Eq.(3.6) and Eqs.(2.11) and (2.12), both of the latter equations in III, are neglected, since they are of the higher order correction in Γ/B to the energy of $J=2$ rotons.

The other parts of the transformed Hamiltonian, which bring us the correction linear in Γ/B to the energy of the

J=2 rotons, are the followings:

$$\begin{aligned}
 S^{-1}h_3S &= h_3 - g(0)\langle 20|z_2|00\rangle\langle 10|z_2|10\rangle\{\sum_j f_{22}(0,j)\} \\
 &\quad \cdot [\sum_m b_m^\dagger(0)b_m(0)+b_0^\dagger(0)b_0(0)] \\
 &\quad + 2\sum_j \sum_{mm'} \sum_{\mu} g(j)\langle 2m|z_\mu|2m'\rangle\langle 30|z_2|10\rangle f_{\mu 2}(0,j)b_m^\dagger(0)b_{m'}(0) \\
 &\quad + (\text{remainder}) , \tag{3.15}
 \end{aligned}$$

where the remainders linear in Γ/B are non-diagonal in the unperturbed energy levels and hence may be neglected.

Let us consider the Green's function of the J=2 roton and the correction terms of the self-energy part. Then, from the second and the third terms of Eq.(3.15) we obtain the correction to the self-energy parts $\tilde{\Delta\Sigma}$, being diagonal in $|JM\rangle$:

$$\tilde{\Delta\Sigma}_{00} = 60.5, \quad \tilde{\Delta\Sigma}_{1\pm 1\pm} = 30.3, \quad \tilde{\Delta\Sigma}_{2\pm 2\pm} = 64.4, \tag{3.16}$$

in units of Γ^2/B and with double signs in order. The other processes bringing the correction are represented by the diagrams shown in Fig. 4. The corresponding values are given in Table II. The net results are estimated to be

$$\tilde{\Delta\Sigma}_{00} = 64.1, \quad \tilde{\Delta\Sigma}_{1\pm 1\pm} = 47.3, \quad \tilde{\Delta\Sigma}_{2\pm 2\pm} = 83.5 . \tag{3.17}$$

The curve for the Raman intensity with the corrections thus obtained is shown in Fig. 5, where the previous result

without correction is also plotted. As can be seen in Fig. 5, we have achieved a closer agreement with experiments, though the intensity at high frequency side is less well.

Appendix

In this Appendix we shall show how to get the previous results by Harris et al. by dropping partially the diagrams taken into account in our paper. Let us confine ourselves to the site diagonal parts of the correction to the self-energy as shown in Fig. 6. If the virtual creation processes are assumed to occur to the nearest neighbors, the estimated corrections to the self-energy $\tilde{\Sigma}_{11}^v$ are given in the same figure. The correction to $\tilde{\Sigma}_{11}^v$ from the second terms in Eq.(2.13) is equal to $77.1\Gamma^2/B$. The net correction is proved to be $45.9\Gamma^2/B$, which is identical with the result of Harris et al.

References

- 1) W.N. Hardy, I.F. Silvera and J.P. McTague, Phys. Rev. B12 (1975), 753.
- 2) T. Nakamura, H. Miyagi and M. Fujio, in Proc. of the 20-th Intern. Conf. of Low-Temp. Phys., edited by Eizo Kanda (Academic of Japan, Kyoto, 1970). The corrected figures are seen in Ref. 1) as a private communication by T. Nakamura.
- 3) A.B. Harris, A.J. Berlinsky and H. Meyer, Phys. Rev. B7 (1973), 4720.

Table I Comparison of the $k=0$ libron energy with
the Raman experiment

| | Libron energy | | $\Gamma_{\text{eff}}^{\text{a)}$ | |
|-------------|--|--|--|---------------------------------|
| | Experiment ^{b)} (cm^{-1}) | Theory ^{c)} (without J=3 corrections) | without J=3 corrections (cm^{-1}) | Present (cm^{-1}) |
| D_2 | | | | |
| E_g | 9.18 ± 0.05 | 11.4Γ | 0.805 | 0.755 |
| $T_g^{(1)}$ | 11.35 ± 0.1 | 14.2Γ | 0.799 | 0.756 |
| $T_g^{(2)}$ | 15.50 ± 0.05 | 20.8Γ | 0.745 | 0.716 |
| H_2 | | | | |
| E_g | 6.75 ± 0.15 | 11.4Γ | 0.592 | 0.577 |
| $T_g^{(1)}$ | 8.58 ± 0.2 | 14.2Γ | 0.604 | 0.591 |
| $T_g^{(2)}$ | 11.80 ± 0.2 | 20.8Γ | 0.567 | 0.558 |

a) Estimates of Γ obtained by fitting theoretical energies to the experimental ones. ($B=30\text{cm}^{-1}$ for D_2 and $=60\text{cm}^{-1}$ for H_2 are used.)

b) Data based on Ref. 1).

c) Anharmonic theory given in part II.

Table II Polarization corrections to the self-energy parts of J=2 rotons.

| Diagram ^{a)} | $\Delta\Sigma_{00}$ | $\Delta\Sigma_{1\pm 1\pm}$ | $\Delta\Sigma_{2\pm 2\pm}$ |
|-----------------------|---------------------|----------------------------|----------------------------|
| (A) | -13.6 | -12.5 | -13.2 |
| (B) | -13.1 | 0 | 0 |
| (C) | -22.3 | -22.1 | -22.9 |
| (D) | 52.6 | 51.6 | 55.2 |

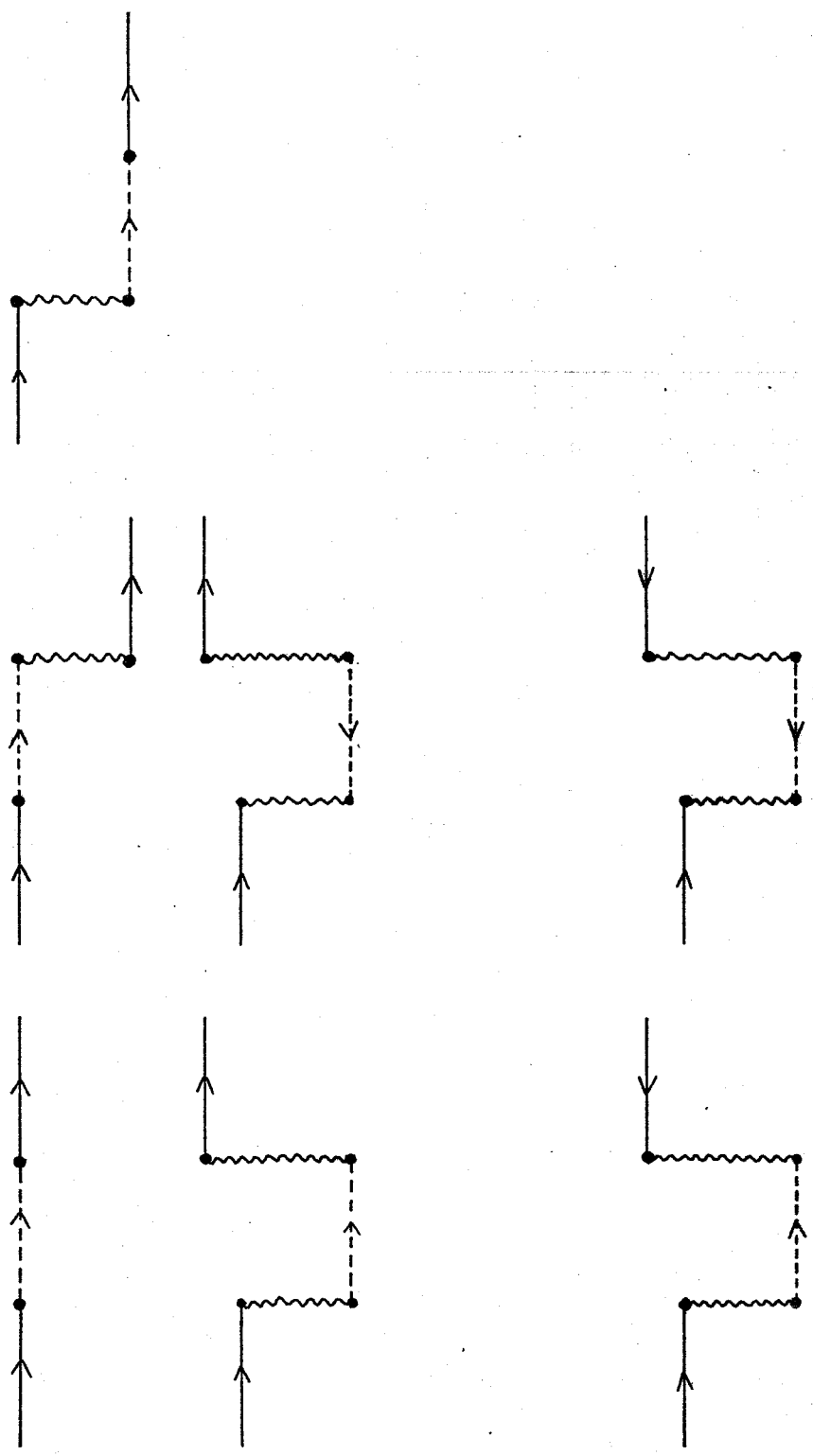
(unit: Γ^2/B)

a) The diagrams are in accordance with Fig. 4.

Figure Captions

- Fig. 1. Diagrams for $\Delta\tilde{\Sigma}_{11}^{\nu}$ and $\Delta\tilde{\Sigma}_{20}^{\nu}$ arising from Eq.(2.4). The solid lines represent the Green's functions of librons and the broken ones those of J=3 rotons. The wavy lines represent the EQQ interaction.
- Fig. 2. Diagrams for $\Delta\tilde{\Sigma}_{11}^{\nu}$ arising from Eq.(2.5). Notations are in accordance with Fig. 1.
- Fig. 3. Diagrams for $\Delta\tilde{\Sigma}_{11}^{\nu}$ arising from Eqs.(2.4) and (2.6). Notations are in accordance with Fig. 1.
- Fig. 4. Diagrams for $\Delta\tilde{\Sigma}_{mm}^{\nu}$. The solid lines represent the Green's functions for J=2 rotons and the dotted broken ones those for J=4 rotons. The broken lines represent the Green's functions for librons or those for J=3 rotons.
- Fig. 5. Raman intensities of J=0 \rightarrow 2 transition for D₂ as a function of (E-6B)/ Γ in the case for the polarization XY+XZ. The broken line represents the theoretical value without polarization effects. The theoretical curve with the polarization effect is represented by the dotted broken line. $\Gamma=0.755 \text{ cm}^{-1}$ and $B=30 \text{ cm}^{-1}$ for D₂ are used (See Table I).
- Fig. 6. Diagrams for $\Delta\tilde{\Sigma}_{11}^{\nu}$ relevant to the previous calculation by Harris et al. The solid lines represent the Green's functions for librons and the broken ones

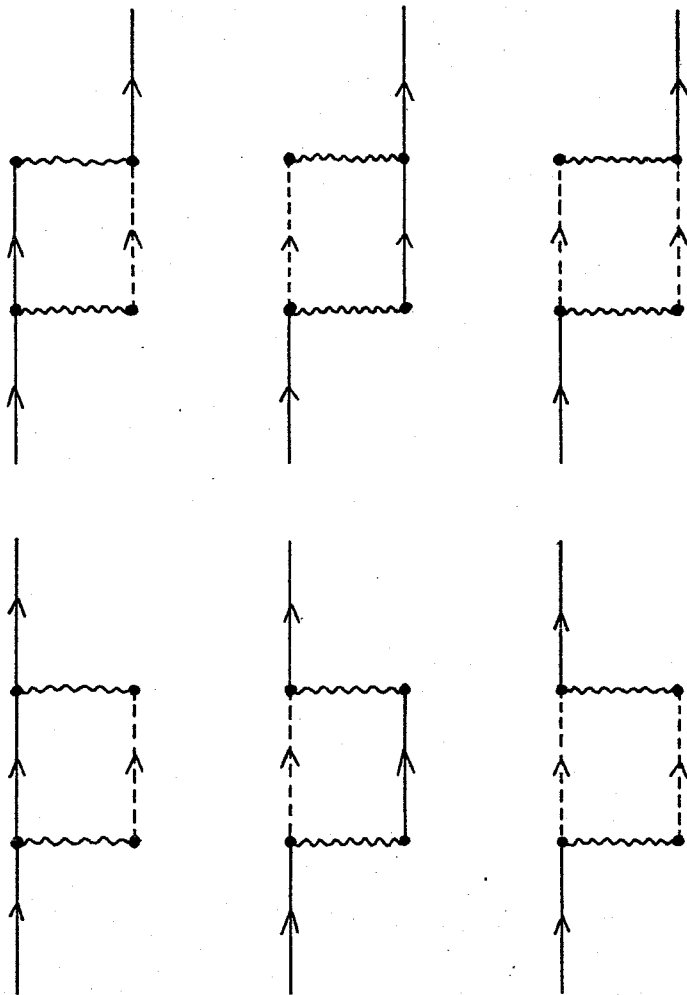
those for $J=3$ rotons in the site representation with i and j the lattice site. The evaluated value for the diagonal part of each diagram is shown in the right hand side of the figure.



$\Delta \Sigma_{11}$

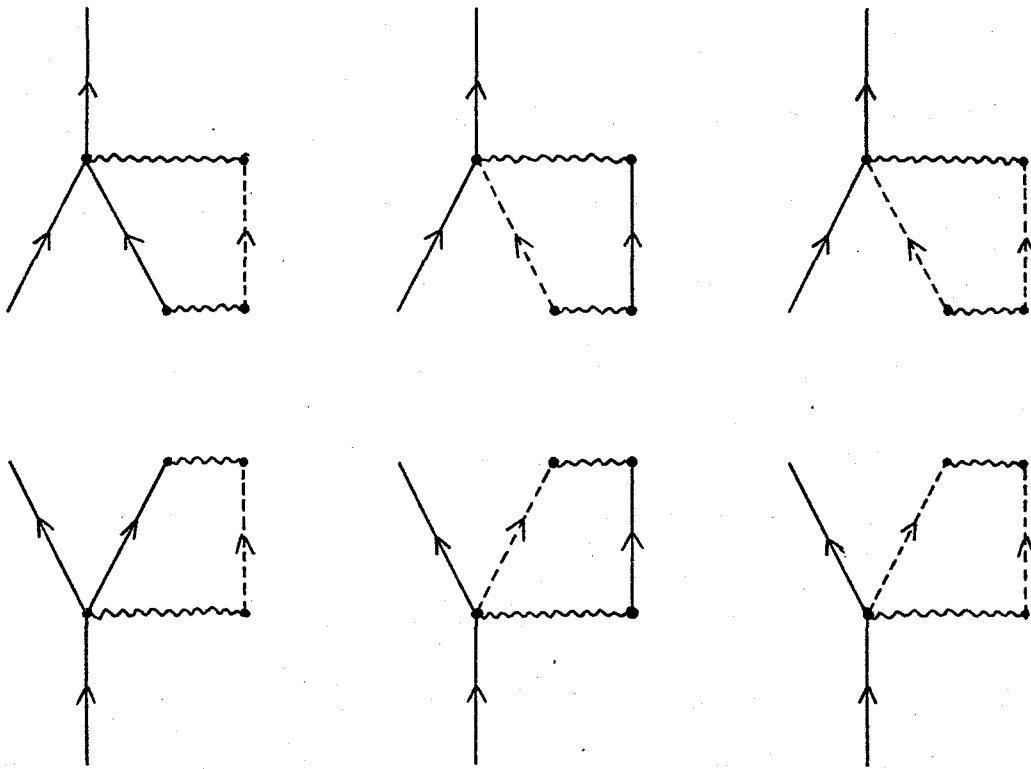
$\Delta \Sigma_{20}$

Fig. 2



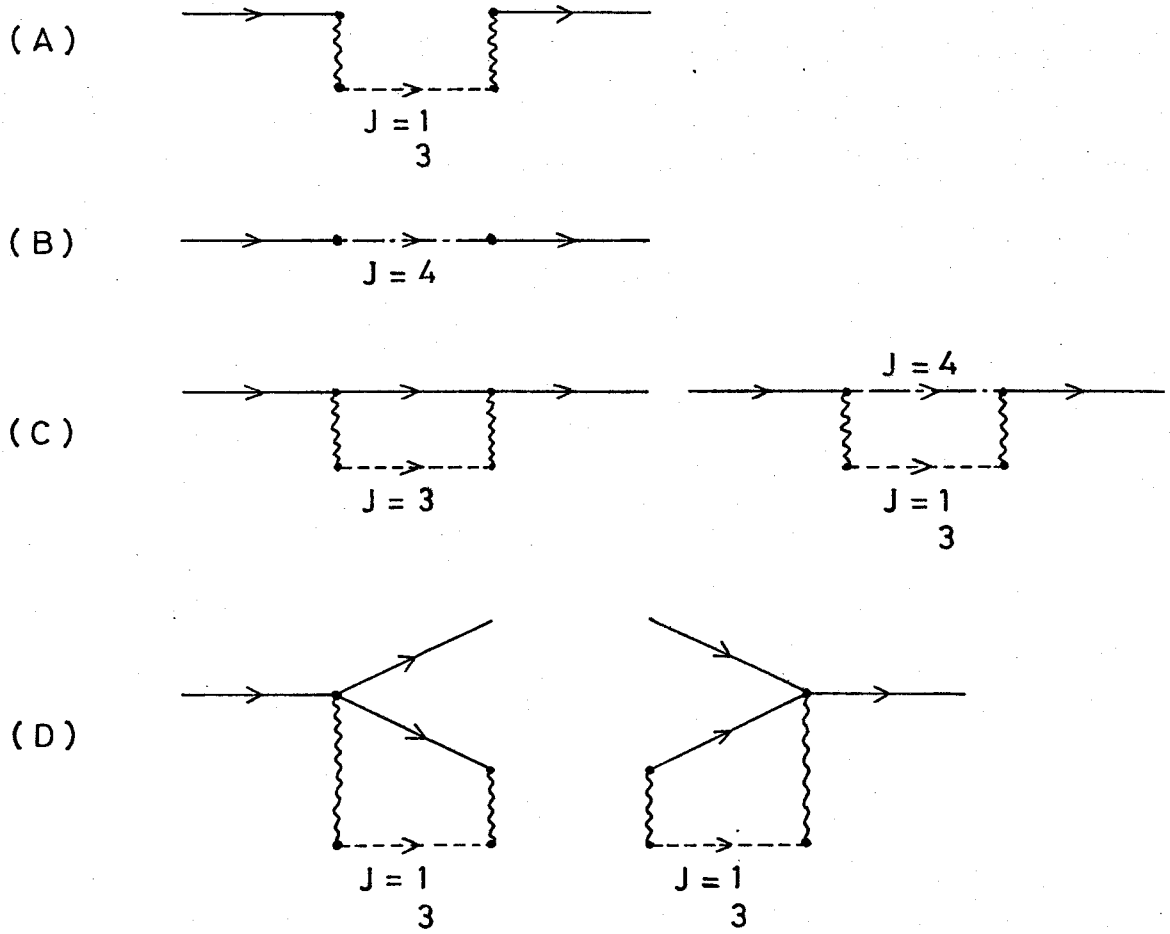
$$\Delta \sum_{11}^{\sim}$$

Fig.3



$$\Delta \sum_{R} 11$$

Fig. 4



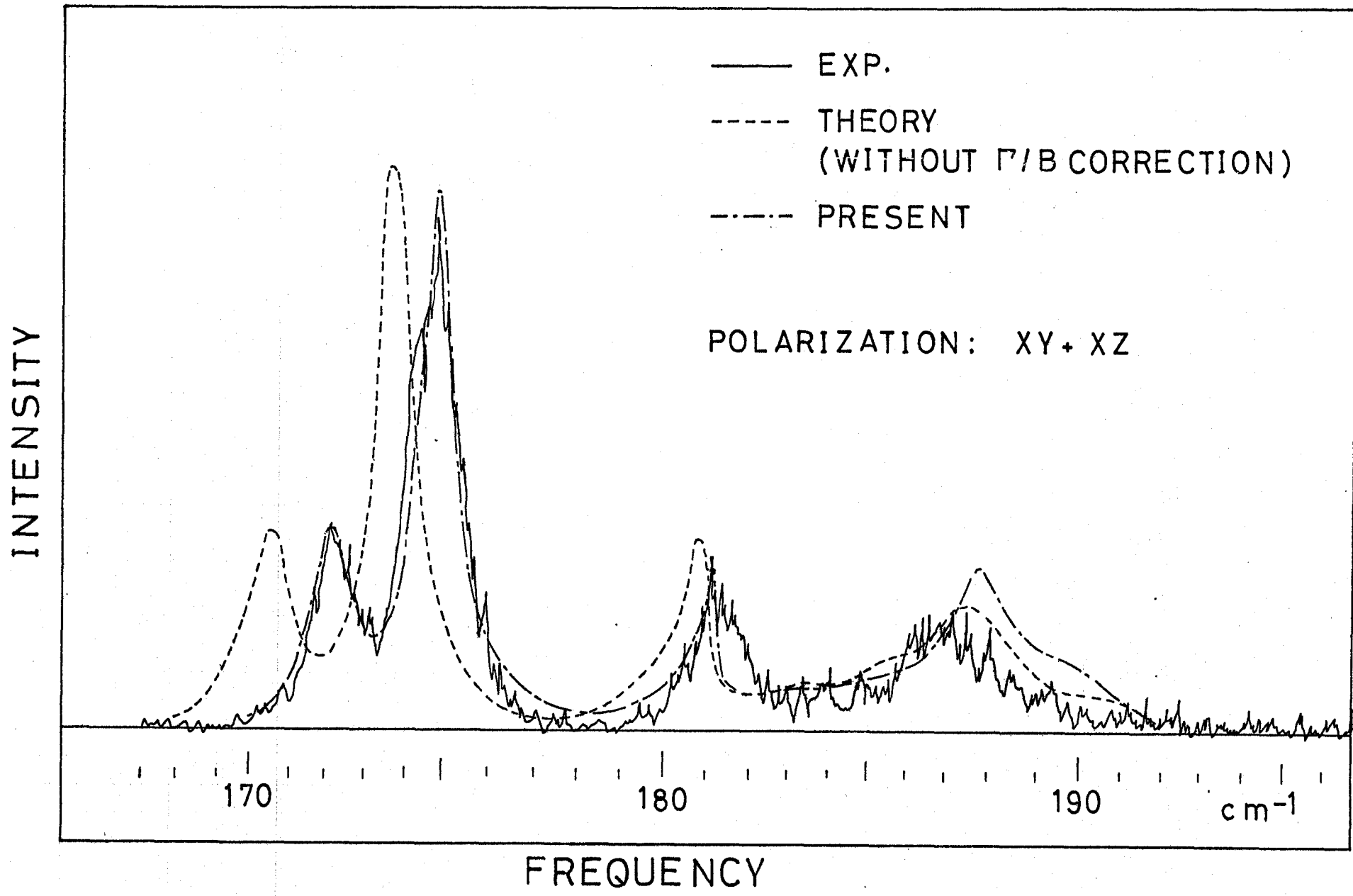
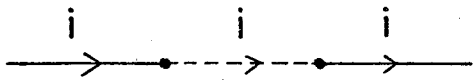


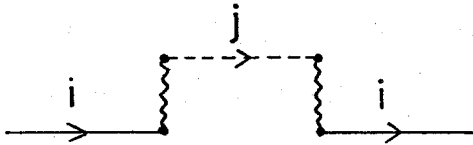
Fig. 5

Fig. 6

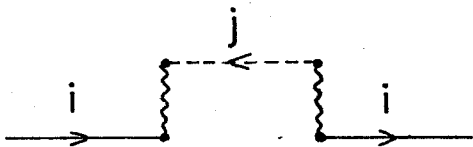
(unit: Γ^2/B)



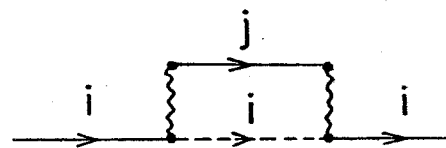
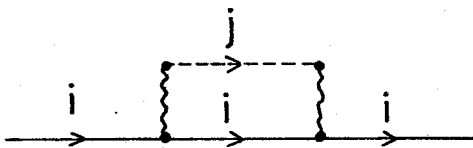
-12.9



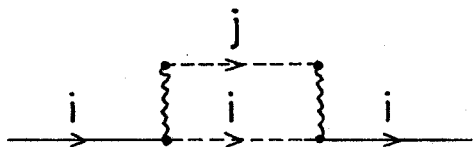
-3.8



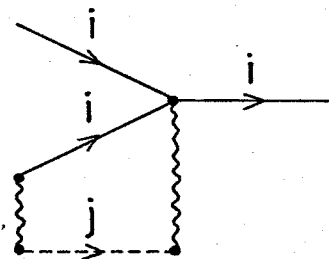
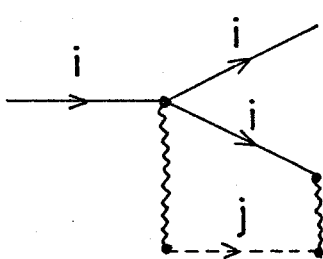
-3.8



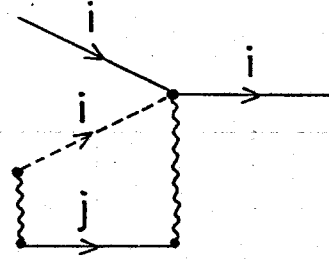
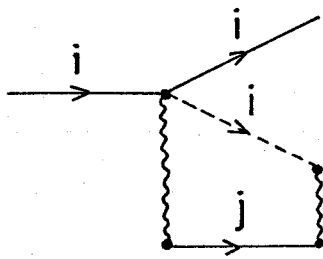
-29.4



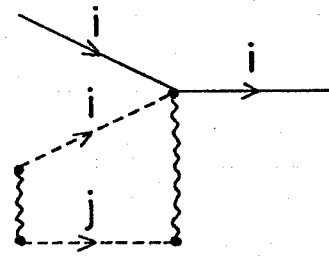
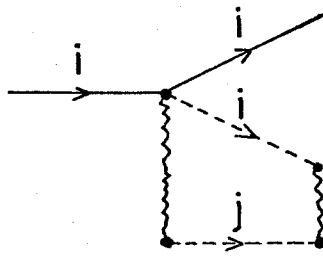
-10.6



11.4



7.6



10.3